



Norwegian University
of Life Sciences

Master's Thesis 2017

Faculty of Sciences and Technology

TESTING ALUMINIUM BASED CHEMICALS FOR FOULING REDUCTION IN MEMBRANE BIOREACTOR

Supervisors:

Dr. Zakhar Maletskyi

Prof. Harsha Ratnaweera

Dawit Kahsay Zigta

Sustainable water and Sanitation, Health and Development

Faculty of Environmental Sciences and Natural resources Management

ABSTRACT

The need for the environment, water and soil protection from human-induced pollutions are increasing from day to day. Improper sanitation and uncontrolled waste discharge are among the main sources of pollutants, which made the decentralized wastewater treatment industries solution as same time source of pollutants. Hence, environmental and economic sustainability are the two factors among many that sustainability of wastewater treatment plants (WWTP) are being evaluated through in recent days. Wastewater contains nutrient pollutants such as organic matter, nitrogen, and phosphorus. Disposal of these contaminants in an uncontrolled manner causes environmental pollution like eutrophication and enhance watercolor development.

To protect the environment from the adverse effect of urban wastewater discharge, urban wastewater directives set stringent standards on discharges quality from WWTPs. The need to meet the quality standards and the enquiry to challenge the water scarcity has led to development of innovative technologies like MBR and MBBR that are generally used in water management sectors. Treatment of used water for reuse involves several process among which the continuously evolving membrane filtration. Membranes such as MBR provides a combination of biological treatment and membrane separation. Membrane bioreactor has significantly contribute to the production of high quality effluent, reduced sludge yield, and effective retention of biomass. The MBR is applied for direct filtration in an activated sludge waste treatment that normally contains suspended particles, colloids and solutes. Thus, MBR is used to perform the critical solid-liquid separation eliminating the need for a secondary clarifier. However, the interaction between the feed material and the membrane causes fouling of the membrane restraining the wider application of the technology. Fouling results as a consequence to precipitation of suspended or dissolved substances on the membrane surface and at the pores of the membrane. Consequently, it reduces membrane performance and productivity, increased energy consumption, membrane cleaning, and use of reagents decreasing economic feasibility of the MBR.

The main purpose of this experimental study was, to physically validate the analytical predictions of using aluminum-based coagulation as fouling reducer in submerged membrane biological reactor. Therefore, membrane fouling reduction through charge driven interaction using $\text{Al}_2(\text{SO}_4)_3$, was studied and compared with results of PAX-18 and PAX XL-61. Improvement on filterability of mixed liquor due to the Influence on the properties of mixed liquor solid were assessed through the change in Zeta potential, Turbidity, floc size and hydrophobicity after coagulant addition. Accordingly, it was found that at lower ranges of concentration Alum enhanced the filterability of the mixed liquor better than the polymers. It could be explained that monomeric aluminum enhanced the charge counter balancing, floc size and hydrophobicity better at pH 4-6 and dosing $1.6 \text{ mM Al. g}^{-1} \text{ MLSS}$. As the experimental investigation revealed the chemicals can be ranked $\text{Al}_2(\text{SO}_4)_3$, PAX-18 and PAX XL-61 in order of their effect on membrane fouling in the given range of dosing.

Acknowledgement

I believe nothing have happened without your will, God thank you for being with me always. I would like to thank the Norwegian University of life sciences (NMBU: Norges miljø- og biovitenskapelige universitet) for granting me the admission to pursue my graduate study and their support throughout my stay.

I am very much grateful of Dr. Zakhar Maletskyi, My Supervisor, for the continuous guidance and advisory help he provided me through the course of this master's thesis. This work wouldn't have been materialized without his constructive criticism and fruitful discussions. I would also like to thank very much Prof. Harsha Ratnaweera, my Co-supervisor, for his advice and unreserved help in my study and during the thesis work.

I am highly indebted to Olga Kulesha, Doctoral candidate at Faculty of Science & Technology, for her Help during the Laboratory works and the constructive discussions. My thanks also goes to Vladislav Shostak for the introduction to the CE-MBR Laboratory facility and his friendly help.

I would like to thank to the IT support, Plant biology and plant biotechnology imaging center, and the Faculty of Science and technology laboratory Floy IV and V for giving me full access to the different facilities and support when I needed it. My thanks extends to the department of Sustainable water and sanitation, health and development for the academic and administration support they delivered during my study.

Abbreviations and Acronyms

AMTA – American Membrane Technology Association

AS – Activated Sludge

BF-MBR – Biofilm Membrane Bioreactor

CAS – Conventional Activated Sludge

DOM – Dissolved Organic Matter

EPS – Extracellular Polymeric Substances

EU-UWWTD – European Urban Wastewater Treatment Directive

F/M – Food to Microorganisms ratio

K – symbol for Element Potassium

LMH – Litter per square Meter per Hour

MBR – Membrane Bio-Reactor

MF – Membrane Filtration

N, N_{Tot} – Nitrogen, Total Nitrogen

SMP – Soluble Microbial Products

SS/MLSS – Suspended Solids/ Mixed Liquor Suspended Solids

MWCO – Molecular Weight Cut Off

PAX-18 – Poly-aluminum chloride coagulant

PAX XL-61 – Pol-aluminum

PCA – Principal Component Analysis

P, P_{Tot} – Phosphorus, Total Phosphorus

PSD – Particles Size Distribution

PVDF – Poly-Vinylidene Difluoride

TMP – Trans-membrane Pressure

UF – Ultra-filtration

WWTPs – Wastewater Treatment Plants

ZP – Zeta Potential

Table of content

Contents

| | |
|--|-----|
| ABSTRACT..... | i |
| Acknowledgement | ii |
| Abbreviations and Acronyms | iii |
| Table of content | iv |
| List of figures..... | vi |
| List of Tables | ix |
| 1. INTRODUCTION | 1 |
| 1.1. General..... | 1 |
| 1.2. Objectives | 2 |
| 1.3. Statement of the Problem..... | 2 |
| 1.4. Thesis Outline | 3 |
| 1.5. Limitations | 3 |
| 2. THEORY | 4 |
| 2.1. Membrane Filtration | 4 |
| 2.2. Understanding Membrane Bioreactor | 5 |
| 2.3. The Need to Use MBR..... | 6 |
| 2.3.1. Footprint..... | 7 |
| 2.3.2. Discharge quality and nutrient recovery | 7 |
| 2.3.3. Carbon budget..... | 8 |
| 2.4. Membrane Fouling..... | 8 |
| 2.5. Membrane Foulants | 10 |
| 2.5.1. Organic Foulants | 10 |
| 2.5.2. Biofoulants..... | 11 |
| 2.5.3. Inorganic Foulants..... | 11 |
| 2.6. Fouling Mechanisms in Membrane Bioreactor..... | 13 |
| 2.6.1. Pore Clogging | 13 |
| 2.6.2. Cake Layer Formation | 14 |
| 2.7. Factors Affecting Membrane Fouling..... | 15 |
| 2.7.1. Membrane Properties | 15 |
| 2.7.2. Operational Conditions | 16 |
| 2.7.3. Feed Material and Biomass Characteristics | 20 |
| 2.8. Fouling Reduction Techniques | 24 |

| | | |
|--------|--|----|
| 2.8.1. | Adsorption..... | 25 |
| 2.8.2. | Coagulation..... | 25 |
| 2.9. | Alum..... | 29 |
| 2.10. | Mechanism of Coagulation in Wastewater..... | 29 |
| 2.11. | Ortho-Phosphate..... | 32 |
| 3. | MATERIALS AND METHODS..... | 33 |
| 3.1. | BF-MBR Mixed Liquor and the Conventional Activated Sludge..... | 33 |
| 3.1.1. | Determination of Sludge Parameters..... | 34 |
| 3.2. | Membrane Type and Characteristics..... | 34 |
| 3.3. | Membrane Fouling Reducers..... | 35 |
| 3.4. | EXPERIMENTAL SETUP..... | 36 |
| 3.5. | ANALYTICAL METHODS..... | 38 |
| 3.5.1. | Zeta Potential (ZP)..... | 38 |
| 3.5.2. | Floc size and morphology..... | 39 |
| 3.5.3. | Turbidity..... | 39 |
| 3.5.4. | Capillary suction time (CST)..... | 39 |
| 3.5.5. | Ortho-Phosphate..... | 40 |
| 3.6. | Data Collection and Processing..... | 40 |
| 4. | RESULTS AND DISCUSSION..... | 42 |
| 4.1. | Aluminum Sulphate as Membrane fouling reducer..... | 42 |
| 4.1.1. | Filtration Phase..... | 42 |
| 4.2. | Supernatant characterization..... | 43 |
| 4.2.1. | pH..... | 43 |
| 4.2.2. | Zeta Potential (ZP)..... | 43 |
| 4.2.3. | Turbidity..... | 44 |
| 4.3. | Precipitate characterization..... | 45 |
| 4.3.1. | Capillary suction time..... | 45 |
| 4.3.2. | Particle size distribution (PSD)..... | 46 |
| 4.4. | Filtrate characterization..... | 49 |
| 4.4.1. | Ortho-Phosphate..... | 49 |
| 4.5. | Summary of comparison between BF-MBR and AS Mixed liquor..... | 50 |
| 4.6. | Comparison with Pre-polymerized MFRs..... | 53 |
| 4.6.1. | PAX XL-61..... | 53 |
| 4.6.2. | PAX-18..... | 54 |
| 4. | CONCLUSION..... | 57 |

| | |
|--|----|
| 5. REFERENCES | 58 |
| APPENDIX I: Processing of data from total recycle test | 62 |
| APPENDIX II: Particle Size Growth and Distribution..... | 68 |

List of figures

| | |
|---|----|
| Figure 1. Schematic representation of fluid transport through a membrane. | 4 |
| Figure 2. Shows types of membrane and particles they separate..... | 4 |
| Figure 3. Phosphorus resources peak production curve and human excreta, urine, and food wastes contain nutrient fertilizers required to produce our daily food..... | 7 |
| Figure 4. Shows the different fouling mechanisms that decrease the filtration rate | 9 |
| Figure 5. Chart illustration of the formation of the three types of fouling and elimination of removal and irremovable fouling's..... | 10 |
| Figure 6. Schematic illustration of the relationship of EPS, membrane foulants and fouling mechanisms in MBR..... | 12 |
| Figure 7. Membrane fouling mechanisms in MBR..... | 13 |
| Figure 8. Illustration of size range membranes pores, foulants and filtration processes | 14 |
| Figure 9. The gradual TMP development and corresponding Fouling stages a..... | 18 |
| Figure 10. Schematics of EPS components (a), EPS cell structure (b), and adsorption of EPS on Hydrophilic membrane (c)..... | 21 |
| Figure 11. SEM (200x) Images illustrating the change in sludge flocs after addition of coagulants: | 26 |
| Figure 12. The change in charge neutrality and specific resistance to filtration/filterability..... | 27 |
| Figure 13. The concentration of monomeric hydrolysis products of Al^{3+} in equilibrium..... | 30 |
| Figure 14. Illustration of the dilution, hydrolysis, and polymerization of Al^{3+} | 31 |
| Figure 15. Flow sheet of BF-MBR Pilot plant and Bekkelaget Wastewater treatment plant | 33 |
| Figure 16. Shows the cross section of flat sheet membrane structure..... | 35 |
| Figure 17. Schematic illustration of the principles of the experiment set up..... | 36 |

| | |
|---|----|
| Figure 18. A Graphical demonstration of the variation in TMP over the filtration time | 37 |
| Figure 19. Flowchart showing sequences of the experiments and analytical measurements..... | 38 |
| Figure 20. Schematic illustration of Zeta potential and the formation of Electrical Double layer around a particle | 39 |
| Figure 21. Schematic representation of the CST testing apparatus and photo of actual set-up | 40 |
| Figure 22. The filtration duration, change in MLSS and normalized permeability as well as flux at working MLSS 3.53 g.l ⁻¹ BF-MBR..... | 42 |
| Figure 23. Graphic illustration of the change in pH as a function of dosing at MLSS (a) 3.53 g.l ⁻¹ SS BF-MBR and (b) 4.72 g.l ⁻¹ SS AS. | 43 |
| Figure 24. The variation of electrical charge of particles as a function of dosing at a working MLSS of (a) 3.53 g.l ⁻¹ from BF-MBR and (b) 4.72 g.l ⁻¹ from AS. | 44 |
| Figure 25. Turbidity evolution as a function of dosage at MLSS concentration (a) 3.53 g.l ⁻¹ from BF-MBR and (b) 4.72 g.l ⁻¹ from AS. | 45 |
| Figure 26. The change Capillary suction time as a function of dosage (a) 3.53 g.l ⁻¹ MLSS BF-MBR and (b) 4.72 g.l ⁻¹ MLSS AS. | 46 |
| Figure 27. Light microscopy image demonstrating particle size growth and distribution of the Non-flocculating and Flocculated micro-particles | 47 |
| Figure 28. Graphical illustration of particle size distribution as a function of dosing | 48 |
| Figure 29. Demonstrates the change in Ortho-Phosphate concentration (ppm). | 49 |
| Figure 30. The contrast between the influences on the Suspended Solid concentration (a), filtration Phase (b), Zeta potential (c), turbidity (d), CST (e) and Ortho-phosphate (f)..... | 51 |
| Figure 31. PCA signifying the increase in filtration congruently with zeta potential..... | 52 |
| Figure 32. pH change before dosing and after dosing as function of the dose | 53 |
| Figure 33. The variation of zeta potential and filtration phase as function of dosing..... | 53 |
| Figure 34. Graphical representation of the change in the CST in correlation with filtration phase..... | 54 |
| Figure 35. The contrast between the filtration cycle and Turbidity as a function of dosage. | 54 |
| Figure 36. Change in pH before and after dosing as function of dosing..... | 54 |
| Figure 37. Evolution of surface net charge and its impact on filtration phase..... | 55 |

| | |
|--|----|
| Figure 38. The contrast between the filtration cycle and zeta potential (a) and Filtration cycle versus CST (b) as a function of dosage..... | 55 |
| Figure 39. Turbidity indices in relation of the filtration phase as function of dosing..... | 55 |
| Figure 40. Change in TMP as function of time at 0.21 mM Al | 62 |
| Figure 41. TMP as function of time at 0.43 mM Al | 62 |
| Figure 42. Change in TMP as function of time at 0.53 mM Al | 62 |
| Figure 43. The Evolution of TMP as function of time at 0.64 mM Al | 63 |
| Figure 44. The three-stages of TMP as function of time at 0.74 mM Al..... | 63 |
| Figure 45. The variation of TMP as function of time at 0.85 mM Al..... | 63 |
| Figure 46. The Evolution of TMP as function of time at 0.96 mM Al | 64 |
| Figure 47. The change in TMP as function of time at 1.06 mM Al..... | 64 |
| Figure 48. TMP increase as function of time at 1.3 mM Al | 64 |
| Figure 49. Evolution of TMP as function of time at 1.5 mM Al | 65 |
| Figure 50. TMP increase as function of time at 0 mM Al | 65 |
| Figure 51. The change in TMP as function of time at 0.21 mM Al..... | 65 |
| Figure 52. Evolution of TMP as function of time at 0.43 mM Al | 66 |
| Figure 53. The variation of TMP as function of time at 0.53 mM Al..... | 66 |
| Figure 54. The change in TMP as function of time at 0.64 mM Al..... | 66 |
| Figure 55 the evolution of TMP as function of time at 0.74 mM Al | 67 |
| Figure 56. Illustrations of the particle size growth and distribution at dosing 0 mM Al | 68 |
| Figure 57. Graphical description of the particle size growth and distribution at dosing 0.21 mM Al..... | 68 |
| Figure 58. The particle size growth and distribution at dosing 0.42 mM Al | 68 |
| Figure 59. Graphical illustration of particle size growth and distribution at dosing 0.53 mM Al | 69 |
| Figure 60. Shows the particle size growth and distribution at dosing 0.00064 mM Al..... | 69 |

| | |
|--|----|
| Figure 61. Graphical illustration of particle size growth and distribution at dosing 0.74 mM Al | 69 |
| Figure 62. Graphic descriptions of the particle size growth and distribution at dosing 0.8 mM Al | 69 |
| Figure 63. Illustrations of particle size growth and distribution 1.0 mM Al..... | 69 |
| Figure 64. The change in particle size and distribution at dosing 1.1 mM Al | 70 |
| Figure 65. Shows the particle size growth and distribution at dosing 1.3 mM Al..... | 70 |
| Figure 66. Display the particle size growth and distribution at dosing 1.5 mM Al | 70 |
| Figure 67. The particle size evolution and distribution at 0 mM Al | 71 |
| Figure 68. The improvement of the particle size and distribution at dosing 0.2 mM Al..... | 71 |
| Figure 69. Graphical illustration of particle size growth and distribution at dosing 0.42 mM Al | 71 |
| Figure 70. Illustrations of the growth in particle size and distribution at dosing 0.53 mM Al | 71 |
| Figure 71. The influence on particle size and distribution at dosing 0.64 mM Al..... | 72 |
| Figure 72. Graphical illustrations of particle size growth and distribution at dosing 0.74 mM Al..... | 72 |

List of Tables

| | |
|---|----|
| Table 1. Shows the mechanism how the different reagent types influence the fouling factors and enhance filtration | 28 |
| Table 2. Properties of the mixed liquor from BF-MBR and Activated Sludge from Conventional Process used for this study | 33 |
| Table 3. Membrane properties and operation condition | 34 |
| Table 4. Information on physicochemical properties of the reagents. Based on the Kemira Safety data sheet for each chemical, all are in liquid form and completely soluble in water. | 35 |
| Table 5. Correlation matrix..... | 51 |
| Table 6. Summary of the effect of the MFRs on the filtration Phase and ZP at Given MLSS, pH and optimal dose..... | 56 |
| Table 7, Filtration phase data source BF-MBR | 67 |
| Table 8. Filtration phase data source AS | 67 |

1. INTRODUCTION

1.1. General

Water scarcity has forced the world to develop new approaches such as water re-use and adapt to scarcity. Water might be recycled for potable supplies for human, industrial, agricultural and smaller scale utilities. The main challenge with this approach is that effective distribution and the water produced from, for instance, wastewater should be safe to use. Moreover, tighter control on the discharge of wastewater treatment has necessitated more expensive perhaps environment friendly solutions than the conventional biological treatment systems. Therefore, new technologies such as membrane bioreactor are attracting interest in the wastewater treatment industry due to the advantages they pose over the conventional activated sludge.

Membrane bioreactor (MBR) allows treatment of high sludge concentration wastewater at higher loading rate, provides high effluent quality and reduce the sludge yield owing to effective retention of biomass (Fang et al., 2006). Since its development starting 1970s (Bouhabila et al., 2001) Membrane bioreactor has been preferred to assist activated sludge replacing the clarifier; giving complete removal of impurities, process flexibility towards influent changes, reduced sludge production, improved nitrification (Lin et al., 2014), and 30-50% compactness (AMTA, 2017). However, for MBR to operate at the required efficiency it must be cleaned or replaced at some point due to a fouling problem, which eventually increases the operation and maintenance costs. Its high installation and operational costs, high air demand due to lower oxygen mass transfer consequent to high viscosity sludge are other disadvantages of MBR. Nevertheless, biological removal of Nitrogen requires significant bioreactor volume, which could be attained through MBR fitted in the conventional biological treatment.

Pore blocking by colloidal particles, biofilm growth, cake formation, and adsorption are some mechanisms of fouling while extracellular substances (EPS), soluble microbial particles (SMP) and colloidal materials are regarded as the main cause of the membrane fouling. Many studies have focused on alleviation of the fouling (Breite et al., 2015; Hwang et al., 2007; Koseoglu et al., 2008; Wu et al., 2006). Backwashing, aeration, intermittent suction, module modification and the addition of inorganic coagulant were tested in an attempt to reduce/solve membrane fouling problem. Moreover, application of cationic polymers has emerged as promising membrane fouling reducer though its details are not well understood. Coagulation has become common practice to remove colloids and soluble organic substances in water and wastewater treatment through aggregation to larger flocs. Iron and Alum salts are most used coagulants due to that they are more effective. Membrane fouling in the MBR is still not well understood which is why a subject of many ongoing researches.

The purpose of this study was to add to the better understanding of the use of Membrane fouling reducers (MFR) for fouling abatement. Particularly, the thesis focuses on charge-driven

mechanisms of interaction with membrane surface to elucidate membrane fouling reduction mechanism, aiming to validate the analytical predictions of using Aluminum based coagulants as fouling reducer in submerged membrane biological reactor. Specifically, an analytical experiment was conducted to determine the influence of Alum, PAX-18 and PAX XL-61 on Zeta potential, Turbidity, Hydrophobicity and particle properties as fouling factors.

1.2. Objectives

The main objective of this experimental study was, to physically validate the analytical predictions of using aluminum-based coagulation as fouling reducer in submerged membrane biological reactor (MBR).

Specifically,

- To experimentally study the influence of Aluminum based coagulation on Charge, Turbidity, hydrophobicity, and floc size. And
- To estimate the efficiency of Aluminum Sulphate ($\text{Al}_2(\text{SO}_4)_3 \cdot n\text{H}_2\text{O}$), PAX-18 and PAX XL-16 as fouling reducers.

1.3. Statement of the Problem

Fouling is the most significant drawback of MBR that restricts the application of the technology due to that it causes high operational and maintenance cost. Hence, membrane-fouling mitigation in MBRs has been one of the key areas of extensive research in order to enhance the wider application of the MBR technology in wastewater engineering. Experimental and pilot studies were performed to reduce fouling through Backwashing, aeration, intermittent suction, module modification and addition of an inorganic coagulant. And significant progress has been attained. However, many questions still remain unanswered in particular regarding controlling mechanism, which is an ongoing research.

The highly heterogeneous and presence of the microorganism in biomass matrix for different flow and composition, the different operational conditions applied in different MBR plants and the interaction between the activated sludge and the membrane makes fouling complex; hence, is insufficiently understood. Besides, this may have lead many of the researches done to focus on monitoring either one, combinations of two or three factors such as hydrophobicity, size of flocs, charge, and turbidity. This implies most studies have generally been limited to single or two treatment system. However, a unified study that focuses on the collective effect of the above parameters hasn't published yet, which this dissertation has focused on improving the understanding of the effect of coagulants on fouling reduction and filterability through combined influence on these fouling factors experimentally.

1.4. Thesis Outline

Chapter One: provides a general description of the necessity of treating water from water reuse perspective to overcome water scarcity and environmental pollution, the advantages of applying MBR as a new technology was sought after its advantages for wastewater treatment as a significant improvement of the conventional activated sludge technology. The problems associated with applying MBR mainly fouling as a primary MBR growth restraining factor and insight of researches on controlling the problem were introduced. The chapter concludes with a description of the objectives, statement of the problem that this dissertation aimed to address, short outline of thesis and of course limitations during the study.

Chapter two: is dedicated to literature review where a general background and theoretical mechanism of membrane fouling in water and wastewater treatment are studied. Understanding of the MBR, the need to use MBR technology from sustainable water and resource management perspective, the definition of fouling, mechanism of fouling, determinant factors and remediation techniques were discussed as to give a detailed understanding of MBR fouling problem.

Chapter three: Specific description of the materials used as impute for this experimental study, the experimental procedure, analytical methods and techniques of data collection and processing are given in this chapter. In general, it's a chapter dedicated to materials and methodologies description.

Chapter four: in this chapter, the findings from the experiment are presented schematically and described subsequently. The results are discussed and interpreted with respect to scientific literatures with a similar thematic area, which are mainly reviewed in the second chapter of this thesis, and theoretical background acquired through the course of my study.

Chapter five: a conclusion chapter where a summary of key points from the study are concluded and further recommendations are proposed.

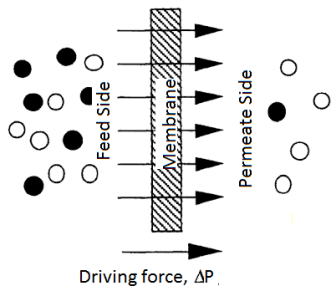
1.5. Limitations

As this was a short-term research, it was practically difficult to incorporate all phenomenon associated with fouling. Time constraint was the main limiting factor working with this thesis. Consequently, it wasn't possible to conduct the total recycle test experiment using the polymerized MFRs but data was borrowed from similar experiment conducted by WESH group for comparison.

2. THEORY

2.1. Membrane Filtration

Filtration process could be defined as the application of a selective barrier between two phases (Mulder, 2012). In the case of water or wastewater treatment, the barrier would be a membrane that is a material consisting fine porous medium that allows water to pass through and hold back constituents incorporated in the water. The components retained are materials with a larger size than the membrane pores. Water transported through the membrane occurs due to the applied



pressure gradient as a driving force, namely transmembrane pressure (TMP). Hence, the flux of water from the inlet side, usually called feed side, to the outlet side also called permeate side is determined by the height of TMP and the resistance to flow developed due to the accumulated particle on the membrane surface (Figure 1).

Figure 1. Schematic representation of fluid transport through a membrane. modified from (Mulder, 2012).

Based on their pore size four types of membrane are distinguished in Water and wastewater treatment (figure 2).

| Size, μm | 0.001 | 0.01 | 0.1 | 1 | 10 | 100 | 1000 |
|---------------------|---------|------------|--------------|-------------|-----------------------------------|----------|-------|
| MWCO | 100 200 | 1000 10000 | 20000 100000 | 500000 | | | |
| Materials | Metals | Salts | Viruses | Humic acids | Clay | Bacteria | Algae |
| | | | | | Silt | Cystes | Sand |
| Process | RO | NF | UF | MF | Conventional filtration processes | | |

Figure 2. Shows types of membrane and particles they separate (Van Dijk et al., 2001 in (Geilvoet, 2010))

Accordingly, the flat sheet microfiltration of 0.1 μm going to be used in this dissertation could completely retain particle sizes larger than clay, bacteria and to some extent humic acids. During filtration, deposition of particles on and in the membrane is inevitable consequently reducing the membrane filtration performance. This decrease in performance is called membrane fouling (Geilvoet, 2010).

2.2. Understanding Membrane Bioreactor

Development of Membrane bioreactor (MBR) is dated back to 1970s (Bouhabila et al., 2001). MBR, in general, means the application of a perm-selective membrane; Ultra- or Micro-membrane, integrated with biological processes as a discrete tertiary step. Hence, MBR is applied for direct filtration in an activated sludge waste treatment, which normally contains suspended particles (bacteria flocs and inert materials), colloids and solutes (Rosenberger et al., 2005). Thus, MBR is used to perform the critical solid-liquid separation eliminating the need for a secondary clarifier. This makes MBR an interesting innovation in wastewater treatment as it overcomes the drawbacks of conventional activated sludge method such as the large space requirement for secondary clarifier, production of excess sludge, the limitation with the removal of recalcitrant in addition to the liquid-solid separation issue. Application of MBR reduces 30-50% footprint of the conventional activated sludge facility that includes secondary clarifiers and media tertiary filtration (AMTA, 2017).

MBRs have been choice of both municipal and industrial wastewater treatment and reclamation due to the advantages it provide; high quality effluent, higher volumetric loading rate, shorter hydraulic retention time (HRT), longer solid retention time (SRT), less sludge production and potential for simultaneous nitrification/denitrification in long SRTs (Iorhemen et al., 2016). The more stringent discharge standards, the steady decrease of membrane costs and increased water reclamation needs together with the above advantages stimulates extensive researches and application of MBR for biological WWT (Lin et al., 2014).

Gravity-driven (Vacuum) and pressure-driven systems are the two working principles of MBR. The vacuum system is immersed that employ hollow fiber membrane installed in either the bioreactor or subsequent membrane tank whereas the pressure driven system is connected to the bioreactor externally in-pipe cartridge system (AMTA, 2017).

Membrane bioreactor is widely used because of its Exceptional separation capacity, high biodegradation efficiency, smaller sludge production, and compactness. The smaller pores (<0.5 μ m) provide very high clarity and significantly reduced pathogen concentration effluent discharged to sensitive receiving bodies or reclaimed for urban irrigation or toilet flushing.

However, MBR technology has disadvantages such as higher energy costs, the need to control membrane fouling problem, potential high cost of periodic membrane replacement and installation costs. Among these problems, membrane fouling remains the major drawback of using MBR. Several studies described the faster development of this reactor was constrained due to membrane fouling (Bouhabila et al., 2001; Iorhemen et al., 2016; Rosenberger et al., 2005).

2.3. The Need to Use MBR

The need for the environment, water and soil protection from human-induced pollutions are increasing from day to day. Improper sanitation and uncontrolled waste discharge are among the main sources of pollutants, which made the wastewater treatment industries solution as same time source of pollutants. Hence, environmental and economic sustainability are the two factors among many factors that sustainability of wastewater treatment plants (WWTP) are being evaluated through in recent days. Wastewater contains nutrient pollutants such as organic matter, nitrogen, and phosphorus. If these contaminants are disposed of in an uncontrolled manner, they can cause environmental pollution like eutrophication and enhance watercolor development. To protect the environment from the adverse effect of urban wastewater discharge, urban wastewater directives set stringent standards on discharges quality from WWTPs. For instance, the EU urban wastewater treatment directive has stated standards on the design and set requirements for discharge from WWTPs (EU-UWWTD, 1991). To mention;

- WWTPs must be designed or modified to that representative sample of incoming wastewater and treated effluent can be found before discharging to make sure it does not adversely affect the environment
- A process involving biological treatment with a secondary settlement or another process should have minimum percentage of reduction 70-90 % organic matter, 90% suspended solids, 80% phosphorus, and >70% Nitrogen.

Hence, biological WWTPs based on activated sludge (AS) were upgrading to more advanced treatment technologies to meet the desired quality of effluent. Consequently, new technologies such as membrane bioreactor are attracting interests in the wastewater treatment industries due to the advantages they provide over the conventional activated sludge and their application has been growing through time. More than 2500 MBR plants were reported to have been in operation worldwide and had a growth rate of 10.5% during 2008 -2013 (Meng et al., 2012 in (Lin et al., 2014)). The advantages include excellent effluent quality, good disinfection capability, higher volumetric loading, reduced footprint, processes flexibility towards influent changes, reduced sludge production, and improved nitrification (Lin et al., 2014). Moreover, membrane costs are decreasing and the need for water reclamation of nutrient resources and water itself is increasing (Lin et al., 2014). When describing the drivers for the application of the MBR (Geilvoet, 2010) summarized the following important factors from the study by Judd (2006);

- Space scarcity,
- The suitability of MBR to retrofitted in existing conventional activated sludge (CAS)
- Local water scarcity
- Increasing confidence and acceptance of MBR technology
- State incentives to encourage improvement in wastewater technology and recycling

The first two factors elucidate the need of new technologies with reduced footprint requirement while the last three factors indicate the need for the world to adopt new approaches to water scarcity and the excellent effluent quality produced using MBR. Decreasing investment cost also was another factor that promotes the implementation of MBR.

2.3.1. Footprint

Nowadays space constraint is becoming a concern in conventional treatment plants. Due to increase in population at a certain period and future predictions in many parts of the world, the incoming volume of wastewater into treatment plants grow from time to time. Besides the biological treatment for Nitrogen removal requires significant bioreactor volume. The application of MBRs fitted in the conventional biological treatment provides both usage of a reduced area as well as flexibility in influent volume. Studies have indicated MBR provides process flexibility towards influent changes (Lin et al., 2014) and areal reduction up to 50% of the conventional activated sludge (AMTA, 2017).

2.3.2. Discharge quality and nutrient recovery

Water, organic matter, nitrogen, and phosphorus are nutrient resources that wastewater is composed of when it reaches the treatment industries. In excess availability of these resources; organic carbon, nitrogen, and phosphorus in a certain environment could adversely affect the ecological system. Therefore, the urban wastewater treatment directorate passes rules that promote utmost retention of these pollutants. MBR has been sought from this perspective and reported to provide excellent effluent quality and effective retention of biomass (Fang et al., 2006; Melin et al., 2006). This implies the improvement of the discharge quality of a plant with biological processes using MBR. The effective retaining capacity also means that resources such as Phosphorus and organic carbon are well preserved in the sludge, which can be applied back into the soil. Consequently, MBR contributes to the recent attitude of viewing waste as a resource.

A conservative analysis using industry data suggested peak phosphorus production could be reached exactly in 15 years, 2033 (figure 3) from now (Cordell et al., 2009). In contrast, the Blackwater that we simply discharged was reported to contain 90% N, 80% P, 80% K and 40-75% organic matter (Ratnaweera, 2017; Vinnerås and Jönsson, 2002).

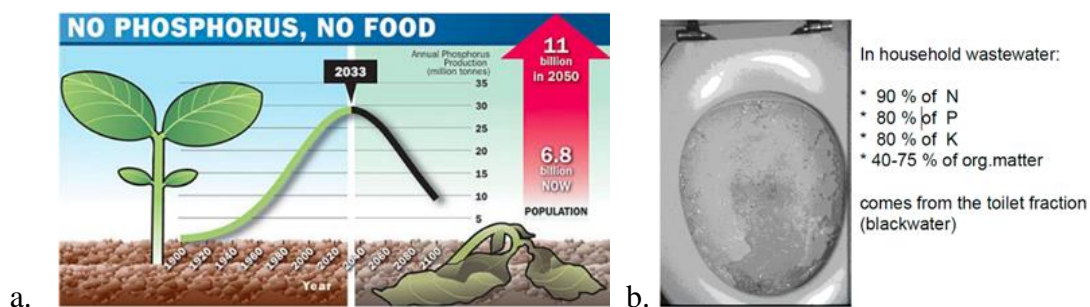


Figure 3. Phosphorus resources peak production curve (a) and human excreta, urine, and food wastes contain nutrient fertilizers required to produce our daily food (b).

Studying the MBR technology for wastewater reclamation and reuse with main focus on emerging pollutants (Melin et al., 2006) indicated, biological removal of Phosphorus $P_{Tot} < 0.3 \text{ mg.l}^{-1}$ and complete nitrification-denitrification with effluent quality $N_{Tot} < 10 \text{ mg.l}^{-1}$ (cool climate); $N_{Tot} < 3 \text{ mg.l}^{-1}$ (warm climate). Given the values are below the standard limits $P_{Tot} < 1 \text{ mg.l}^{-1}$ and $N_{Tot} < 10 \text{ mg.l}^{-1}$, MBR provides both excellent effluent quality and recovery of the nutrients from the sludge.

Moreover, the application of low-pressure membrane filtration Micro membrane (MF) or Ultrafiltration (UF) enables significant elimination of pathogens; bacteria and Virus (when UF applied). (Melin et al., 2006) have summarized that MBR has achieved log removal of 6-8 for bacteria and 3-5 for viruses, showing satisfactory microbiological effluent quality adequate for many water reuse applications with slight chlorine disinfection. Water reuse now days sought as a solution for prevalent water scarcity in less developed countries, is also an important approach for sustainable management in areas were currently no shortage of water.

2.3.3. Carbon budget

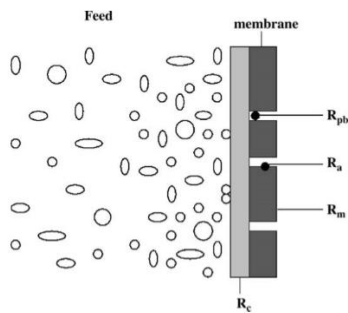
The household wastes (kitchen and toilet), wastes discharge from industries (fish and pulp) and storm erosion increases the wastewater organic matter (carbon) content. Their discharge to aquatic and marine environments creates favorable conditions for bacterial decomposition eventually contributing to CO_2 emission which affecting the carbon cycle. The longer solid retention time in the MBR operation was identified to contribute in less sludge production (Iorhemen et al., 2016). One of the implication could be due to the high microbial population enhances oxidation and decomposition of organic matter, reducing the organic carbon flowing to water bodies. This significantly reduces the transportation of organic matter to seas eventually less effect on the carbon cycle and production of carbon dioxide. Recent advancement on membrane bioreactors studied by (Meng et al., 2009) recognized the high removal efficiency of biological oxygen demand (BOD) and chemical oxygen demand (COD) of MBRs which also allows water reclamation.

Therefore, the effective conservancy of these resources from the wastewater in the sludge is both environmentally and economically advantageous since they could be reused as fertilizer (Phosphorus) and soil gel (Organic Carbon).

2.4. Membrane Fouling

The international union of pure and applied chemistry (IUPAC) defines membrane fouling as a process resulting consequence to precipitation of suspended or dissolved substances on the membrane surface, at the openings or in the pores (Koros et al., 1996). Similarly, (Rosenberger et al., 2005) indicated, In the processes of filtering activated sludge, retained particles may form a cake on the membrane, some may block the pores, others adsorb at the membrane surface or in the membrane pores depending on their physicochemical properties. Another study added,

the physical and chemical interactions taking place between mixed liquor matrix and membrane



material results in membrane fouling (Iorhemen et al., 2016). Hence, it could be said fouling is due to interaction of feed components with the membrane in one or many of the above factors. Rosenberger et al. describe the above factors as fouling mechanisms that could be expressed by filtration resistance (total resistance to filtration Eq. 2.1 and Fig. 4).

$$R = R_{\text{cake}} + R_{\text{poreblocking}} + R_{\text{adsorption}} + R_{\text{membrane}} \dots\dots 2.1$$

Figure 4. Shows the different fouling mechanisms that decrease the filtration rate

Membrane fouling reduces membrane performance and membrane lifespan, which leads to increased maintenance and operation costs reducing productivity (Iorhemen et al., 2016). Membrane performance is a function of transmembrane pressure (TMP), which can be described as the difference in pressure between two sides of a membrane and may vary for different membranes. A low transmembrane pressure indicates a clean, well-functioning membrane. On the other hand, a high transmembrane pressure indicates a dirty or too fouled membrane with reduced filtering abilities. Fouling is attributed to suspended particles, colloids, solutes, and sludge flocs as they can precipitate and /or clog the pores. Membrane fouling, as indicated in (Meng et al., 2009) occurs due to following causes;

- Adsorption of solutes or colloids Within/on membrane
- Deposition of sludge flocs on to membrane surface
- Formation of cake layer on membrane surface
- Detachment of foulants due to shear forces, and
- Spatial and temporal change of foulant composition during operation (e.g. change of bacterial community and biopolymer components)

The heterogeneous nature of suspended solids and active microorganisms in mixed liquor suspended solids (MLSS), and the nature of membrane makes the membrane fouling inevitable challenge in long-term MBR application in the wastewater industry. Membrane fouling could be two types; reversible and irreversible fouling (van der Marel et al., 2010).

Reversible foulants or fouling cake could be removed by physical cleaning, however, irreversible foulants also called pore clogging are removed by chemical cleaning. Therefore, applying physical cleaning discriminate between reversible and irreversible fouling. (van der Marel et al., 2010) added that cake layer can be removed by relaxing and backwashing; however, gel layers, compressed cake layers and pore blocking as well as adsorption hardly removed by these physical methods. In contrary, (Meng et al., 2009) suggested irreversible fouling to be defined as fouling that can't be removed by any method even chemical cleaning. The naming irreversible for a removable fouling seems confusing or incorrect form in connection with the meaning of the word itself. Hence, more elaborated classifications would avoid the confusion and (Meng et al., 2009) has categorized fouling into three components as follow;

- Removal fouling – attributed to cake layer formation and can be removed by physical cleaning,
- Irremovable fouling - caused by pore blocking strongly attached foulants which can be eliminated applying chemical cleaning, and
- Irreversible fouling that is permanent fouling, which can't be removed by any of the above approaches.

The irreversible in this case could possibly be the collective contribution of compacted cake or gel layer formation and pore blocking predominated by SMP or EPS.

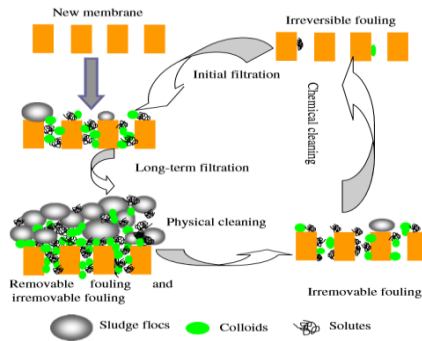


Figure 5. Chart illustration of the formation of the three types of fouling and elimination of removal and irremovable fouling's (Meng et al., 2009).

Similarly, another study also agreed with the approach of three component definitions of fouling and proposed reversible, irreversible and irrecoverable fouling (for the irreversible fouling in Meng et al.) based on the required cleaning methods (Geilvoet, 2010) (fig. 9).

2.5. Membrane Foulants

Membrane foulants is a terminology used to define substances causing membrane fouling in MBR. Substances such as EPS, SMP, dissolved organic matters (DOM), biopolymer clusters (BPC), colloids, sludge flocs, and other inorganic substances are identified as foulant particles (Lin et al., 2014). Several of the studies have focused on different substance as major foulants such as EPS (Fang et al., 2006), SMP (Yoon et al., 2005), colloidal (Koseoglu et al., 2008) and bacterial growth (Vanysacker et al., 2014). Colloids are recognized as primary membrane foulants and are classified as organic macromolecules and rigid inorganic colloids (Lin et al., 2014). Organic macromolecules are the substance like protein, polysaccharides and fluvic compounds whereas rigid inorganic colloids include silica, Alumino-silicate minerals and iron oxy-hydroxide (in aerobic MBR), struvite and calcium carbonate (in Anaerobic MBR). Generally, depending on their biological and chemical characteristics membrane foulants could be grouped into three as bio-foulants, organic and inorganic foulants (Spettmann et al., 2007).

2.5.1. Organic Foulants

Biopolymers in the MLSS and metabolic products of microorganisms namely polysaccharides and proteins, generally described as EPS were identified as major foulants (Fang et al., 2006; Iorhemen et al., 2016; Lee et al., 2007; Meng et al., 2009). Moreover, organic solutes often termed as soluble microbial products (SMP) contributes to the formation of cake due to their larger size relative to

EPS (Wang et al., 2011). Examining the effect of MPE, membrane performance enhancer (Yoon et al., 2005) against SMP as major membrane foulant and their result showed a reduction by half with 100 mg.L⁻¹ MPE addition. Other study identified SMP as soluble EPSs and specified they are subdivided into two as biomass associated products and substrate-utilization associated products (Lin et al., 2014). Clusters of Extracellular polymeric substance and SMP also produces larger organic solutes that easily retained by the membrane and contribute to fouling (Wang et al., 2011).

EPS (polysaccharides and proteins) carries ionizable functional groups such as carboxyl, phosphoric and hydroxyl groups that dissociation of e.g. Carboxyl attains EPS negative charges at near neutral pH; affecting the surface charge usually characterized with Zeta potential (Lin et al., 2014). This might affect the surface charge, which is an important control of the stability of fine particles suspension. Stability of the sludge flocs is mainly controlled by the intermolecular interactions like van der waal, acid-base, electrical interactions, ion bridging, and polymer entanglement among floc structure and EPS plays central role acting as a glue keeping the cells together (Lin et al., 2014). Furthermore, this study indicated EPSs could be seen as the material base or medium of membrane fouling processes in MBRs through which other foulants directly or indirectly contribute to the membrane fouling.

2.5.2. Biofoulants

Biofilm growth on the membrane surface is the main cause of the permeability decline/loss. The populations of microorganisms that are concentrated at the interface (liquid-solid) surrounded by extracellular polymeric slime matrix were defined as bacterial biofilms (Lee et al., 2007). Another study described, the deposition, growth, and metabolism of bacterial flocs as biofouling (Meng et al., 2009) and the fouling components biofoulants. The bacterial attachment to the surface of the membrane leads to the growth of bio-cake and reduce permeability. Biofouling starts with single bacterial attachment and multiplication of bacteria, and their metabolic processes contribute to the fouling described (Vanysacker et al., 2014). A Scanning Electron Microscope (SEM) examination of cake layer morphology portrays that bacteria clusters covered with biopolymers caused a biofouling on the membrane surface (Meng et al., 2007). Moreover, SMP and EPS which are secreted by the bacterial cells enhance the formation of biological foulants and cake layer on membrane surface (Meng et al., 2009).

2.5.3. Inorganic Foulants

Precipitates of some inorganic substances on the membrane surface and pores might cause fouling through hydrolysis that lowers the pH, oxidation and mineral scaling. Investigating the impact of calcium on membrane fouling (Arabi and Nakhla, 2008) indicated, low concentration of Ca²⁺ (280mg.L⁻¹) contributed for cation bridging with EPS, but high concentration (830 mg.L⁻¹) increases sludge retention due to significant precipitation. (Lin et al., 2014) referring to (Choo and Lee, 1996) stated struvite deposition together with organic colloids and flocs (EPSs) played the key role in the formation of strongly attached cake layer restraining membrane permeability. Moreover, (Meng et al., 2007) stated that metal cations Si⁴⁺, Ca²⁺, Mg²⁺, Al³⁺, and Fe³⁺ are the origins of inorganic fouling. Their XRF analysis showed major inorganic elements in the cake

layer were P, Si, Ca, S, K, Fe, Al, and Mg in the order of dominance. (Meng et al., 2009) also summarized that Carbonates of Ca^{2+} , Mg^{2+} and Fe^{3+} can crystalize increasing potential for membrane fouling as CO_2 produced from biological reaction could affect the pH and supersaturation of carbonates. Moreover, Fe^{3+} was found responsible for clogging membrane pores together with organic matter by aiding precipitation of negative charge organic complexes such as DOM, the carboxylic group of Uronic acid and humic acid on to the negatively charged PVDF membrane (Lyko et al., 2007). This may possibly contribute to severe membrane fouling. In addition, Fe^{2+} were also observed to complex with organic matters and produce oxidation resistance complexes even in the presence of dissolved oxygen (Lyko et al., 2007). It could be for this reason that (Meng et al., 2009) stated inorganic fouling could occur through biological precipitation other than chemical precipitation.

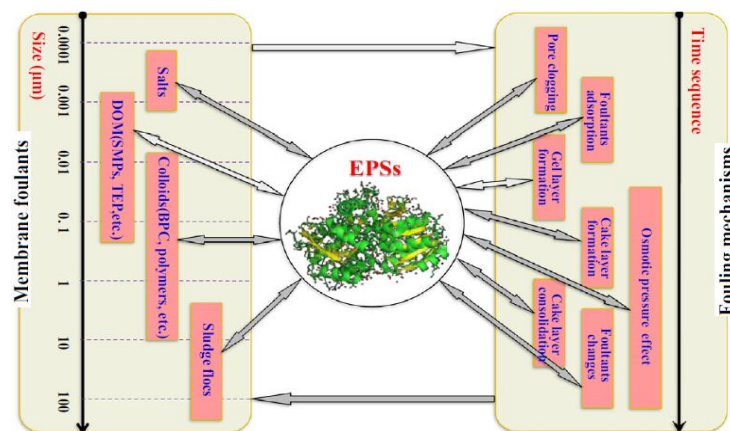


Figure 6. Schematic illustration of the relationship of EPS, membrane foulants and fouling mechanisms in MBR (Lin et al., 2014)

Based on most of the literatures reviewed here, membrane fouling in MBR looks to be governed mainly by organic and bio-foulants than inorganic foulants. A similar observation by (Meng et al., 2009) indicated most researches attributed MBR fouling to deposition of bacterial cells and biopolymers. However, inorganic foulants can sometimes be equally significant contributors as organic foulants to membrane fouling. A study on sludge supernatant polymeric compounds characterization and retention mechanisms in full-scale municipal MBR found metal ions such as Ca^{2+} and Mg^{2+} in the same concentration range in the permeate showing their unrestricted passage through the MBR (Lyko et al., 2007). This study also indicated the examination of the fouled membrane showed the metal ions mainly Fe^{3+} were as significant as the biopolymers and they were not extractable by mechanical stress rather by chemical elution in citric acid. Pretreatment of feed water could reduce inorganic foulants, which in some cases was defined beneficial as the lower concentration of some cations (e.g. Ca^{2+}) support flocculation (Meng et al., 2009).

2.6. Fouling Mechanisms in Membrane Bioreactor

There are different fouling systems in MBR (Fig. 2); pore narrowing, pore clogging, cake formation (Iorhemen et al., 2016) and gel layer formation (Lin et al., 2014). Pore blocking is dependent on the size of the flocs, the membrane opening, and attachment of the substances due to the stickiness of the particles while the cake is formed consequent to continues accumulation of bacteria clusters, biopolymers and inorganic matters on the membrane surface (Iorhemen et al., 2016).

Another study identified cake formation and biofouling are the major fouling mechanism through parameters such as particle concentration (MLSS), particle size distribution, sludge hydrophobicity and sludge viscosity influence membrane filtration performance (Rosenberger et al., 2005). For instance, MLSS concentration $>12\text{g/l}$ increases fouling (Rosenberger et al., 2005).

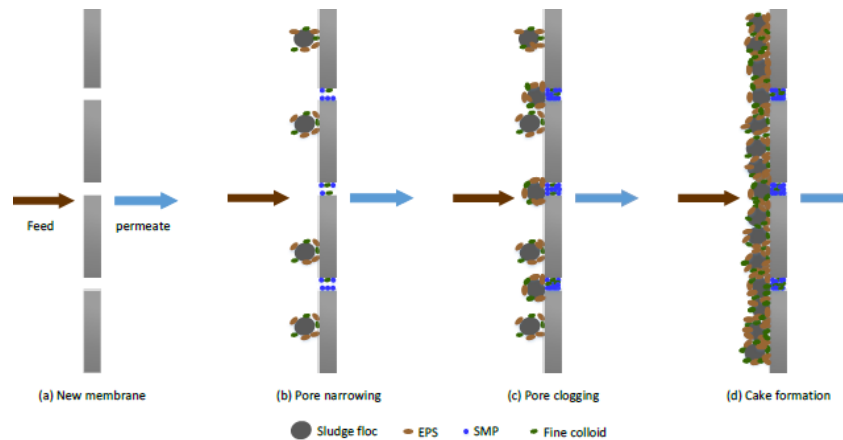


Figure 7. Membrane fouling mechanisms in MBR (Iorhemen et al., 2016)

Different characteristics of mixed liquor such as Viscosity, Extracellular polymeric substance (EPS), particle/floc size, colloidal and soluble organic substance affect the filterability of the membrane.

Concentration polarization defined by the IUPAC, higher level of solute concentration profiling near the membrane surface, was also described as other cause of membrane fouling mechanism (Koros et al., 1996) because of osmotic pressure exerts back transport of solvent from the permeate side that requires higher TMP (Geilvoet, 2010). However, MBR uses low-pressure membranes (MF & UF) that makes it less probable to occur. Hence, it could be summarized that membrane performance/permeability reduction is mostly due to pore blocking and cake layer formation.

2.6.1. Pore Clogging

Microfiltration (MF) and Ultrafiltration (UF) are the two microporous structures mostly used in MBR technology. The working principle is that, foulants larger than the pore sizes (fig. 3) are rejected but smaller particles have the potential to penetrate through. However, some sticky materials attached to the membrane surface in the pores narrow the pore opening leading to

clogging of the pores (Fig. 2a &b). Most soluble organics such as SMP stated (Lin et al., 2014) could enter to the micropores and partly accumulate in the pores due to their sticky properties. They also indicated that the surface properties of foulants and membrane pores, matching of the size, and the amount of predominant effective foulants possibly determines the significance of pore clogging. Similarly, (Wu et al., 2006) identified colloidal and soluble organic substances have a more complicated effect on membrane filterability and fouling by adsorbing to macromolecules and clogging the pores.

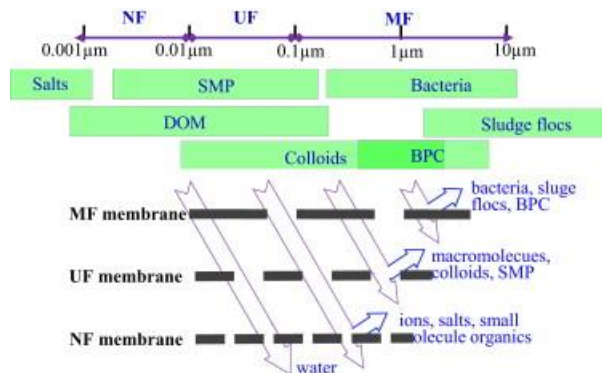


Figure 8. Illustration of size range membranes pores, foulants and filtration processes (Lin et al., 2014). MF and UF are two most commonly used membranes in MBR.

When pores are clogged the transmembrane pressure (TMP) rapidly rises, which is also called TMP jump (Fig. 4).

2.6.2. Cake Layer Formation

Continues operation of MBR and gel layer formation leads to cake layer formation (fig. 2d). indicating EPS as main membrane foulant (Lin et al., 2014) regarded floc adhesion and cake formation as the second stage of membrane fouling in MBR. Moreover, (Yoon et al., 2005) comparatively stated larger microbial flocs bigger than several micrometers hardly deposited on membrane surface but soluble microbial products (SMP) easily do, hence are the major cause of membrane fouling. Accordingly, strong back transport mechanism such as inertial lift, shear-induced migration, and electrostatic repulsion averts larger microbial flocs precipitation on the membrane surface. The components forming the cake layer, however, are constituents that comparatively are larger than the pores; and are present in higher concentration consequent to the high volume of activated sludge in MBR (Meng et al., 2009).

Cake layer formation was suggested as a hydrodynamic and thermodynamic process where the hydrodynamic forces are responsible for the foulant approach to the membrane surface and thermodynamic forces cause the attachment on the membrane surface (Hong et al., 2013; Lin et al., 2014). They added, the thermodynamic interaction between the membrane surface and the foulants are dependent on the distance among them and their surface charges. Moreover, forces such as van der waal (LW), acid-base (AB) and electrical (EL) interactions together contribute to the highly attractive total interaction in MBR but AB interaction contributed most when membrane

and foulant contacted each other, which is attributed to the abundance of functional groups of EPSs (Hong et al., 2013). This indicates that the surface charge and surface tension majorly affects the thermodynamic interaction which determines particle attachment on the membrane and cake formation. In addition, (Hong et al., 2013) indicated the reason why fine particles adhere to membrane surface easily was that they possess higher attractive interaction energy per unit mass as their findings depicted the proportionality of interaction energy per unit mass to the inverse of particle size squared. Selective deposition of foulants and long-term change of cake layer affect the composition as well as characteristics of cake layer relative to the bulk sludge and initial cake sludge (Lin et al., 2014). Long-term changes such as compaction of the cake layer affect the permeability of the layer.

A detailed cake layer characterization was made to define an optimum range of operating parameters for MBR (Meng et al., 2007). Accordingly, two forces mediate cake layer formation namely permeate drag and back transport. The permeate drag a suction from trans membrane pressure encourages particles adherence and back transport was shear stress that alleviates membrane fouling by reducing the cake formation consequence to the lifting effect during aeration scouring (Meng et al., 2007). Therefore, Colloids and macromolecules (biopolymers) contribute significantly to membrane fouling as they readily deposit on the surface by the permeate drag and are difficult to be detached by the low velocity cross flow.

2.7. Factors Affecting Membrane Fouling

Membrane fouling occurs as result of the interaction of feed material and the membrane. Beside to the characteristics of feed material, the membrane material, the module geometry, and the working mode seem to influence the fouling. Hence, factors affecting membrane fouling in MBR are categorized into three as membrane properties, feed material and biomass characteristics, and operating conditions (Iorhemen et al., 2016).

2.7.1. Membrane Properties

Physico-chemical characteristics, affinity towards water and surface charge and roughness are characters through which the membrane contribute to the fouling. The characteristics of membranes differed based on the materials they are made from.

2.7.1.1. *Types of Membranes*

polymeric membranes; the most commonly used membrane, were described to possess good chemical and physical resistance but tend to easily foul due to their hydrophobic nature (Breite et al., 2015; Iorhemen et al., 2016). Hydrophobic membranes appear to easily be affected by adsorption. A hydrophilic Polyvinylidene difluoride (PVDF) with pore size 0.1 μm was made hydrophobic and had half lower critical flux of the hydrophilic PVDF due to adsorption (van der Marel et al., 2010). A possible explanation was that the feed constituents are commonly hydrophobic and tend to accumulate on the hydrophobic membrane. Moreover, different adsorption was observed between two membranes PVDF 0.07 μm and 0.03 μm , which the PVDF 0.07 μm was more hydrophobic and had high adsorption (van der Marel et al., 2010).

The second type called Ceramic membranes (Cembrane) are chemical resistance, inert and hydrophilic, which make them fouling resistance compared to the polymeric membrane (Hofs et al., 2011). They are made from inorganic materials such as oxides of Aluminum, titanium, zirconia and other glassy materials (Mulder, 1996). Nevertheless, their fragileness and fabrication cost was described as uneconomical for MBR application (Iorhemen et al., 2016). Hence, their application was limited to specific circumstance example for industrial waste treatment and anaerobic biodegradation. Recently though, Silicon carbide ceramic membrane was described as the latest evolution of filtration and termed as new generation membrane (Cembrane, 2015). This Cembrane was chosen for this study due to its hydrophilic surface, flat sheet, reduced bio and Oil fouling, the ability for high solid loading, stable operation even in MLSS upsets and longer life (Cembrane, 2015).

The composite membrane is made to combine both the above behaviors to overcome the fouling shortcoming of the polymeric membrane by coating the active surface with a hydrophilic polymer. A study by (Breite et al., 2015) indicated the hydrophobic affinity of membranes attract substance like protein that increasing membrane fouling and suggested treating to hydrophilize the membrane would reduce the effect.

2.7.1.2. *Membrane Surface Charge and Roughness*

Membrane surface roughness and charge are other factors that influence fouling. Rough surface membranes are noted to foul faster as the uneven surface accumulates colloidal particles relative to the even surface. This may influence fouling in two ways; through increased mass accumulation and negatively charged colloids could react with cations such as Ca^{2+} , Al^{3+} and contribute to inorganic fouling (Iorhemen et al., 2016).

Some particles are smaller than the pore sizes of the applied membrane in MBR due to which pore blocking occurs. Therefore, with increased volume of larger pore size there provides a larger chance of pore blocking that increases fouling. When explaining this (van der Marel et al., 2010) defined membranes with larger pores also have larger surface porosities that increase the critical flux and lowers transmembrane pressure whereas pore morphology (structure and interconnectivity) affects the amount of internal fouling (van der Marel et al., 2010). This implies that increased pore size and surface porosity reduces membrane fouling by lowering local flux through the pores, hence, smaller retention of feed constituents. However, Membrane with smaller pores ($\leq 0.1\mu\text{m}$) had lower critical flux explained by faster adsorption of feed constituents and tortuous path in some of the membrane that are responsible to irreversible fouling (van der Marel et al., 2010). Besides, interconnected pore structures fouled slowly due to that permeate can bypass blocked pore via the interconnections compared to track etched straight pores (van der Marel et al., 2010).

2.7.2. *Operational Conditions*

Different operational conditions are applied in MBRs that may not have a direct effect on the fouling but determine the characteristics of the activated sludge. There are two membrane operation conditions in MBR; constant permeate flux with variable transmembrane pressure

(TMP) and variable permeate flux with constant TMP. In the first case, the flow is kept constant while TMP increases in time whereas in later one the flux reduces with time with TMP being fixed. The Constant Permeate flux and variable TMP is commonly practiced in MBR operation where transmembrane pressure (TMP) used as an indicator of the degree of the fouling. In this approach, the flux was below the so-called Critical flux, flux above which excessive deposition of particles and colloid occurs in the membrane surface (Diez et al., 2014). This operational method was chosen for this study too.

2.7.2.1. Critical Flux

Increase in membrane fouling reduces the permeate flux that in turn increases the transmembrane pressure. Since the flow through the membrane is unidirectional and according to (Geilvoet, 2010) could be considered as a laminar flow, the flux might be calculated using Darcy's law for groundwater flow (eq. 2.2).

$$J = \frac{Q}{A} \dots \dots \dots 2.2$$

Where;

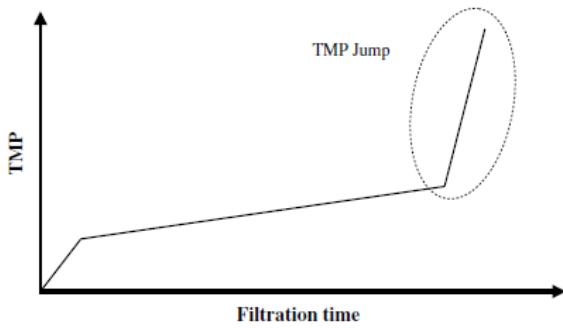
J= flux (m.s⁻¹) for this dissertation L.m⁻².h⁻¹ is used

Q = flow rate (m³.s⁻¹)

A = area of membrane surface (m²)

As membrane fouling occurs gradually the TMP increase accordingly and is normally described as a three-stage process (Iorhemen et al., 2016; Meng et al., 2009). The initial stage also called conditioning caused when the pores start blocking and solute adsorption while further precipitation on the surface of the membrane, pore blocking as well as biofilm causes gradual TMP build up; which is the second stage (Iorhemen et al., 2016).

Successive closure of pores, changes in critical flux values (localized higher flux occur due to uneven blockage of pores) consequent to increase in fouling, and an abrupt change of cake layer structure causes a rapid sudden increase in TMP. This stage is third stage also called TMP jump (Meng et al., 2009), indicates severe membrane fouling and membrane cleaning would be necessary. Several researches on how to reduce membrane fouling (Breite et al., 2015; Fang et al., 2006; Lee et al., 2007; Wu et al., 2006) have been conducted using different techniques that look to influence the fouling development before it reached stage three.



(a) The three-stage increase in TMP is related to fouling progresses before it becomes severe indicated by TMP jump (Meng et al., 2009).

b. Type of Fouling as a function of time and TMP for constant flux operation, and cleaning mechanisms (Geilvoet, 2010).

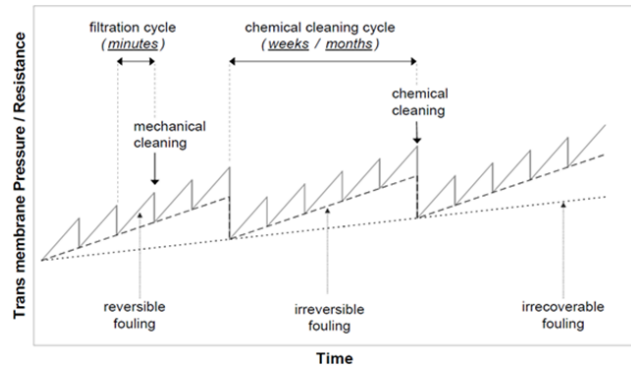


Figure 9. The gradual TMP development (a) and corresponding Fouling stages (b) as function of time for steady flux MBR operation.

Furthermore, there are two modes of flow in membrane operation; dead-end and crossflow. Dead-end filtration allows only one directional flow, the feed material to pass the membrane and retain components that could not pass through. However, crossflow filtration applies two flows perpendicular to each other to produce a shear force that prevents deposition of particles on the membrane surface. With MBR treating a high volume of sludge the tangential (with respect to the membrane) shear force helping reduce fouling and the crossflow filtration method was chosen in this thesis.

2.7.2.2. Temperature

Temperature is a key influence parameter on the efficiency of MBR. Optimum temperature is an important factor for biodegradation but the decline in temperature let occurrence of filamentous bacteria that produce SMP, increased deflocculating releases EPS, lower biodegradation of COD and increase MLSS viscosity reducing shear stress by course bubbles (van den Brink et al., 2011). Deflocculating of sludge flocs also occur due to increase in temperature which is why operating at ambient temperature is so important. Besides, it’s also described temperature impacts membrane filtration through the influence it has on permeate fluid viscosity and can be compensated through the following equation (Le-Clech et al., 2006).

$$J_{C,t} = J_{C,20} * 1.025^{t-20} \dots\dots\dots 2.3$$

2.7.2.3. Aeration

In addition to working mode, aeration rate could also affect fouling both positively and negatively. Increase in aeration aids scouring depositing substance but at higher intensities, it could also break large flocs increasing SMP production (Meng et al., 2009) and increase MLSS. Hence, the positive

effect of aeration could be halt unless the optimum intensity is found. The increase in MLSS accumulation might also lead to higher SRT, which increases sludge viscosity an indication of high matter accumulation that increases fouling.

It has been reported that dissolved oxygen (DO) affects the membrane fouling rate (Lee et al., 2007). Similarly, another study indicated that at lower DO the concentration of SMP increases and these organic compounds are reported to contribute more to fouling than colloids and EPS (Meng et al., 2009). Moreover, another study also defined that low DO in aerobic MBR facilitates the occurrence of filamentous bulking causing more EPS production and sever membrane fouling (Lin et al., 2014). Hence, maintaining constant oxygen flux and/or increasing the SRT lowers the SMP concentration. In this thesis, the Dissolved Oxygen supply through the compressor was assumed to remain constant.

2.7.2.4. Solid Retention Time (SRT)

Solid retention time could affect treatment performance and characteristics of biomass in MBR operation. A study explored effects of SRT on fouling and bacterial structure in MBR and MBMBR operating under SRT of 20, 10 and 5 days. They found that both membranes were less susceptible to fouling when operated at 20 days SRT (Fu et al., 2017). However, operating at shorter SRT, about 5days, appears to affect some bacterial population such as Nitrospira, a nitrifying bacteria. It reduces from 8.4% to 2.3% of the total bacteria at 20 days and 5days SRT respectively (Fu et al., 2017). Similarly, (Ng and Hermanowicz, 2005) investigated performance and characteristics of biomass in MBR at short solid retention time and reported that nitrification completely ceased under SRT below 2.5 days. Furthermore, findings from both studies indicated the concentration of organic matters DOM, EPS, and SMP increased with a decrease in SRT. Controlling solid retention time is suggested as means of keeping the SMP low, (Yoon et al., 2005) however doubted its feasibility due to an occasional upset of biological system and change of flow rate.

Nevertheless, (Fu et al., 2017) depict possible reason for decreased protein and carbohydrate concentration when the SRT was high;

- lower production due to a decrease in growth rate of biomass with increase SRT,
- increased degradation as a result of Lower F/M ratio at high SRT, and
- They were utilized as a substrate to sustain the higher biomass at higher SRT.

However, (Liao et al., 2001) investigated the influence of SRT on sludge hydrophobicity and indicated that surface hydrophobicity increased at higher SRT of 12,16, and 20 days. Change in surface hydrophobicity was attributed mainly to the variation in the protein and total carbohydrate with SRT than total EPS content. Accordingly at lower SRT of 4 and 9 days, the presence of a large amount of carbohydrate contributed to the hydrophilicity whereas proteins (e.g. amino acids) with high hydrophobicity characterize the sludge at higher SRT.

Though increasing SRT enhance membrane performance through reduction of foulants, extremities would have negative effects. Hence, working at very high or low SRT mainly attributed to change in EPS concentration increases membrane fouling significantly (Meng et al., 2009). An increase in EPS was observed when (Ng and Hermanowicz, 2005) increased the SRT from 0.25 to 5 days. Signifying the importance of operating at optimum SRT (Meng et al., 2009) reported favorable SRT for EPS production and membrane fouling control ranges between 20 to 50 days. This implies longer SRT provides time for the microorganisms to breakdown the biopolymers consequently decreasing their concentration. Reduction of biopolymers diminishes the probability of cake layer formation hence membrane fouling. Stating the contribution of MLSS to cake layer formation (Fu et al., 2017) indicated that relatively severe membrane fouling at the shorter SRT with a low MLSS concentration in the MBR.

On the contrary, a different approach with an assessment of reusing organics in wastewater comprehended operating at short SRT as advantageous (Ng and Hermanowicz, 2005). The organic matter in sludge could be digested to produce $\text{CH}_4(\text{g})$ saving energy and giving ecological benefits. From their findings (Ng and Hermanowicz, 2005) indicated that with decreased SRT the amount of EPS declines. Their image from optical microscope showed the abundance of non-flocculating microorganisms and was attributed to the lack of binding substrates (EPS) to form bio-flocs. Furthermore, they explain the presence of high non-flocculating microorganisms was advantageous for organics removal in such a way that the effluent from the MBR operating at extremely short SRT 0.25 days had COD 10.7 mg.L^{-1} (Ng and Hermanowicz, 2005).

2.7.2.5. pH

The nitrification process in the biological reactor produces lower pH which normally is adjusted by feeding alkaline substance. But lower pH contributes to (inorganic) chemicals precipitation that leads to fouling. Adding extra alkalinity would balance the pH, though (Meng et al., 2009) indicated CaCO_3 could precipitate at high pH (8-10). An investigation on the impact of calcium on membrane fouling found that Ca^{2+} concentration $> 800 \text{ mg.L}^{-1}$ might cause substantial fouling but at lower concentration (e.g. 280 mg.L^{-1}) aids binding EPS (Arabi and Nakhla, 2008).

2.7.3. Feed Material and Biomass Characteristics

MBR is different from the conventional membrane because it includes biomass. The characteristics of the wastewater and interaction between the constituent biomass as well as the membrane affect the membrane fouling.

2.7.3.1. Mixed Liquor Suspended Solution (MLSS)

One of the advantages of MBR over the conventional activated sludge process is, it enables the biological process to operate at high MLSS. However, MLSS contains colloids, bacterial flocs, EPS and solutes that are described as major foulants (Fang et al., 2006; Koseoglu et al., 2008; Vanyacker et al., 2014). The concentrations of all these constituents increase with the increase in MLSS. Hence, operating at higher mixed liquor suspended solid by itself is a factor affecting the membrane permeability and increase fouling. (Iorhemen et al., 2016) have summarized that

membrane fouling increases with increase in MLSS due to the subsequent increase in fractions of polysaccharides, proteins, the chance of filamentous bulking, and SMP production.

The higher MLSS also increases the viscosity of the sludge consequently decreasing the shear stress and demand high air scouring. When microbial aggregation occurs due to increase in the bound EPS, it alters the flocculation ability, surface charge, hydrophobicity, and sludge viscosity. as collected by (Geilvoet, 2010) though, MLSS concentration might have a negative, positive or insignificant effect on fouling and inferred MLSS concentration alone should not be used as fouling propensity indication parameter. Nevertheless, a range of MLSS concentration (12 g.l^{-1}) was specified by some studies to indicate an increase in MLSS stimulates fouling (Rosenberger et al., 2005).

2.7.3.2. Extracellular polymeric substances (EPS)

EPS are complex of high molecular weight mixtures of polymers excreted by microorganisms, produced from cell lysis and absorbed organic matter from wastewater (Sheng et al., 2010). Carbohydrates, proteins, humic acids and nucleic acid are main components of these group. Functional groups of these components found to significantly affect the surface characteristics, microbial aggregation properties, adsorption ability and sludge stability (Sheng et al., 2010). Hence, EPS plays a crucial role in the physicochemical properties of microbial aggregates. Since there are many functional groups such as carboxyl (CO_3^{2-}), phosphoric (PO_4^{3-}), sulfhydryl (SO_4^{2-}), phenolic and hydroxyl (OH^-), EPS have a very high binding capacity that influences the surface charge (Sheng et al., 2010). EPS has a tendency to bind with organic pollutants (benzene, toluene, and m-xylene), metal cations like Ca^{2+} and Mg^{2+} , as well as complexing with heavy metals. Adsorption of the later compound may release the cations e.g. Ca^{2+} into the solution which will aid either binding or membrane fouling depending on its concentration (Arabi and Nakhla, 2008; Sheng et al., 2010). The tendency of EPS to adsorb organic pollutants and cations implies EPS are amphoteric; possess hydrophobic mainly protein and hydrophilic the carbohydrate groups (Lin et al., 2014; Sheng et al., 2010).

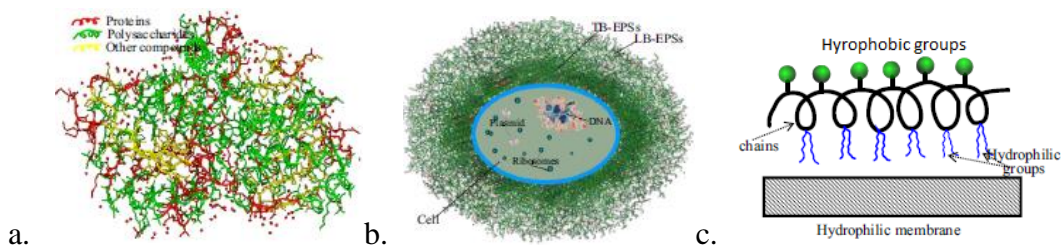


Figure 10. Schematics of EPS components (a), EPS cell structure (b), and adsorption of EPS on Hydrophilic membrane (c) after (Lin et al., 2014)

This also indicates the EPS plays a key role in thickening and dewatering processes of the sludge. Pressure filtration is used as a means of sludge dewatering in this study and the specific resistance to capillary suction time characterizes the dewaterability of the sludge. The increase in EPS was described to contribute for poor sludge dewaterability because of the following reason (Sheng et al., 2010).

- due to the steric force EPS generate prevents contact between cells
- EPS causes retention of much water in the sludge flocs consequently increasing interstitial water in the flocs. And
- The stable gel EPS form prevents water seepage from the pores of flocs deteriorating dewaterability of the sludge

Therefore, removal of the EPS would increase the dewatering ability of the sludge. However, a study suggested the concentration EPS determines whether to enhance or deteriorate dewaterability of a sludge (Houghton et al., 2001). The binding property of the sludge aids flocculation thereby thickening the sludge by bringing the flocs together, which implies lower EPS content improves sludge dewaterability. Whereas, a further increase in EPS content increases the retention of more water consequent to the above listed three reasons that decline dewaterability of the sludge (Houghton et al., 2001; Sheng et al., 2010). Therefore, it could be summarized that EPS have the higher contribution to membrane fouling.

2.7.3.3. *Properties of Sludge Flocs*

Sludge floc size, surface charge, and surface roughness are the different properties through which sludge flocs affect membrane fouling.

2.7.3.3.1. *Floc size*

The feed MLSS comprises different fractions of sludge floc size and looks that smaller flocs play important role in membrane fouling. Small flocs include microorganisms, colloids, bound EPS, and cell debris (Lin et al., 2011). A study on cake characterization conducted particle size distribution analysis on suspended sludge and found macromolecule matter and colloids particles dominating (Meng et al., 2007). They supposed these particles could penetrate into the membrane pores easily and cause severe pore blocking. another study which investigate characteristics of different fractions of small and large size sludge flocs and their role in membrane fouling, indicated the small flocs possess higher bound EPS and a fraction of dimension than the large flocs (Lin et al., 2011).

Constituents of activated sludge subject to membrane filtration are normally categorized as suspended solids ($>1\mu\text{m}$), Colloids ($0.01 - 1\mu\text{m}$) and solutes ($<0.01\mu\text{m}$) and fouling is the collective effect of all these particles. Small flocs account fewer amounts of the bulk sludge however they seem to take major responsibility in membrane fouling. This was demonstrated by the filtration resistance of cake layer in MBR $10^{14} \text{ m.kg}^{-1}$ (Ping Chu and Li, 2005) compared to that of activated sludge $10^{11} \text{ m.kg}^{-1}$ (Buyukkamaci, 2004) as summarized in (Lin et al., 2011). Smaller size flocs easily penetrate into pores and adhere to the membrane surface. The tendency of small flocs to adhere to the surface of membrane was reported as result of deriving hydrodynamic force, the lesser effect of back transport force on these particle and thermodynamic interaction causing the binding (Hong et al., 2013; Lin et al., 2014). Provided hydraulic forces forward both large and small particle sizes, and a decrease in energy barrier with an increase in floc size (Shen et al., 2015) suggested that larger particles get closer to membrane surface more

easily in contrary to many studies that submitted hydrodynamic forces were responsible for smaller particles to adhere easily.

However, they demonstrate the reason was that once small flocs attached to the membrane or are at a short separation distance, $<2.5\text{nm}$ as their experiment show, they are difficult to detach or transport back by aeration. This was similar to the findings of (Meng et al., 2007) that indicated particle size $<50\mu\text{m}$ could easily deposit on membrane surface worsening membrane permeation while larger particles could be detached because of the aeration. Besides, (Hong et al., 2013) depicted the proportionality of interaction energy per unit mass to the inverse of particle size squared explains the smaller flocs are important parts of the cake layer on the membrane surface. This implies the ease precipitation of fine particles due to the higher attractive interaction energy per unit mass.

From filtration test (Lin et al., 2011) demonstrated that the small flocs fraction liquor had six times larger specific resistance ($1.26 \times 10^{14} \text{m.kg}^{-1}$) than larger flocs liquor, indicating the larger responsibility of small flocs for high cake layer filtration resistance. They also indicated that the cake layer formed from the small flocs had lower porosity implying the high fouling effect. Moreover, this study identified small flocs had high bound EPS, denser structure (as result of EPS bridging) and very diverse microbial community that possibly affect the characteristics of these flocs.

As thermodynamic interactions are functions of the separation distance between the membrane and foulants indicating membrane surface roughness can affect the energy of interaction by extending the distance in rough surfaces membranes (Lin et al., 2014).

Particle size distribution analysis made in a study investigating the impact of floc size in membrane fouling revealed that sludge flocs in sludge suspension had the size above a micrometer (Shen et al., 2015). They observed that floc size had minimal effect on membrane fouling due to low pore clogging fouling following the match between the membrane pores $0.3\mu\text{m}$ and flocs size $>1\mu\text{m}$. Hence, it could be understood that the relationship between particle size and membrane pore size was the major factor for pore clogging.

it was also suggested that Comparatively small flocs foul membranes severely than larger flocs as they form denser cake layer leading to higher specific cake resistance (Lin et al., 2011; Meng et al., 2007). This possible explanation was because smaller flocs form cake layer with small pores and low permeability, and particularly when biopolymer clusters (BPC) present in the pores creating a large binding site for counter ions rising Osmotic (pressure induced) resistance (Shen et al., 2015).

2.7.3.3.2. Surface charge

Zeta potential of sludge flocs is generally measured based on electrophoretic mobility in an electric field using zeta analyzer. For sludge flocs, zeta potential was reported between -50mV to -10mV in MBR (Lin et al., 2014). Proteins, humic acids, uronic acids, and nucleic acids in EPSs carry abundant ionizable functional groups, which are the source of surface charge. There are two

methods of measuring surface charges of sludge flocs, namely; dye exchange titration and colloid titration. The surface charge of sludge is determined by the ionizable groups present on the sludge surface and was defined as proportional to the ratio of EPS components; protein to Carbohydrate (Liao et al., 2001). Operational SRT affects the concentration of these components, which determines the hydrophobicity/hydrophilicity of EPS and surface charge. The significance of the ratio of protein to carbohydrate in determining the surface charge could possibly be explained by the unique charge properties of proteins. The amino acid group carries positive charges which could neutralize the negative charges from the carboxyl and phosphate groups decreasing the net negative charge of the sludge flocs (Liao et al., 2001). Hence, the implication of these outcomes are that EPS content affects the surface charge hence the flocculating ability of the sludge. Due to significant dissociation of functional groups in EPSs at higher pH, the absolute value of EPS surface charge increase with pH (Lin et al., 2014). It's also stated that excess growth of filamentous bacteria causes extra EPS release and increase the zeta potential of sludge flocs (Meng et al., 2006).

2.7.3.3.3. *Salinity*

MBRs are used to treat Industrial wastewater, which has large amount of salt. Additionally, the presence of large number of cations such as Ca^{2+} , Mg^{2+} , Al^{3+} and Fe^{3+} and anions; PO_4^{3-} , SO_4^{2-} , CO_3^{2-} and OH^- in the feed water create concentration polarization that leads to high concentration of retained salt on the membrane surface (Meng et al., 2009). A study investigated the effect of salinity on biomass and membrane fouling and identified an increase in membrane fouling with salinity but microbial diversity reduces due to the death of microorganisms that contribute to the increased turbidity (washout of solids and dead biomass) in the effluent (Jang et al., 2013). They demonstrated this by increasing the salt concentration from 5 g.l^{-1} – 20 g.l^{-1} , which reduced the time TMP (27kPa) reached critical flux by half from 132h to 60 h. The same study infers that high amount of EPS were released under high salt concentrations attributed to plasmolysis, the release of intracellular constituents and accumulation of incomplete degradation of organic substances (Jang et al., 2013). Therefore, increase in salinity accelerates membrane fouling. Another observation in this study was, Increase in salt concentration reduced Zeta potential consequent to increased carbohydrate content and significantly increased the floc sizes. This implies high salinity altered biomass characteristics (more EPS produced for self-defense), floc size and zeta potential, increased pore blocking resistance and reduced filtration eventually resulted in increased membrane fouling (Jang et al., 2013).

2.8. Fouling Reduction Techniques

Different techniques were applied to reduce membrane fouling; increase air bubbles to reduce settling on the membrane, periodic backwashing to improve permeability, adding flocculation-coagulation agents to aggregate the colloidal fraction and reduce internal clogging of the membrane (Bouhabila et al., 2001). Testing four different membranes, Hofs et al. find that the least backwashing required for irreversible fouling was best in a polymeric membrane. The finding was not statistically significant, however such factors as pore size is more decisive for level of TMP (Hofs et al. 2011).

Some studies focused on reducing the cake layer to control fouling, as it was seen major flux resisting factor (Chang and Lee, 1998; Hwang et al., 2007; Lee et al., 2001). Colloidal and solute organic substances were identified as important fractions to cause membrane fouling by adsorption of macromolecules and progressive pore clogging (Wu et al., 2006). Hence, adding adsorbents or coagulants were sought as possible solutions.

2.8.1. Adsorption

Improvement of the mixed liquor by adding powdered activated carbon (PAC) was applied in an attempt to control membrane fouling. Addition of PAC to MBR forms the biological activated carbon (BAC), which cause significant uptake and entrapment of soluble organics as well as colloids. A study on biofouling mitigation using PAC and cationic polymer specified, PAC addition facilitated adsorption and flocculation of dissolved organics, fine particles, and colloids (Khan et al., 2012). Moreover, PAC modifies the sludge characteristics and the composition as well as permeability of cake layer on the membrane. Their findings also shown that PAC exhibited the highest sorption of EPS with 40% capacity, which 66% of removed was Carbohydrate (Khan et al., 2012).

Another study by (Fang et al., 2006) investigated the effect of activated carbon on fouling reduction and found out strong adsorption of EPS to Virgin activated carbon (AC_v). The AC_v reduces the film filtration resistance by about 22% (6.4×10^{12} to $5 \times 10^{12} \text{ m}^{-1}$) from the control (Fang et al., 2006). They have also specified polysaccharide and humic substances affect the filtration resistance, particularly polysaccharides because of their ability to penetrate through to the pores and cause fouling. Since, polysaccharides are sought as major foulants for MF/UF, using ceramic membrane suggested as means of significantly reducing from organic fouling (Hofs et al. 2011).

2.8.2. Coagulation

Coagulation is a common practice in water and wastewater treatment industries for removal of colloidal and soluble organic fractions by aggregating the particles to larger flocs. In wastewater, salts of aluminum and Iron have been used with prime treatment objective of particle and Phosphate removal (Ødegaard et al., 1992). Similarly, another study stated, coagulants are widely used to remove natural organic matter and suspended solids through sweep floc, charge neutralization and bridging (Wong et al., 2016). The dosing of coagulant in MBR system would normally be greater than water and wastewater treatments.

Colloids are the major fouling components, coagulating/flocculating the activated sludge and binding the colloids and other MLSS possibly enhances the filterability. Quoting other studies (Koseoglu et al., 2008) showed several laboratory experiments were done to determine the effect of different chemicals on enhancing flux/filterability and reduction of fouling. Among all, the coagulating/flocculating method was promising as it reduces the foulants soluble substance in the bulk phase. Moreover, the study also indicated cationic polymers were found effective due to their influence on extracellular polymer substance (EPS) in addition to the activated sludge.

Another study compared polymeric (PFS and PAC) and monomeric ($\text{Al}_2(\text{SO}_4)_3$ and FeCl_3) Aluminum and ferric salts to investigate their effect on mixed liquor and fouling control. Applying dosing of 0-3mM of AL and Fe per liter, they found the polymeric coagulants (PAC and PFS) effectively improve filterability and reduce the supernatant organic fractions (Wu et al., 2006). The polymeric coagulants supply more positive charges for the organic fractions and form larger flocs by charge neutralization. Furthermore, the addition of the coagulants delayed the TMP increase as the growth of foulants decelerated, stable foulants are removed from the membrane surface and cake layer formation was restrained. A TMP surge delay for 5-30days was found out with the addition of 30 -100mg.L⁻¹ membrane performance enhancer (Yoon et al., 2005). Their result also showed that an average decrease of polysaccharide concentration from 41mg.L⁻¹ to 21mg.L⁻¹ when 100 mg.L⁻¹ coagulant was added. Wu et al also noted that Al-salts had higher organic substances removal about 73% and this was due to that Al- salts were removing substance by bridging in addition to charge neutralization. Their findings show that coagulant addition has increased sludge filterability, sludge floc properties (e.g. enlarged the floc size), and lowered the supernatant organic substance content. They indicated that the PFS was more effective in fouling control with a dosing rate of 1.0 mM of Fe (Fig. 3).

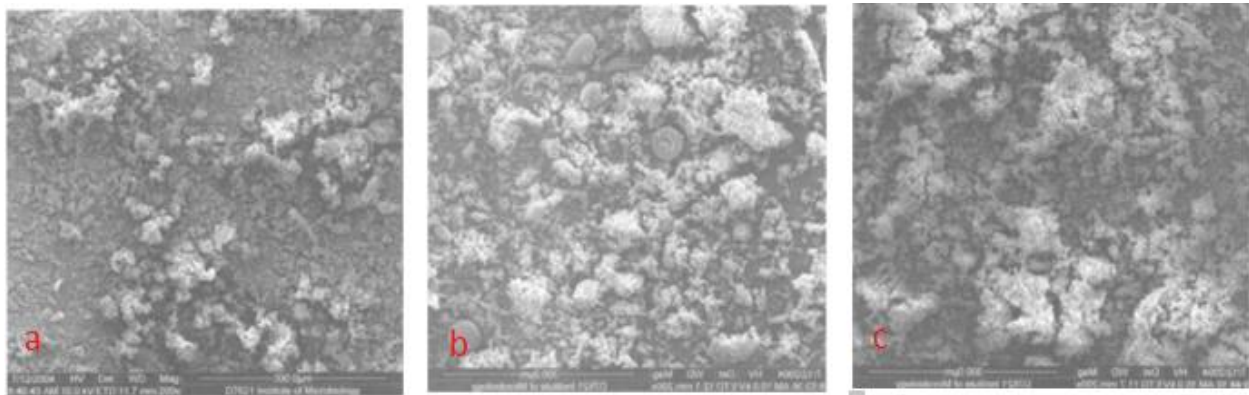


Figure 11. SEM (200x) Images illustrating the change in sludge flocs after addition of coagulants: (a) without coagulant addition; (b) with PAC addition; (c) with PFS addition (Wu et al., 2006).

pH decreases with the increase of coagulant addition. When pH lowers below 6.0 it could affect the quantity, species, and activity of microorganisms as well as the hydrolysis products of coagulants and mechanism of coagulation (Wu et al., 2006). They measured Zeta potential to determine the interaction between the added coagulants, sludge flocs, and supernatant organic matter that expresses the stability of the colloids. It was found that the Zeta potential increased towards the positive charge indicating the negatively charged colloids were neutralized by the hydrolyzed coagulants (Wu et al., 2006). Comparatively, it showed the ability of the polymer coagulants to deliver positive charges was higher as they rank the coagulants in such a way $\text{PFS} > \text{PAC} > \text{Al}_2(\text{SO}_4)_3 > \text{FeCl}_3$. When the coagulants added, positive charges are generated consequent to the hydrolysis process. Adsorption of the positive charges on the surface of flocs and neutralizing the negative charges weakens the repulsion between flocs and colloids causing

flocculation. Consequently, flocs became larger in size than the pore opening increasing filterability (Wu et al., 2006). Therefore, the more positive charges the coagulant supplied, the higher coagulating ability and the lesser chance of membrane fouling.

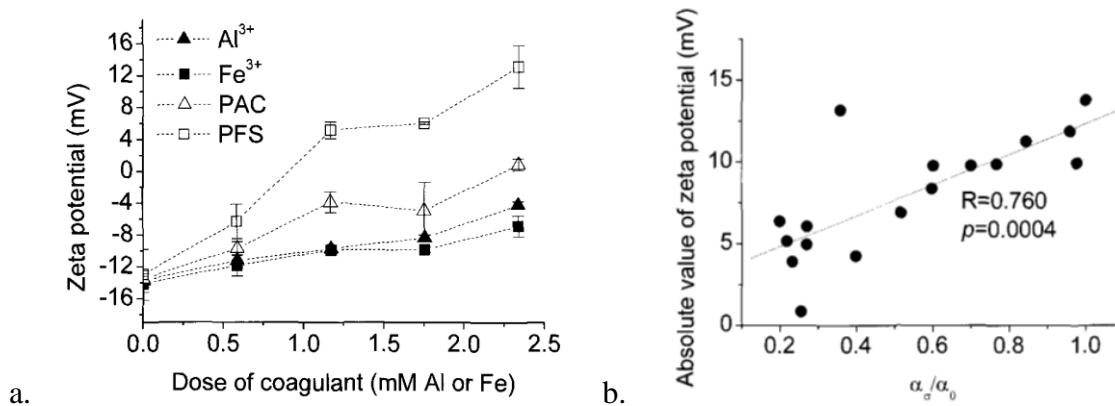


Figure 12. The change in charge neutrality (a) and specific resistance to filtration/filterability with as a function of coagulant dose (Wu et al., 2006).

From their findings (Wu et al., 2006) described that addition of cationic polymers has a great effect on membrane fouling reduction by restraining gel layer formation, remove foulants from the membrane surface, and decelerate development of foulants. Similarly, (Lee et al., 2007) stated the recently developed cationic polymers have a significant impact on membrane fouling reducers (MFR) though how the MFR reduces the fouling was not clarified yet. Hence, they analyze changes in biofilm architecture to elucidate how MFR mitigates membrane fouling. Accordingly, the addition of MFR creates larger flocs through flocculation of activated sludge, lower attached biomass on the membrane surface and higher bound EPS that eventually enhance the filterability.

Altering the surface property of the membrane itself was also considered as one means of membrane fouling reducing mechanism. Most membrane bioreactors are hydrophobic in nature. A study on membrane surface charge hinted hydrophobic reaction (e.g. with proteins) could precipitate fouling layer that decline the membrane performance (Breite et al., 2015). Hence, they suggest hydrophilizing the membrane by either grafting, electron beam irradiation or plasma treatment could increase the membrane fouling resistance consequent to the water film built up on the membrane surface repelling hydrophobic foulants.

It looks that finding sustainable membrane fouling mitigation strategies in MBRs has been one of the main concerns for over the last two decades and still ongoing research. Hence, this study was also conducted to investigate the influence of charge driven mechanism of coagulation on sludge characteristics and membrane fouling. Monomeric coagulants like FeCl₃, alum and polymers of both iron, and aluminum (PFS & PAC) were identified as effective in enhancing membrane filterability and limit membrane fouling (Wong et al., 2016; Wu et al., 2006). Hence, aluminum-based coagulants were considered in this study and the mechanism how the chemical affects the fouling are given below.

- Using Zeta potential as a measure of positive charge supply, the PFS from the polymers and Alum from the monomeric coagulant showed a better charge neutralization effect.
- Aluminum salts were identified as effective in removal of TOC compared to Iron salts (Wu et al., 2006) and removal of TOC has a positive effect on fouling reduction due to lowering of macromolecules organic matter that contributes to gel layer formation.
- To keep the pH around neutral (Wu et al., 2006) suggested an optimal dosage of 1.6 and 3.0 mM Al for Alum and PAC, 1.4 and 2.2 mM Fe for FeCl₃ and PFS respectively. Their result showed relative high pH reduction with Iron based coagulants. Furthermore, from an economic point of view lesser chemical is used in the monomeric coagulants. Besides, another study also showed charge neutralization occur at alum dosing of less than 0.1mmol/l where increasing further cause sweep flocculation (Li et al., 2006).

Table 1. Shows the mechanism how the different reagent types influence the fouling factors and enhance filtration

| Reagent type | | Mechanism of fouling reduction |
|-----------------|--|---|
| Monomeric | Al ₂ (SO ₄) ₃ .nH ₂ O | <ul style="list-style-type: none"> - Increase sludge floc size and reducing fractional dimension – Charge neutralization & bridging (Li et al., 2006; Wu et al., 2006) floc fractional dimensional decrease in such order Sweep floc > charge neutralization > bridging (Li et al., 2006) - Cake porosity increase and specific resistance decline – Reducing cake and gel layer formation (Lee et al., 2007) |
| Pre-polymerized | PAX | <ul style="list-style-type: none"> - Reduce the fractions of organic pollutants (EPS & SMP) through Increase sludge floc size and filterability – Charge neutralization (Wu et al., 2006) - |

- Alum was chosen in this study because of its cost effectiveness and relatively better in bridging than Fe-based coagulants.
- The more positive charges the coagulant supplied, the higher coagulating ability and the lesser chance of membrane fouling. However, in this study we want to keep the flocs in suspension that means settling is not required and hence pre-polymerize coagulants wouldn't be a choice.

Membrane relaxation, backwashing, intermittent aeration chemical enhanced backwashing and maintenance cleaning are other fouling controls through enhancing the filtration processes.

2.9. Alum

Alum, believed first mentioned by Pliny, has been applied for water purification since ancient time around 77 AD (Duan and Gregory, 2003). Effect of different concentration of alum was evaluated by applying 1 g.L⁻¹, 3 g.L⁻¹ and 5 g.L⁻¹ for enhancement of membrane fouling control (Wong et al., 2016). Accordingly, MBR with low alum concentration of 1 g.L⁻¹ was found to have better filterability performance which was attributed to the agglomeration of flocs and biodegradation mechanism.

Sodium aluminate (NaAlO₂), aluminum sulfate (Alum: Al₂(SO₄)₃), and poly-aluminum chloride (PAC) are the most commonly used form of aluminum-based coagulants. Application of aluminum and coagulant in general increases the sludge volume. (Wong et al., 2016) indicated that an increase in MLSS with increasing dosage of alum, 5 g of Alum per liter addition being the highest. They also have summarized that excessive alum possibly retards the growth of filamentous bacteria leading to subsequent floc size reduction which they have also observed in their results. Hence, they suggest the early increase in TMP in the reactors where high (3 & 5 g.L⁻¹) alum was added might be due to the attachment of smaller particles to the pores of membrane surface following the increment of MLSS.

Therefore, it could be said that addition of excess alum contributes to membrane fouling through the effects it induces on the concentration of MLSS, pH, and EPS (Protein and Polysaccharides) concentration instead of reducing the problem based on (Wong et al., 2016) evaluation of the effects of alum on membrane fouling. It was reported that alum has high COD removal capacity which was attributed to the adsorption and binding effect (Wu et al., 2006). Similarly, (Wong et al., 2016) found the highest removal of the COD at a low concentration about 1 g.L⁻¹ alum compared to the others due to the binding ability of alum which provides simultaneous agglomerating and biodegradation effects. The mechanism of Alum application selected for this study was batch dosing, where a concentration range of 1-7 mmol Al.L⁻¹ was applied.

2.10. Mechanism of Coagulation in Wastewater

Addition of coagulant reagents produces metal ions and hydroxides through hydrolysis which leads to chemical precipitation of dissolved substances. Three mechanisms of coagulation are reported responsible for removal of organic matter and suspended solids in water and wastewater treatment; namely charge neutralization, sweep flocs and bridging (Li et al., 2006; Wong et al., 2016). A study on Coagulation–flocculation mechanisms in wastewater treatment plants through zeta potential measurements applied coagulant to create chemical precipitation of metal hydroxide, which was possible through the following general reaction (López-Maldonado et al., 2014).



The Mⁿ⁺ stands for metal ion and M(OH)_n represents the precipitating Metal hydroxide. But In this case the equation could be rewritten;



Where $\text{Al}(\text{OH})_n$ represents Aluminum hydroxide $\text{Al}(\text{OH})^{2+}$, $\text{Al}(\text{OH})_2^+$, $\text{Al}(\text{OH})_3$, and $\text{Al}(\text{OH})_4^-$ in order of increasing pH.

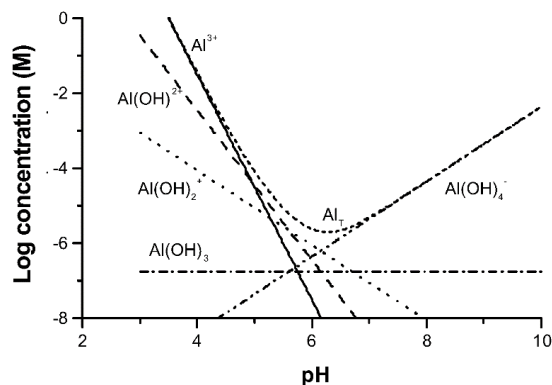


Figure 13. The concentration of monomeric hydrolysis products of Al^{3+} in equilibrium with the amorphous hydroxides, at zero ionic strength and 25°C (Duan and Gregory, 2003).

Defining charge neutralization of negatively charged colloids and incorporation of impurities in an amorphous hydroxide precipitates as two distinct mechanisms of coagulation, (Tang et al., 2015) stated the significance of both mechanisms depends on pH and dosage. Conducting series of laboratory experiments (Chowdhury et al., 1991) have also inferred the rate and stoichiometric aluminum hydroxide precipitation depends not only on pH and Al dosage but also HCO_3^- , SO_4^{2-} and natural organic matter concentrations (NOM) concentrations. Their observation showed the OH to Al ratio (OH/Al) increased in presence of NOM at pH 6.5. The ratio also increases with pH; stoichiometry of $\text{Al}(\text{OH})_2^+$, $\text{Al}(\text{OH})_3$ and $\text{Al}(\text{OH})_4^-$ where observed in the order of increasing pH at 5.5, 6.5 and 7.5 respectively (Chowdhury et al., 1991). In addition, they also discussed, the HCO_3^- and SO_4^{2-} increase the rate of Al complexation with naturally occurring ligands through increasing $\text{Al}(\text{OH})_2^+/\text{Al}^{3+}$ ratio.

Besides, the low solubility of aluminum contributes to increasing dosing that leads to excessive aluminum hydroxide precipitation. The availability of excessive aluminum hydroxides might indicate, sweep flocculation could be the main aluminum coagulation mechanism. A study on floc characterization at various coagulation mechanisms indicated low dosage causes particle destabilization through charge neutralization. However, the addition of sufficiently high metal salt cause precipitation of metal hydroxides which possibly enmesh colloidal particles on their way down (Li et al., 2006). Similarly, (Tang et al., 2015) described the addition of aluminum salts in to water cause hydrolysis reaction to occur as result of aqueous chemical equilibrium and transformation of the monomers, dimers, and trimers into oligomers and polymers. Accordingly, this hydrolysis polymerization stage reaches a strength of obstruction of further access of clusters and reduction of the net charge of polymers due to hydroxylation which causes precipitation (fig.6). (Tang et al., 2015) have also indicated that Alum adsorbs mainly with the precipitate of amorphous $\text{Al}(\text{OH})_3$ by attraction and adhesion.

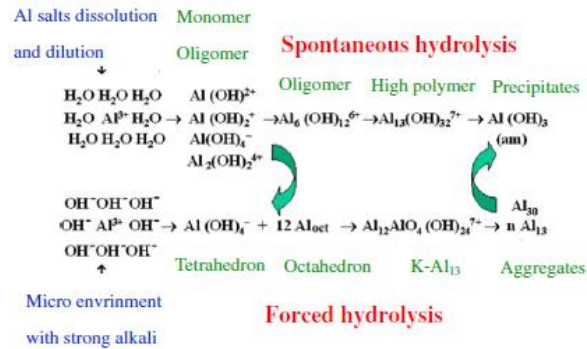


Figure 14. Illustration of the dilution, hydrolysis, and polymerization of Al^{3+} (Tang et al., 2015).

Generally, it could be described that coagulation by addition of Al occurs as result;

- *Charge neutralization of negatively charged colloids by cationic hydrolysis products*
- *Incorporation of impurities in an amorphous hydroxide precipitates (Sweep flocculation) through adsorption, aluminum-ligand complexation, co-precipitation.*
- *Adsorption of polymer chain on more than one particle links the particles and form Bridging.*

The properties and fractional dimensions; size, structure, and strength of flocs formed under the different flocculation mechanisms were stated to be different (Li et al., 2006). This study stated that floc size was the balance between growth and breakage implying the positive relation between floc size and strength with respect to shear strength. Their result showed that floc strength in an increasing order charge neutralization, sweep floc and bridging; indicating the physical bonding between the polymers chain is tighter relative to the flocs formed through charge neutralization. Moreover, flocs structure through sweep flocculation was most compact whereas the flocs structured as result of bridging were loosest (Li et al., 2006).

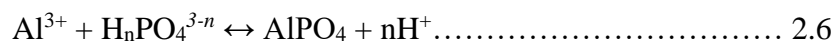
In this study treated MBBR-MBR mixed liquor parameters were measured and compared to analytical predictions of using alum coagulants to reduce fouling by influencing charge, hydrophobicity, and size of sludge flocks. The addition of Alum encourages the formation of larger particles by agglomeration of colloids and smaller particles, neutralize the net surface charge by delivering cations and hydroxyl functional groups with positive surface charge, and enhance the dewaterability of the sludge through increased release of molecularly bound water consequent to coagulation. Hence, the fouling factors are influenced in such a way that particle size increases so that they don't fit the pores, sludge hydrophobicity property increases, the net surface charge increases towards zero and mixed liquor suspended solids is also expected to increase with the increasing dose.

The study takes into account that high reagent addition lowers the pH which in-turn affects the biomass, might increase precipitation of aluminum and particularly for this experiment suspension of particles is main interest. Therefore, the Concentration of the coagulant is kept low. (Wong et al., 2016) stated that the performance of membrane bioreactor was improved as the concentration

of the reagent was low, around 1g/l. this study added that high addition of Alum reduced the particle size, which was contrary to their expectation; and increased MLSS with dosing. Therefore Fouling is inevitable in MBR process and the membrane filterability will decrease consequently, which cause pressure build up and the TMP to increase with time. I contemplate the addition of the MFR would extend the time of the rise in TMP significantly, possibly doubled. To conclude with, the analytical results are expected to signify the effectiveness of alum as MFR by influencing the above fouling factors as described.

2.11. Ortho-Phosphate

The release of phosphorus to the environment is nowadays seen carefully as its limiting nutrient for the growth of photosynthetic algae and cyanobacteria. The Phosphorus content of municipal wastewater ranges 5-20 mg/l and synthetic detergent was identified as main source (Lenntech, 2018). The average contribution of inhabitants estimated about 2.8 g/inhabitant. Feasibly uncontrolled release of phosphorus from households and treatment plants could damage the ecosystem enhancing blossom growth of plants and microorganisms namely called Eutrophication. Hence, it has to be removed from the effluent discharged to the environment to prevent Eutrophication and should be recovered as a resource for food growth. In water treatment, this is often done chemically and most recently biologically or simultaneously. The first method uses aluminum and iron Oxy-hydroxides and aluminum-based coagulants are most extensively used in wastewater treatment. Addition of $Al_2(SO_4)_3 \cdot nH_2O$ form $Al(OH)_3$ through hydrolysis and adsorb soluble phosphorus in its structure (Omoike, 1999). This study added that orthophosphate is removed from solution as aluminum hydro-oxy phosphate. The reaction between alum and phosphate occurs in such a way (Lenntech, 2018);



The above reaction implies effectiveness of Phosphate removal depends on the existing pH. An experimental study described the occurrence of low ion exchange on to aluminum oxy-hydroxides at acidic and alkaline pH (Tanada et al., 2003). They observed greater adsorption at pH 4. The same study also indicated that aluminum oxy-hydroxide selectively adsorb phosphate ion and this affinity makes the reagent suitable for phosphate removal (Tanada et al., 2003). Accordingly, its expected substantial concentration of aluminum might be used up by phosphate in the experiment. Orthophosphate and polyphosphate are the two forms of phosphate found in aqueous solution. Orthophosphate is an interest for this dissertation since orthophosphate is available for biological metabolism without further breaking down (Lenntech, 2018). The current standard limit for Total Phosphorus in wastewater effluent being required $\leq 1 \text{ mg.l}^{-1}$ (EU-UWWTD, 1991). Hence, the target in this experiment is to lower the Phosphorus (P) concentration in the solution below 0.3 mg P.l^{-1} , a typical P release in most Norwegian wastewater treatment plants (Rusten and Ødegaard, 2007).

3. MATERIALS AND METHODS

In this chapter, the materials used for the purpose of this study are described briefly and so are the methods.

3.1. BF-MBR Mixed Liquor and the Conventional Activated Sludge

Mixed liquors used for this study was sampled from the MBR chamber in the BF-MBR pilot plant for marine boats wastewater treatment study, and from returning mixed liquor suspended solids of AS reactor at Bekkelaget (BEVAS), Oslo’s biggest wastewater treatment plant. A source separation wastewater collection system transports the gray and black water into the tank before BF-MBR pilot plant. A mixture of 10% black water and 90% Grey water flow into the BF-MBR chamber. However, the collection system in BEVAS combines all household wastewater and stormwater together.

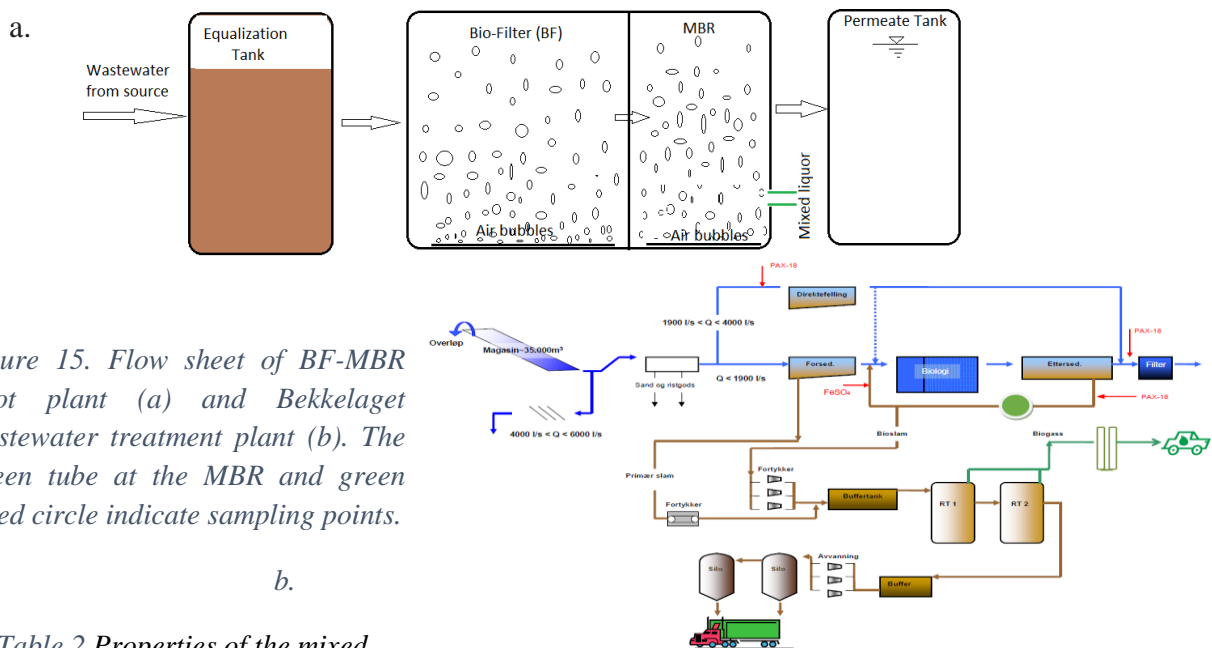


Figure 15. Flow sheet of BF-MBR Pilot plant (a) and Bekkelaget Wastewater treatment plant (b). The Green tube at the MBR and green dotted circle indicate sampling points.

Table 2. Properties of the mixed liquor from BF-MBR and Activated Sludge from Conventional Process used for this study

| Parameters | Ranges | |
|--------------------------|-------------|------------|
| | BF-MBR | AS |
| SS (g. L ⁻¹) | 3.53 | 4.72 |
| pH | 6.63 – 7.04 | 7.21 -7.36 |
| Zeta potential (mV) | -14.2 | -8.3 |
| Turbidity (NTU) | 91.1 | 29.7 |
| Viscosity (mPa.s) | 1.05 | 1.11 |
| D _m (µm) | 0.56 -117 | 0.56 - 200 |

3.1.1. Determination of Sludge Parameters

30 ml Supernatant was collected and filtered through a 0.45 μ m filter. The filter paper was rinsed with deionized water, dried in an oven for 30 min at 105 °C and weighed. After a dead-end flow filtration, the suspended solid retained on the filter paper were weighed once dried in an oven for 2hrs at 105°C. Hence, the concentration of the MLSS was determined by the difference between the weight of the mass retained and filter paper dividing to the sampled volume of Solution (e.q. 3.1).

$$MLSS = \frac{M_2 - M_1}{V} \dots\dots\dots 3.1$$

Where;

M_2 – Weight of filter paper and Suspended solids after drying for 2hrs at 105 °C

M_1 – Weight of filter paper after drying in oven for 30 minutes (105 °C)

V – Impute volume of solution for filtration (in this case 10ml)

Detail properties of the mixed liquor sampled from BEVAS and the pilot plant are listed in Table 2.

3.2. Membrane Type and Characteristics

Flat sheet silicon carbide membrane (SICFM-00145) were used for this experiment. The Cembrane is a hydrophilic material, chemically inert and has excellent recovery rate. The applied flux rate was 50LMH and the membrane was backwashed after every step of the experiment for 5 minutes. The membrane characters and operation conditions are described in table 3.

Table 3. Membrane properties and operation condition

| Membrane Properties | Ranges |
|---|-----------------------------|
| Surface area (m ²) | 0.043452 |
| Nominal pore size (μ m) | 0.1 |
| Type and material | Flat sheet, silicon carbide |
| Flux (Lm ⁻² h ⁻¹) | 50 |
| Back wash flux rate (Lm ⁻² h ⁻¹) | 500-600 |
| Operating suction pressure (bar) | 0-0.7 |
| Backwashing pressure (bar) | 1-3 |

In the outside-in flow filtration, the membrane retains particles and microorganisms above 0.1 μ m, and bacteria up to log 4. In addition, Cembrane poses the following advantages to be chosen for this study.

- Simple to operate
- Low fouling potential
- High solid loading capacity

- Can be stored dry or wet
- Stable operation
- Resistance to solvents, oil, grease, high temperature and high pressure.
- Highest recovery rate
- Limited use of chemical needed
- Minimal pressure loss due to its asymmetric structure

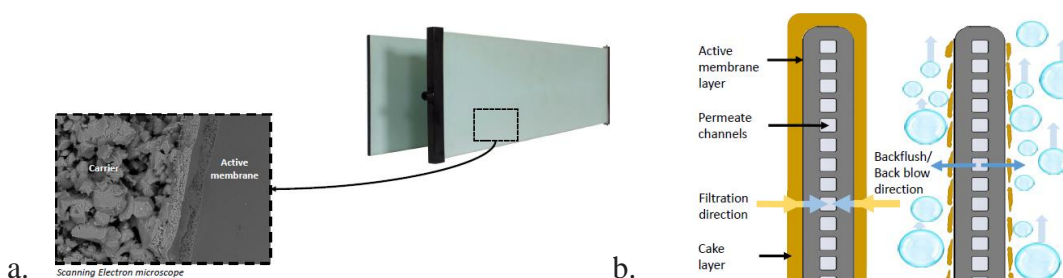


Figure 16. Shows the cross section of flat sheet membrane structure (a) and during filtration and backwashing operations (b) (Cembrane, 2015).

3.3. Membrane Fouling Reducers

Though both Iron- and Aluminum-based coagulation are listed possible Membrane fouling enhancers, Aluminum-based coagulants are selected in this study. Monomeric aluminum sulfate (ALS-LC), and polymeric aluminum chlorides PAX-18 and PAX XL-61 from Kemira Kemi AB, Sweden were used as membrane fouling reducer (MFR) alternatives. Physicochemical properties of the reagents can be read in Table 4.

Table 4. Information on physicochemical properties of the reagents. Based on the Kemira Safety data sheet for each chemical, all are in liquid form and completely soluble in water.

| Type of Reagent | Density (g.cm ⁻³) | pH | Basicity (%) | Viscosity (mPa.s) | Color | odour |
|-----------------|-------------------------------|-----|--------------|-------------------|------------------------|----------|
| ALS-LC | 1.30–1.34 | 2.0 | 48.5 | 20 | Colorless, clear | Odorless |
| PAX-18 | 1.34–1.40 | 1.0 | 42±3 | 30-40 | Light yellow, clear | Odorless |
| PAX XL-61 | 1.23–1.27 | 2-3 | 68±5 | - | Light yellowish, clear | Odorless |

The selection of Alum, (Al₂(SO₄)₃) coagulant was in consideration of the following advantages;

- The physicochemical properties it poses: it's colorless, relatively high pH,
- Provided the objective of the study: which mainly focus on charge-driven mechanisms of interaction with membrane surface, and alum could possibly deliver more Al³⁺ for charge neutralization coagulation with low dosage as precipitation was not required to occur.
- SO₄²⁻ increases coagulation: increase the Al(OH)²⁺/ Al³⁺ ratio hence increasing the rate of Al complexation with naturally occurring ligands.

Moreover, a similar experiment was done using PAX-18 and PAX XL-61 and will be used for comparison later. For this experiment, a range of 1-7 mM Al was selected and Different doses were applied in batch to the mixed liquor samples.

3.4. EXPERIMENTAL SETUP

Flat sheet micro-filter membrane was submerged into the MBR tank that was filled with feed wastewater sludge. The mixed liquor was sampled from the plant a day prior to starting the experiment. The reactor had a volume of $(0.2 * 0.15 * 0.1 \text{ m}^3)$ 3L and working volume was 2.2L. The experiment was operated over a period of a month. After adding the reagent, the sample was mixed by applying aeration for 30 seconds rapid mixing and 90 seconds slow mixing before starting the permeate suction. This was done in such a way;

- The pressure gauge and air supplier were connected to permeate flow line and the reactor respectively
- A chemical coagulant 1-7 mM Al was added to the reactor step by step; dosing in batch
- Air was supplied through the compressor for 120 seconds to create bubbling and floc formation before starting the experiment. The first 30 seconds were for rapid mixing of the reagent with the mixed liquor and the remaining $1\frac{1}{2}$ minutes were cooling time/ slow mixing for flocculation. This step was repeated for each dosing throughout the experiment. And,
- A data logger connected to permeate pump was used to monitor TMP change as a function of time.

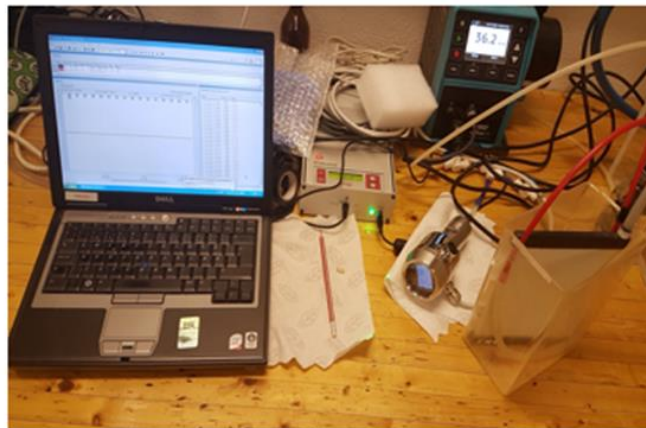
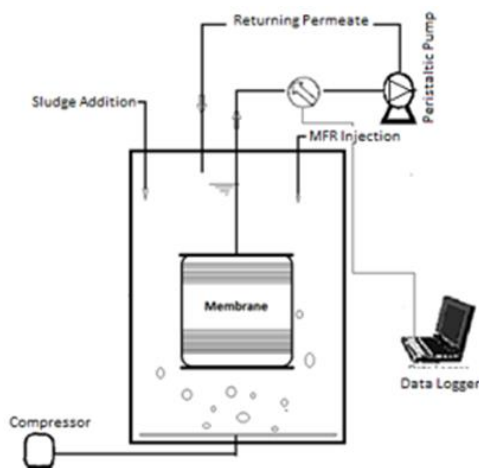


Figure 17. Schematic illustration of the principles of the experiment set up and Photo of actual set-up

Prior to the main experiment, a deionized water test was conducted. 2 liters of deionized water was filtered through the membrane for integrity exploration. A constant flow and variable

transmembrane pressure operation condition were applied. The applied flux was $350 \text{ L.m}^{-2}.\text{h}^{-1}$ and the change in TMP was controlled through data logger from which the maximum pressure read - 0.35 bars (negative sign implies suction pressure).

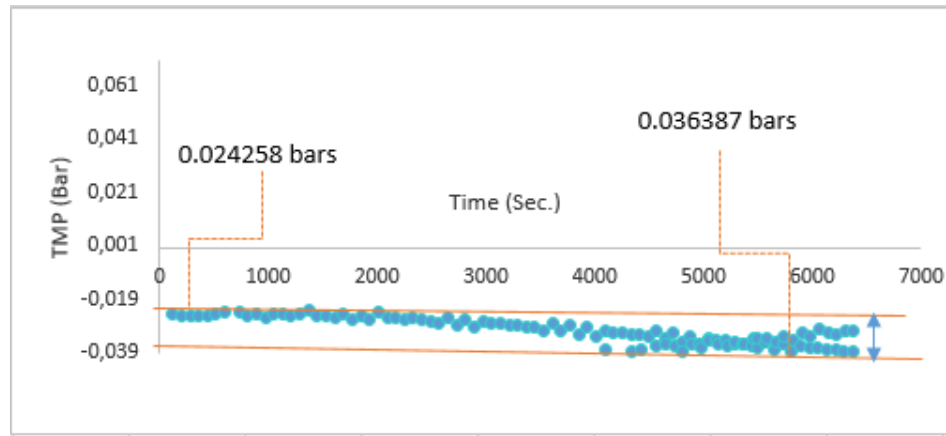


Figure 18. A Graphical demonstration of the variation in TMP over the filtration time. Values are TMP initial and TMP final.

Then a total recycle test was carried out to estimate the efficiency of aluminum sulfate ($\text{Al}_2(\text{SO}_4)_3$) as membrane fouling reducer and the reagent was applied in batch. The peristaltic pump was connected to the membrane to extract permeate (outside-in filtration) at a flux rate of $50 \text{ L.m}^{-2}.\text{h}^{-1}$ and permeate was returned to the tank. Returning permeate keeps the reactor volume constant and was assumed it wouldn't affect the biomass as it originates from the same reactor according to (Lee et al., 2001).

Aeration was supplied from the bottom of the tank (fig.15) so that it could reduce colloid and solute precipitation due to the shear force created along the surface of the membrane through scouring coarse bubbles beside providing air for the biomass. It's considered that the Dissolved Oxygen supply through the compressor remains similar through all the experiment steps. This was done through two perforated plastic tubes connected to a compressor, laid down at the bottom of the tank along each side of the membrane. Online TMP measurement was conducted through easyView software by using a data logger connected to the pressure transmitter line of the suction pump. Continues measurement of transmembrane pressure (TMP) was used to control the degree of fouling and the continuous flux was maintained until the TMP reaches $1.5 \cdot \text{TMP}_{\text{in}}$ (initial pressure).

The temperature of the mixed liquor was monitored for each experiment and pH was controlled using pH-meter. Zeta potential of the supernatant, flocs size (microscopy), residual turbidity and capillary suction time were measured to characterize treated sludge.

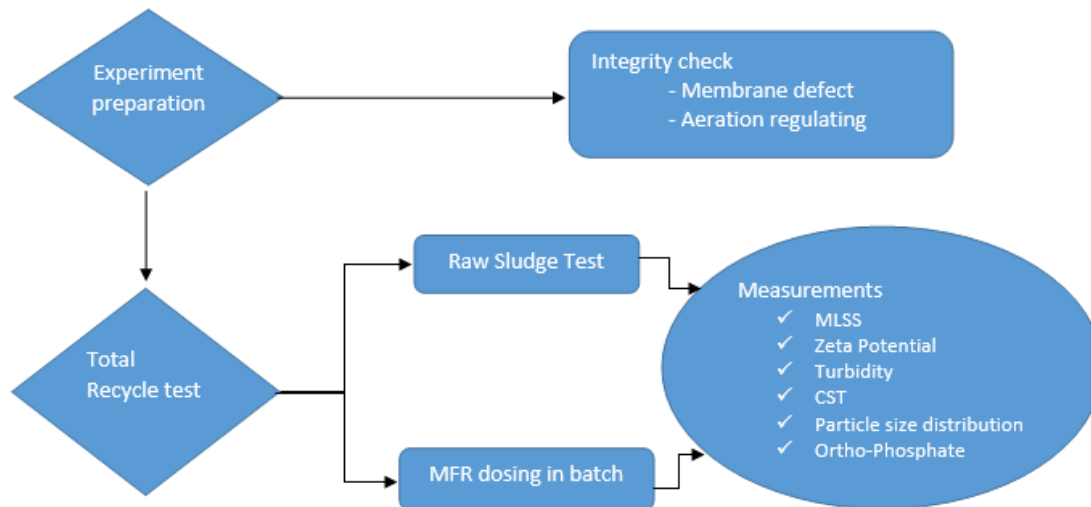


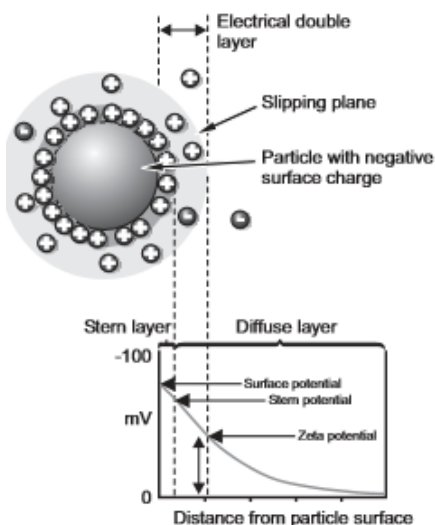
Figure 19. Flowchart showing sequences of the experiments and analytical measurements conducted.

3.5. ANALYTICAL METHODS

150ml supernatant was sampled 10 minutes after the filtration process started from which the fouling factors Zeta potential, Turbidity indices, and Suspended solid (SS₁₀) was analyzed. Residual sludge was used to analyses Capillary suction time and change in particle size distribution. The effectiveness of Alum as fouling reducer is going to be evaluated through the changes it produces on these factors. The capillary suction is used as an indirect measurement of Hydrophobicity in this study.

3.5.1. Zeta Potential (ZP)

10 ml of suspended solid was sampled, a plastic glass cuvette was used to contain the liquid samples inserted into the ZP analyzer (Malvern Zetasizer Nano Z from Malvern instruments limited, UK). ZP measurements were used to get information on the surface charge of the sludge



flocs. ZP of particle is the electrical potential at the boundary of double layer that develop from net charge at the particle surface resulting increased concentration of counter ions. The objective of this study focused on charge driven coagulation which surface charge would play a significant role in determining the particles tendency to coagulate (Nano, 2017). The ZP values would be used to indicate the electro-neutralization after the addition of alum, or repulsion between charged particles before and after coagulation. Supernatant samples were filtered using 8-12 μ m filter paper prior to ZP analysis and three measurements were made for each experiment.

Figure 20. Schematic illustration of Zeta potential and the formation of Electrical Double layer around a particle (Nano, 2017).

3.5.2. Floc size and morphology

Images captured through a Light microscope was used to analyze the morphology of the sludge flocs. Objective lens 10X magnification were used to control particle size variation at the different doses. Three measurements were made for each sampling. Floc size was analyzed through light scattering system given as frequency per volume. Hence, average sizes of flocs in this regard are given based on volume equivalent diameter. Samples were measured with a standard deviation of 12-29% for the BF-MBR mixed liquor and 22.8-96% the AS. Images were processed using Image J software from which particles size distribution was calculated and analyzed through pivot Table, and interpreted accordingly.

3.5.3. Turbidity

Turbidity as measure of the total suspended solids (TSS) in the mixed liquor was measured (using 2100N IS turbidimeter hach ISO method 7027, US) to determine the degree of removal of suspended particles in the supernatant. This was also other means of measuring the effect of the reagent alum added to flocculate the suspended solids. Therefore, it could be also used to determine the dosage as lower residual turbidity values indicate high solid-liquid separation. Similar to ZP, the samples used for turbidity analysis were also filtered using 8-12 μ m filter paper. 60 ml was analyzed twice with 30ml cuvette.

3.5.4. Capillary suction time (CST)

CST measurement which is a sludge dewatering test for characterizing sludge filterability and conditionability was done to describe the filterability of the mixed liquor using settled sludge. A hollow cylinder placed over a rectangular unidirectional chromatographic filter paper (whatmanTM n^o17, UK) was filled with 5ml representative sludge. The pressure was applied manually by pressing down as hard as possible and overlying a steel weight 2kg. Consequently, the liquid was sucked into the paper by capillary suction. The filtrate spreads in a concentric shape in relation to the area covered by the mixed liquor based on its filterability. As the liquid traveled across the paper, it reached the two sensors at the inner concentric reference circle on the filter paper and prompted current that triggered the counter. An automatic time counter connected to these two sensors through current records the time required to travel across the area of the paper. The analysis was stopped as the counting become stationary when the filtrate reaches the outermost circle due to change in conductivity and that time was registered as an indicator of water draining rate. Hence, the CST could be described as the time taken by the filtrate to travel the distance between 32 mm to 45 mm diameter. The CST apparatus used in this study was an older version and the chromatography paper serves as a suction medium. Since this was an indirect measurement, five analyses were made for each sampling.

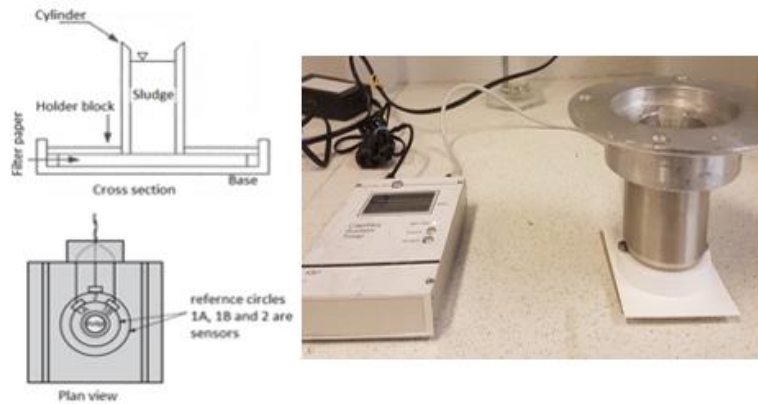


Figure 21. Schematic representation of the CST testing apparatus and photo of actual set-up

3.5.5. Ortho-Phosphate

As a soluble and reactive form of phosphorus Orth-phosphate responds to colorimetric test without preliminary hydrolysis. A discrete analysis of Ortho-phosphate was made using an instrument called EasyChem plus version Rel.1.9.6/2008 from Syntea S.P.A, 03012 Anagni, Italy. Ortho-phosphate (PO_4^{3-} , HPO_4^{2-} , $H_2PO_4^-$ and H_3PO_4 are available for biological metabolism without a further breakdown.

3.6. Data Collection and Processing

During the filtration experiment, suspended solid about 150 ml was sampled 10 minutes after the experiment started from which Zeta potential, residual turbidity, and Ortho-phosphate were analyzed. Standard electrodes (WTW type) were used to monitor temperature ($18^{\circ}C$) and pH (5-7 pH meter) during filtration experiment as they influence the characteristics of the activated sludge. The properties of the MLSS was determined prior to the experiment (Table 2).

80ml of Supernatant solution was filtered through 8-12 μ m filter paper to exclude larger particles prior to analyzing Zeta potential and turbidity. Average of two and three measurement values for turbidity and zeta potential respectively were collected and plotted against dosed concentration.

Permeate flux (J) was calculated based on the volumetric flow (Q) created through the peristaltic pump across the area of the membrane (0.043452 m²).

$$J = \frac{Q}{A} \text{ (L m}^{-2}\text{h}^{-1}\text{)} \dots\dots\dots 3.2$$

the total filtration resistance was obtained using e.q. 3.3 based on the permeate viscosity calculated in accordance with e.q. 3.4 as given by (Geilvoet, 2010).

$$\eta_p = 10^{-3} * \exp^{(0.580-2.520\theta+0.909\theta^2-0.264 \theta^3)} \dots\dots\dots 3.3$$

η_p = Viscosity of the permeate (Pa.s)

θ is an empirical factor calculated from temperature ($^{\circ}C$)

$$\left[3.6610 \cdot \frac{T}{273.1+T}\right] \dots\dots\dots 3.4$$

Moreover, to compensate the impact of temperature on the permeate flux, the permeate flux was normalized to 20 °C based on e.q. 3.5 modified from (Siembida et al., 2010).

$$J_T = F_p * EXP(-0.032 * (T - 20)) \dots\dots\dots 3.5$$

Where J_T is flux normalized to 20 °C.

And permeability (J_{20}) was also normalized to 20 °C according e.q. 3.6.

$$J_{20} = \frac{J_T}{TMP} \dots\dots\dots 3.6$$

The flow was set constant in this experiment. The PC connected to the data logger records the change in TMP as a function of time and graphs are produced accordingly. The TMP increases with time and the filtration was stopped at a pressure 1.5*TMP_{in} (Figure 14).

A Pivot-table analysis was used to process the particle size and distribution. The images captured through light microscopy were explored using ImageJ software to generate area, radius, and diameter of the grains. This process considers the micro-particles are spherical.

4. RESULTS AND DISCUSSION

In this chapter, experimental results of the effects of monomeric and polymeric aluminum reagents on the fouling factors are presented graphically and discussed simultaneously. The effectiveness of the reagents was evaluated through their influence on Zeta potential, Turbidity, Capillary suction time and particle size distribution. The results are mainly displayed in such a way to show how the addition of the reagents $Al_2(SO_4)_3$, PAX-18, and PAX XL-61 have affected the different properties of the mixed liquor solids as a function of dosing. The purpose of the study mainly focuses on evaluating the efficiency of Aluminum-based membrane fouling reducers on charge-driven mechanisms of interaction. Hence, evaluating the change in surface charge properties, hydrophobicity, floc size, turbidity, and mixed liquor suspended solids as a function of the dosing provides better insight on the effect of the positive charges delivered and pH. Consequently, the positive impact it possibly caused on the filterability of the mixed liquor was taken as an indication of the enhanced membrane performance and fouling reduction. Details follow;

4.1. Aluminum Sulphate as Membrane fouling reducer

4.1.1. Filtration Phase

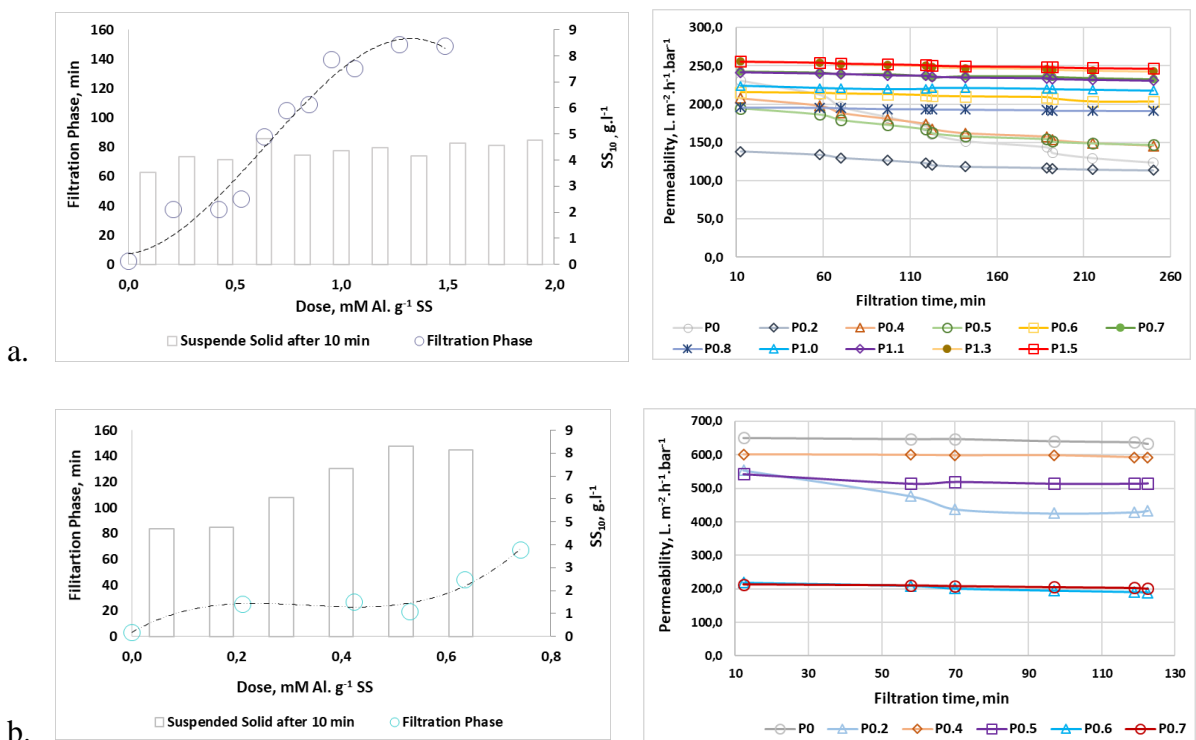


Figure 22. The filtration duration, change in MLSS and normalized permeability as well as flux at working MLSS 3.53 g.l⁻¹ BF-MBR (a) and 4.72 g.l⁻¹ AS (b) as a function of dosages. The permeability and flux were normalized to 20 °C.

At zero dosing, raw sludge, the filtration Phase for the BF-MBR mixed liquor was 2 minutes and for the AS mixed liquor 3 minutes before it reaches 1.5*TMP_{in} for at working MLSS concentration

3.5 g. l⁻¹ and 4.7 g. l⁻¹ respectively. Dosing of 0.21 mM Al. g⁻¹ SS to the BF-MBR mixed liquor extends the filtration phase by 20x. Through the course of the experiment, the filtration phase was enhanced to 150 minutes and the permeability of the filter cake increases by 73% (Figure 22a). The permeability in figure 21 show two clusters groups, which Cluster-1 representing permeability ≤200 L. m⁻².h⁻¹.bars⁻¹ and cluster-2 are groups of permeability above 200 L. m⁻².h⁻¹.bars⁻¹. For the BF-MBR mixed liquor (Figure 22a) Cluster-1 decreases with filtration time but Cluster-2 displays insignificant variation with time. Similarly, the addition of Al₂(SO₄)₃ to the AS mixed liquor have enhanced the Filtration phase up to 1.10hrs and the permeability generally decreases by 32% (Figure 22b). The permeability in Cluster-1 remains constant but Cluster-2 decreases with filtration time.

Basically, it could be observed at the optimum dose (1.3 mM Al. g⁻¹ SS) the BF-MBR mixed liquor filtration phase was improved by 1.15 hours whereas the AS mixed liquor by 23 minutes at dosing 0.74 mM Al. g⁻¹ SS. Accordingly, it could be reflected as an ample indication of the effectiveness of Alum as membrane performance enhancer that attained due to the reduced degree of fouling.

4.2. Supernatant characterization

4.2.1. pH

The pH in the BF-MBR mixed liquor declines from 7 to 5 pH units and in the AS mixed liquor from initial 7.3 to 5.8 pH units. The decrease in pH is attributed to the availability of H⁺ consequent to the hydrolysis of the coagulant as given in equation 2.5.

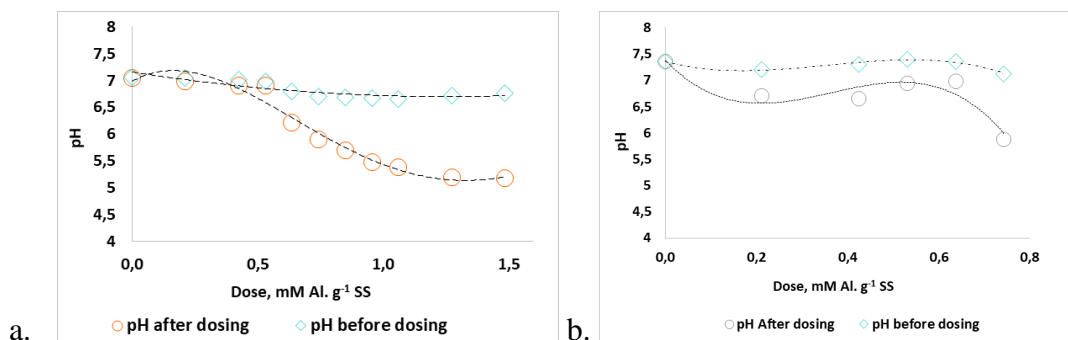


Figure 23. Graphic illustration of the change in pH as a function of dosing at MLSS (a) 3.53 g.l⁻¹ SS BF-MBR and (b) 4.72 g.l⁻¹ SS AS.

4.2.2. Zeta Potential (ZP)

Figure 24 show correlation between the filtration phases and ZP. The filtration phase increased in congruence with the Increasing ZP for the BF-MBR but for the AS the Zeta potential decreases while the filtration phase continues to increases with dosing. Both elucidate the influence on the net charge was major contributor for the enhanced filterability. However, the increase in the filtration phase after the decrease of the ZP in the AS indicates additional factor contributes to the betterment of the filterability.

The trend of the change in the surface properties of the colloidal particles in the suspended liquid display 3-folds different optimum dose. The BF-MBR mixed liquor at working MLSS of 3.5g.l^{-1} shows net surface electrical charge increases from initial -14.3 mV to -6 mV in accordance with Alum dosing. This indicated that the negatively charged surfaces were partially electro-neutralized by the positive charges through reactions with Al^{3+} and adsorbent aluminum hydroxides following the dissociation of Alum (chapter 2-2.10) in the solution. Correspondently, the highest Zeta potential for the given range occurs following the dosing of $1.3\text{ mM Al. g}^{-1}\text{ SS}$.

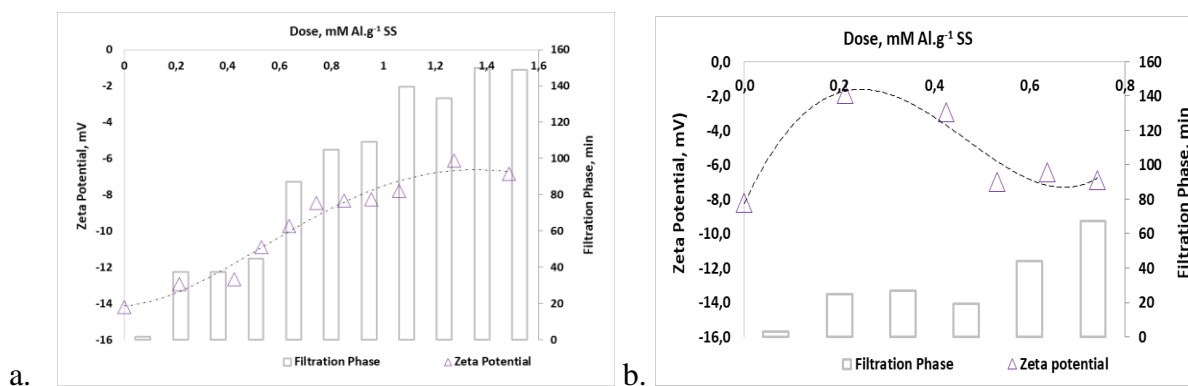


Figure 24. The variation of electrical charge of particles as a function of dosing at a working MLSS of (a) 3.53 g.l^{-1} from BF-MBR and (b) 4.72 g.l^{-1} from AS.

Initially zeta potential for the AS mixed liquor was -9 mV for the working MLSS of 4.7 g.l^{-1} and increases to -2 mV through the course of the test. This indicates the charge on the colloids were counterbalanced largely. Figure 24b shows the optimum dose was $0.43\text{ mM Al. g}^{-1}\text{ SS}$ where a further addition of the reagent caused a decline in the Zeta potential. This can occur due to destabilizations of already formed flocs and consequently release negative surfaced colloids to the solution. The reason behind might be due to the sludge was already been pre-coagulated with PAX-18 from its source (BEVAS) and collectively the dosed concentration might have caused the flocculated colloids to destabilize as depicted by the decreasing ZP, increase in Turbidity and capillary suction time. This agrees with the observation of (Wu et al., 2006) where they state the occurrence of “colloidal re-stabilization” consequent to repulsive force between the packed electronegative macro-molecules at certain dosing. In another expression, the flocs become less stable with increasing dose in the given range due prolonged and intense agitation from the overdosing.

4.2.3. Turbidity

The turbidity and filtration phase have a contrasting relation where the turbidity decrease the filtration phase increased, which was clearly displayed by the BF-MBR. The turbidity indices graph for AS exhibits regardless of the change in the turbidity the filtration phase increases. In the BF-MBR mixed liquor, the decreasing in turbidity is self-explanatory for the increase in the filtration with dosing. At MLSS concentration 3.5 g.l^{-1} , the clouds of microscopic particles decrease from 91 to 6.5 NTU with increased addition of Alum (Figure 25a). This change is in agreement with the effect on zeta potential and the lowest turbidity 6NTU seen at 1.3 mM Al. g^{-1}

SS. The colloidal particles are brought together (form larger size flock) through the positive charges released from the coagulant, which mean they are removed from the solution. As this increased with the addition of alum, the filterability expressed by the bar graphs in figure 25a increases.

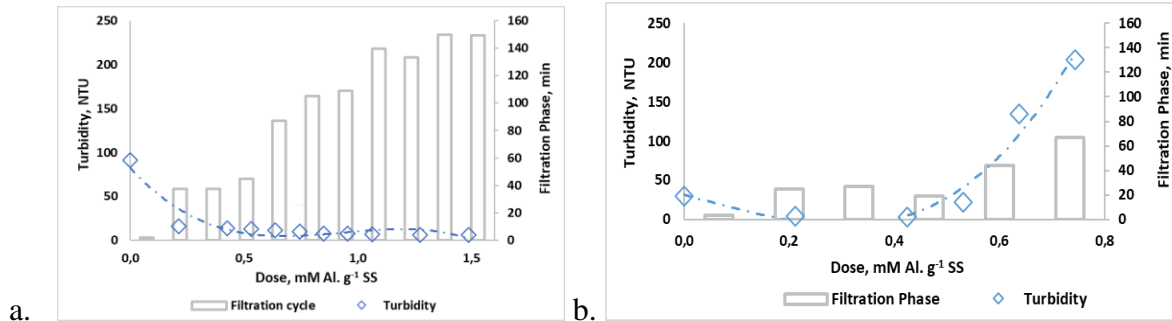


Figure 25. Turbidity evolution as a function of dosage at MLSS concentration (a) 3.53 g.l⁻¹ from BF-MBR and (b) 4.72 g.l⁻¹ from AS.

For the AS mixed liquor, the turbidity initially at 30 NTU for working MLSS of 4.7 g.l⁻¹ decreased to 3 NTU before it started to increase with dosing after the dosing point 0.43 mM Al.g⁻¹ SS. This might elucidate;

- The addition of the coagulant initially disturbed the repulsive force among the colloids, which caused the fine colloids to flocculate consequently reduce the clouds of finely suspended colloids in the solution.
- The increase in colloidal particles in the solution corresponds with the decrease in zeta potential. It could implicate that, further dosing obviously caused high attraction of colloids, however, the dosed concentration might relatively be insufficient to hold all the packed electronegative colloids resulting in the repulsive force to reestablish and thus increased the availability of colloidal clouds in the solution. Or
- The flocs are possibly less stable that they could be broken due to the sheer force through the aeration.

Though the Turbidity increased, the filterability continues to increase. It could be due to that the flocs have already developed different characteristics such as they seem less hydrophilic (the relative increase in CST seem lower when seen in relation to the increase in turbidity and decreasing ZP) and increased sizes relative to the initial colloidal flocs.

4.3. Precipitate characterization

4.3.1. Capillary suction time

The contrary relationship between the CST and the filtration phase seem to have a positive impact on the filterability of BF-MBR mixed liquor correspondent to the increase of dosing (Figure 26a). A decrease in CST declined the filtration initially but the filtration continued increasing though CST increased in between implying a decrease in dewaterability of AS the filtration phase increased rather better. This relation with filtration phase was similar to turbidity and ZP signifying

a factor another than charge neutralization is playing a larger role in enhancing the filterability of the AS.

The BF-MBR mixed liquor showing a decreasing CST reveals the ease release of water from the slurry (figure 26a). The indication would be that the dewaterability of the mixed liquor has increased due to the release of chemically bound water as result of the charge effect. In another expression, its water disliking property has increased. Therefore, it could be discussed that the hydrophobicity of the BF-MBR mixed liquor increased with increase in dosing. Another justification could also be that removal of EPS particles might have contributed to the ease release of water corresponding to the interpretation of (Sheng et al., 2010). The filterability was positively influenced by the increase in the hydrophobicity of the mixed liquor.

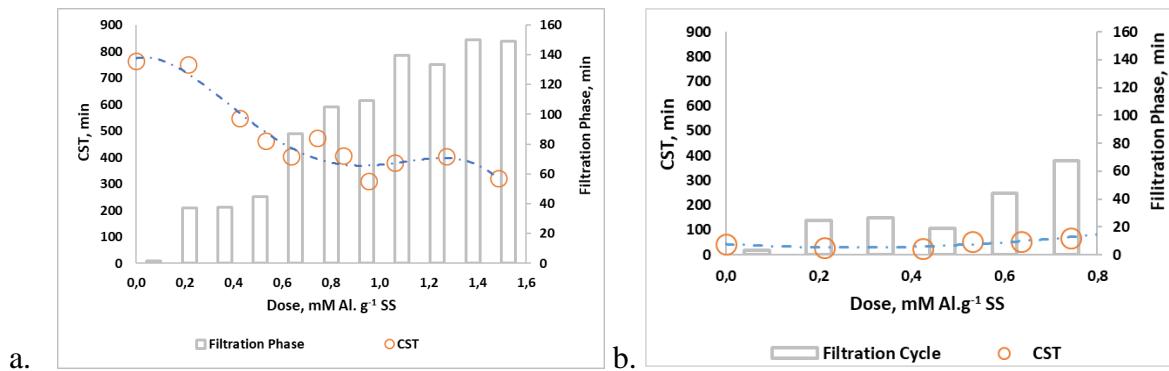


Figure 26. The change Capillary suction time as a function of dosage (a) 3.53 g.l⁻¹ MLSS BF-MBR and (b) 4.72 g.l⁻¹ MLSS AS.

In the same way, the AS mixed liquor display increase in dewaterability until the dosing point of 0.43 mM Al. g⁻¹ SS; However, it decreases afterward (figure 26b). Initially, the charge neutralization caused chemically bounded water to be released. In the later dosing 0.43 – 0.74 mM Al. g⁻¹ SS, the re-stabilization of the colloids may partially restore the hydrophilicity character of the flocs. Moreover, in agreement with the description of (Houghton et al., 2001) where lower EPS content enhances Hydrophobicity but at higher concentration, it increases the water holding capacity of the mixed liquor. The later increases in CST could be due to that the re-stabilization of flocs possibly added back the EPS in the solution that increased the hydrophobicity of the mixed liquor. The increase in the filtration phase possibly indicates the particles in the solution have a relatively higher diameter and the ZP observed in figure 24b is also slightly higher than the initial mixed liquor.

4.3.2. Particle size distribution (PSD)

Microscopic observation of the biomass revealed that the biomass structure in the BF-MBR mixed liquor of 3.5 g.l⁻¹ MLSS was composed of small, weak and uniform-sized flocs mainly dispersed than the AS mixed liquor of 4.72 g.l⁻¹. Comparison of the non-flocculated and flocculated mixed liquor flocs show a general increase in particle size. However, the particles size growth was not evenly as a function of dose. Nevertheless, the reduction of the white background in figure 27a & b with dosing signifies the improved distribution of particle size and dewaterability. Besides,

relative to the raw sludge, the flocculated BF-MBR, and AS mixed liquor showed particles diameter enlargement by 2 to 4 times and 3 to 7 times respectively (Appendix II). The particle sizes were well improved at the beginning of the dosing, better size growth was observed at 0.74 mM Al. g⁻¹ SS for the 3.5 g. l⁻¹ and at 0.43 mM Al. g⁻¹ SS for the 4.7 g. l⁻¹. At higher dosing, the growth of particle size looks less different to that of the non-flocculated particles possibly due to breakage of the flocs as they might become less stable. This could occur as result of the collective effect of the agitation from overdosing and the sheer force of the aeration.

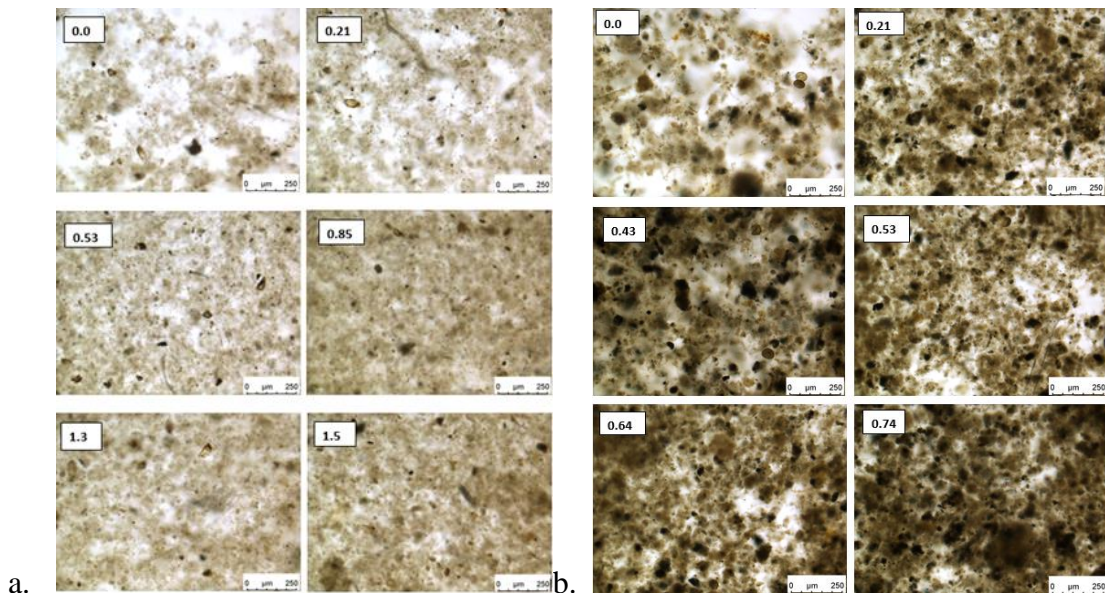


Figure 27. Light microscopy image demonstrating particle size growth and distribution of the Non-flocculating and Flocculated micro-particles of the BF-MBR mixed liquor and the AS with dosing at MLSS 3.53 g. l⁻¹ SS and 4.72 g. l⁻¹ SS respectively. Numbers specify doses in mM Al. g⁻¹ SS.

Moreover, figure 28 indicates with increasing dosing alum has significantly shifted the particle size to a larger than 1μm and hence they wouldn't fit the pore of the membrane. The acute curves have more particles sizes at lower diameter than the wider curves that portray the enhanced particle size growth as well as the distribution of a larger diameter. Therefore, the particle agglomeration was one of the main factors through which alum enhanced the filterability. This could be observed as one explanation for the increase in the filtration phase while the Turbidity and dewaterability increasing in later doses with AS mixed liquor (figure 25b&26b).

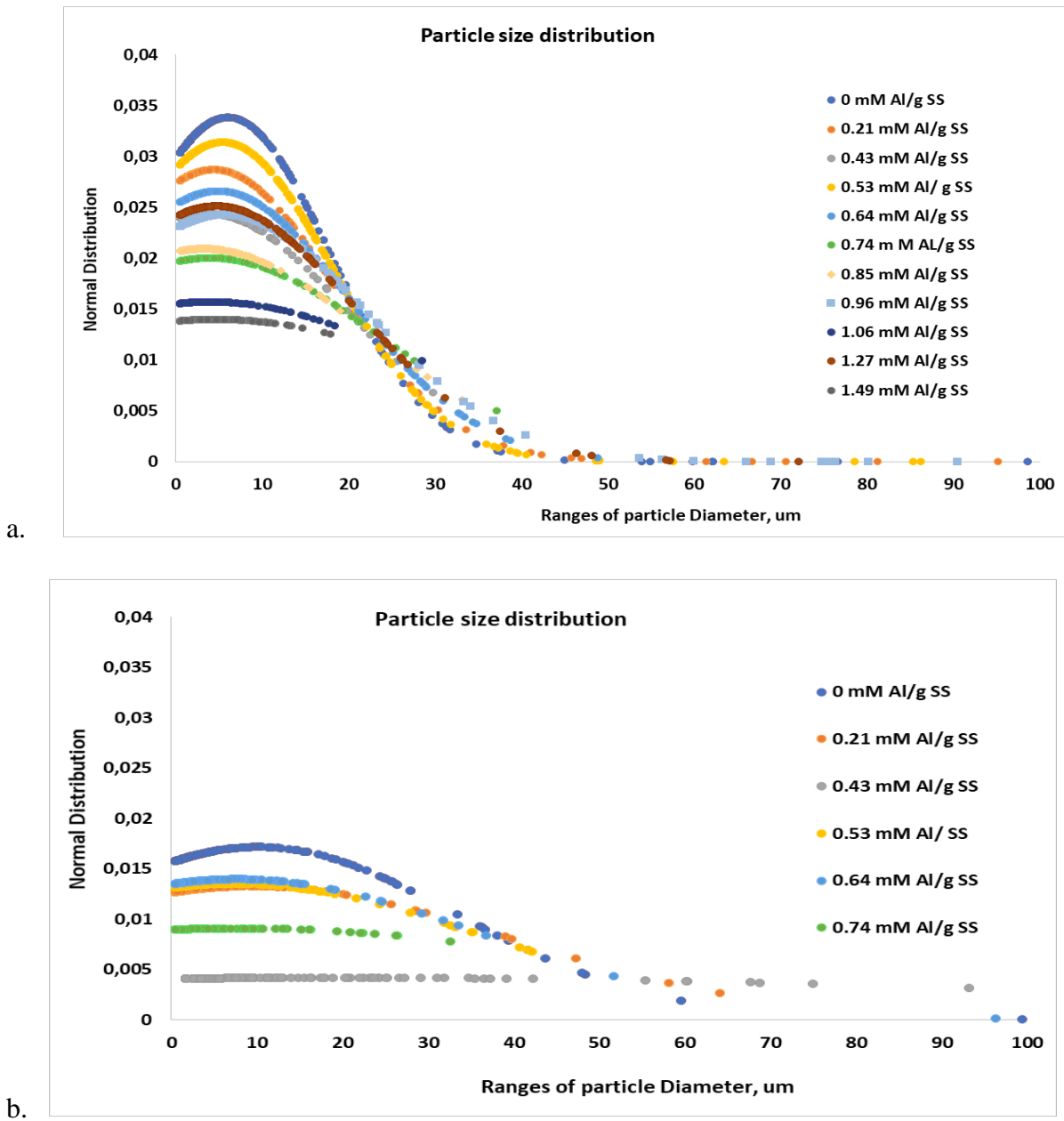


Figure 28. Graphical illustration of particle size distribution as a function of dosing at MLSS (a) 3.53 g.l⁻¹ SS BF-MBR and (b) 4.72 g.l⁻¹ SS AS.

Moreover, the charge driven flocculation looks to play a significant role in reducing the small flocs such as Colloids (0.01 - 1µm) and solutes (<0.01µm) that were described to take major responsibility in membrane fouling.

4.4. Filtrate characterization

4.4.1. Ortho-Phosphate

Both mixed liquors of BF-MBR and AS depict a decreasing general trend of concentration of Ortho-phosphate with increasing dosage. The BF-MBR mixed liquor decreased from initial PO_4^{3-} content 11.410 ppm to 0.058 ppm at 1.06 mM Al. g^{-1} SS dosing. The optimal dose for the PO_4^{3-} to attain the target 0.3 was below 1mM, slightly lower than that of the filtration phase. This might be good for practical aspect; reduce chemical application.

The decrease in PO_4^{3-} concentration as a function of dosage implies the efficiency of Aluminum removing this ion from the solution. However, the mixed liquor from AS had Initial PO_4^{3-} concentration of 0.067 ppm, which is below the targeted value 0.3 mg P. l^{-1} (indicated by dashed line) due it was already treated with PAX-18. Nevertheless, it has further reduced to 0.030ppm.

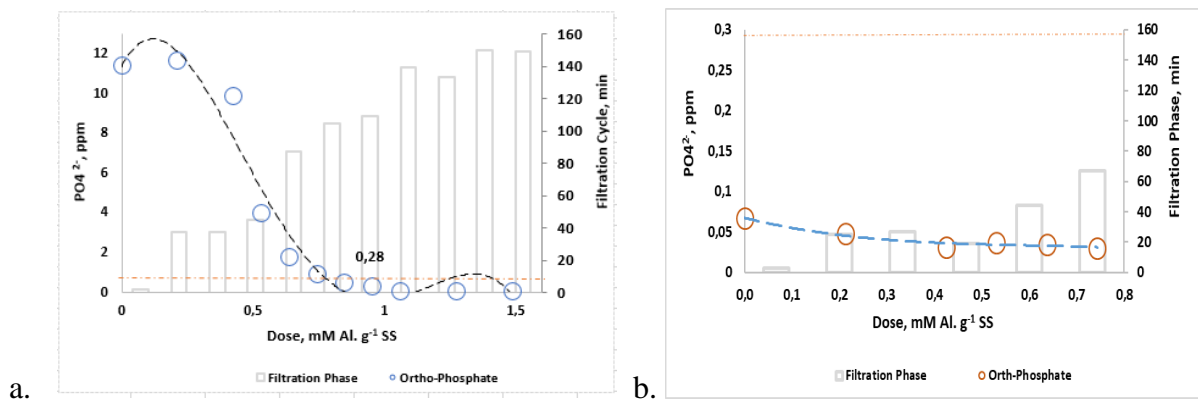


Figure 29. Demonstrates the change in Ortho-Phosphate concentration (ppm) as a function of dosing at MLSS (a) 3.53 g. l^{-1} SS BF-MBR and (b) 4.72 g. l^{-1} SS AS. Dashed line indicates target values.

The greater removal at high dose could be explained by the reduction in pH to 5 at the BF-MBR and 5.8 at the AS mixed liquor (Figure 23). It can also explain that significant concentration of aluminum been consumed through ion exchange with Phosphate ion provided the high affinity to adsorb shown both graphs, particularly figure 29a and agrees with the explanation of (Tanada et al., 2003). They observed a selectivity of phosphorus adsorption to aluminum coagulant and had high adsorption at pH 4-5 with greater adsorption at pH 4, which in this case was pH 5.

Generally, it could be observed that the addition of Alum as MFR enhanced the mixed liquor filtration duration of the BF-MBR by 0.5-1.15hrs at working MLSS 3.5 g. l^{-1} and that of AS by 8-23 minutes at 4.7 g. l^{-1} MLSS. This indirectly means the degree of fouling was considerably reduced. It could also be emphasized by the general increase in ZP, decrease in Turbidity, low CST, and increased particle size distribution after coagulant addition. The availability of positive charges caused a decrease in the net negative charge of colloids from -14 to -06mV as well as -09 to -1.6mV on the mixed liquor from BF-MBR and AS respectively. Change in pH may have influence in the Zeta potential as particles can exhibit net positive and negative charge accordingly. The stability pH relationship from (Duan and Gregory, 2003) given in chapter two indicate, for the given range of concentration the optimum pH ranges for coagulation is around 5. Moreover,

pH measurements show the influence on Zeta potential was greater at 5.2 pH units at 3.5 g. l⁻¹ and 5.8 at 4.7 g. l⁻¹ SS concentration.

Moreover, in terms of turbidity removal efficiency Aluminum looks effective in removing finer particles and was believed mainly through charge neutralization as colloids were considered the main constituent of the MLSS. The lower CST indicates better sludge filtration capability, suggesting the hydrophobicity was well altered by Alum MFR that signify the reduced tendency of the rate of fouling. This may possibly also explained by the TMP (bar) and time (sec) plot showing the filtration cycle length and the stable filtration under the time zone before the TMP reached the maximum $1.5 \cdot \text{TMP}_{\text{in}}$ given in Appendix I.

Though it did not reach up to zero charge, the charge reduction meets the goal of the study and signify the charge driven fouling reduction was an effective mechanism. It has influenced the particles to develop different characteristics than their initial properties. Colloidal flocs have acquired different net charge, became more hydrophobic, size growth and better particle distribution were achieved as result of the charge based interaction through the supplied positive charges from the added Alum. Hence, it could be summarized that electro-neutralization was the major factor through which the filterability was enhanced. Besides, the observed influence on the ZP, CST, flocs size and turbidity emphasize the key role colloids play on the fouling process, which also was recognized (Lin et al., 2014). Though it's also believed Aluminum could remove some particles through bridging at <1.6 mM Al concentration according to (Wu et al., 2006), this might not have occurred as the lower dosing applied would possibly be insufficient to create larger flocs that bridge. Moreover, the stability of the flocs depicted by the breakage at higher dose reflects the main mechanism was charge-neutralization.

4.5. Summary of comparison between BF-MBR and AS Mixed liquor

Below is given a graphical summary of the contrast between the SS, filtration Phase, Zeta potential, turbidity, CST, and Ortho-Phosphate between the two MLSS 3.5 g. l⁻¹ (BF-MBR) and 4.7 g. l⁻¹ (AS). The general observations could be summarized as;

- Addition of the MFR has positively influenced the Filtration phase which was more clearly displayed by the BF-MBR mixed liquor
- The changes in the fouling factors ZP, CST, turbidity, and PSD depict the main influence on the filtration was charge driven in the case of BF-MBR whereas AS mixed liquor effect of both charge and Particle size distribution. The principal component analysis (PCA) given in figure 30 emphasize the effect of ZP with dosing on the filtration phase.
- In the case of AS mixed liquor, Dosing after the ZP start to decline led to permeability decline.

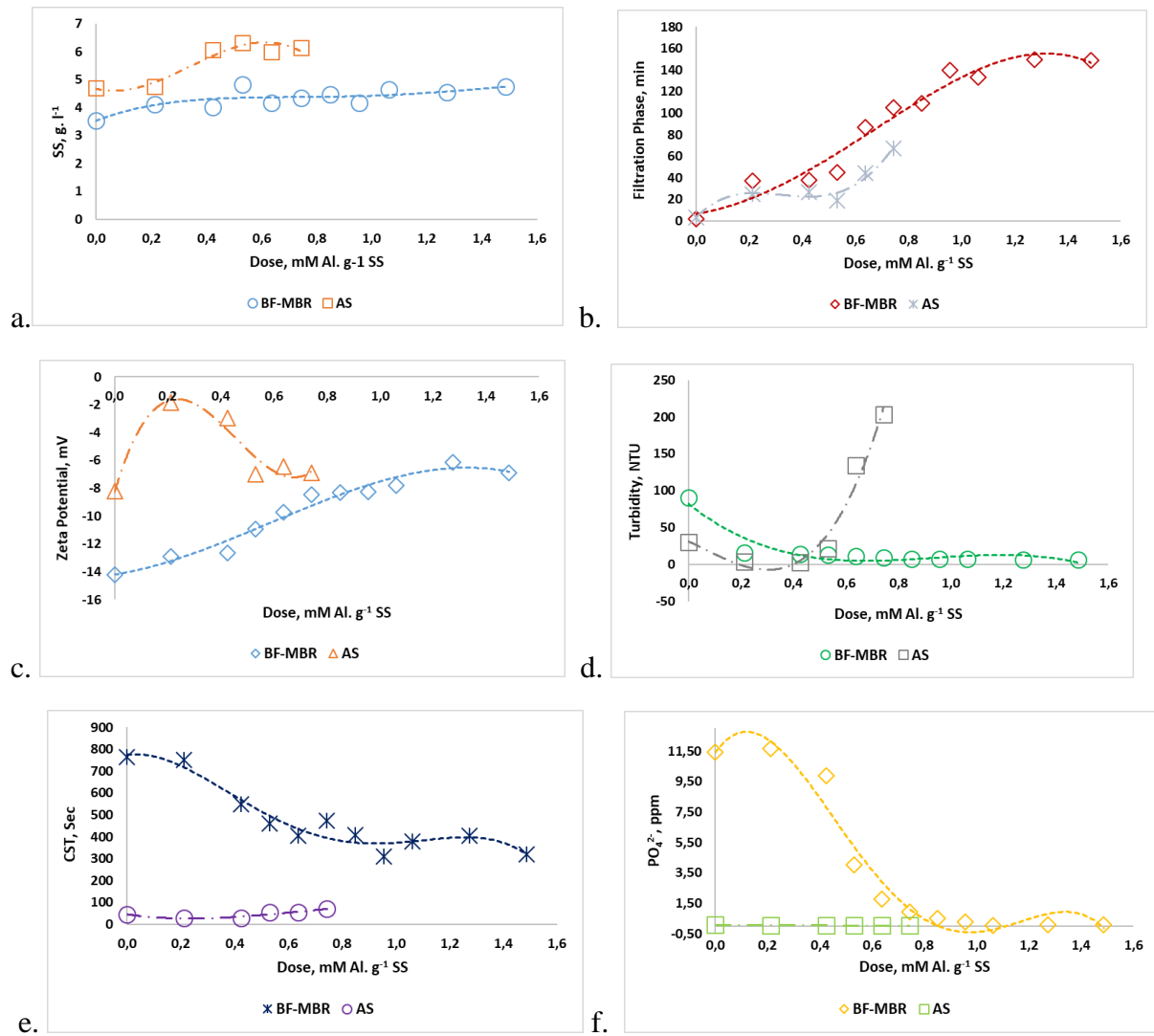


Figure 30. The contrast between the influences on the Suspended Solid concentration (a), filtration Phase (b), Zeta potential (c), turbidity (d), CST (e) and Ortho-phosphate (f) as a function of coagulant dose for both BF-MBR and AS mixed liquors.

Provided the results from the BF-MBR showed a better result that signifies the charge driven influence on the filterability of the mixed liquor, a statistical analysis was conducted to better clarify the main factors that play the major role in improving the filtration phase. Principal component analysis (PCA) is given below and the factors ZP, turbidity, CST, and Dose were expressed as components in this regard.

Table 5. Correlation matrix

| | Dose (D) | ZP (Z) | Turbidity (T) | CST |
|-----------|----------|----------|---------------|----------|
| Dose | 1 | 0.95464 | -0.65182 | -0.86906 |
| ZP | 0.95464 | 1 | -0.66782 | -0.87214 |
| Turbidity | -0.65182 | -0.66782 | 1 | 0.70359 |
| CST | -0.86906 | -0.87214 | 0.70359 | 1 |

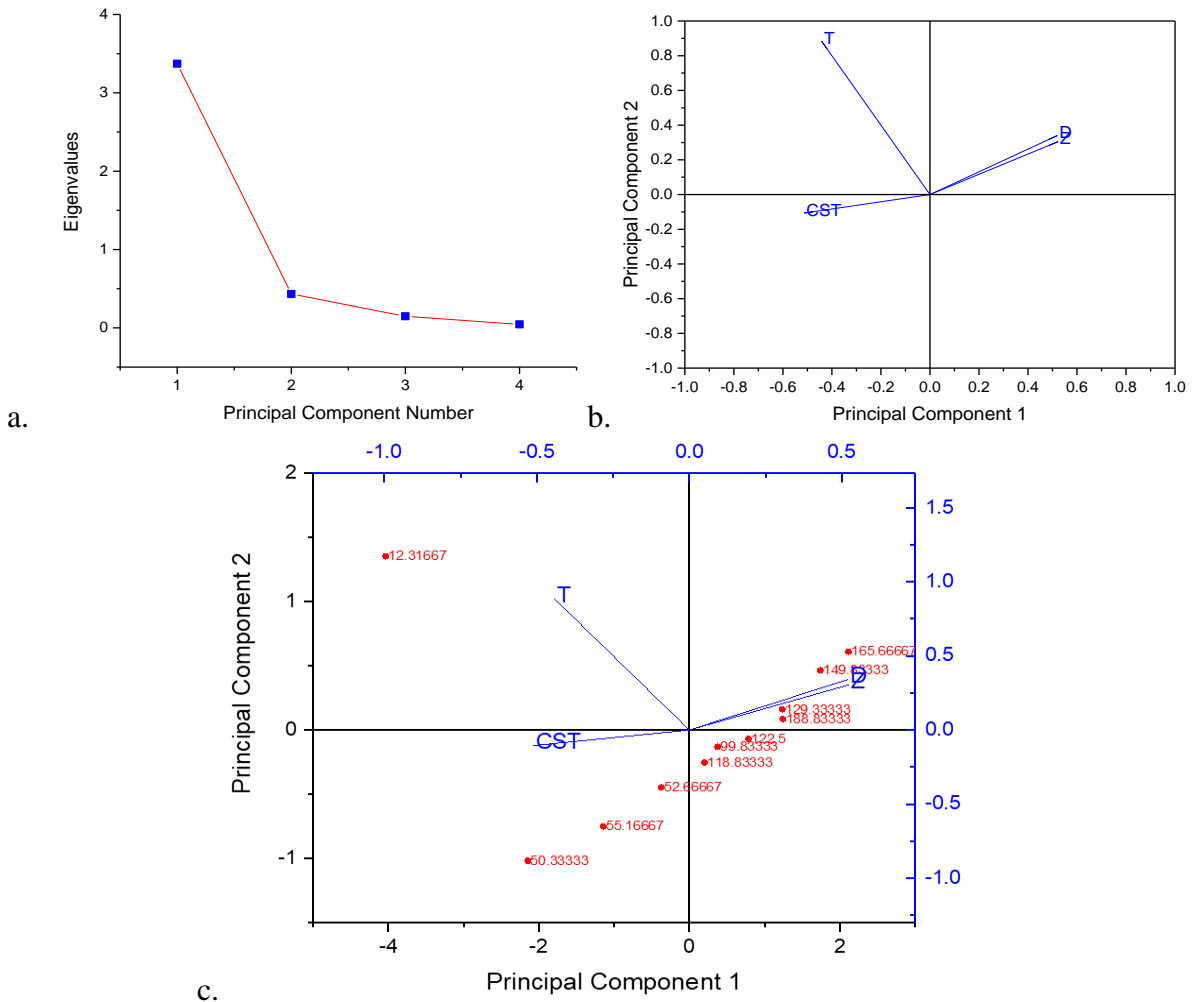


Figure 31. PCA signifying the increase in filtration congruently with zeta potential as function of dosing. a) Scree plot, b) Loading plot, and c) Biplot.

Accordingly, the effect on the surface charge of the particles (ZP) was the major influencing factor on the variability of the filtration phase. This is indicated by the magnitude and variability of the filtration phase values (in Red) in the direction of the Z and D (figure 31c). It's also explained in the scree plot steep curve (Figure 31a) a principal component No.1 having high Eigenvalue and the loading plot with Z close to value 1 in the principal component 1. It could also be observed that Turbidity (T) reduction has played significant role, possibly due to the availability of high finer biomass in the source mixed liquor that later flocculated. It could be concluded that Charge

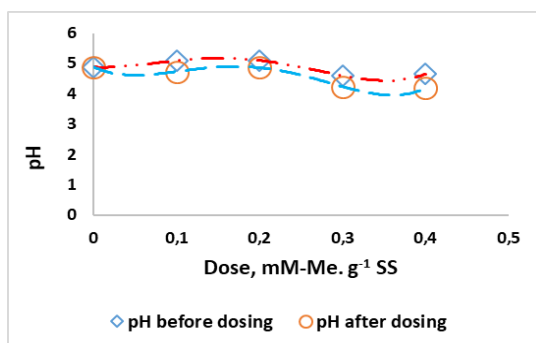
neutralization was the effective mechanism of fouling reduction for alum at dosing below 1.6 mM Al. g^{-1} SS. Similar observation was made by (Li et al., 2006) for dose concentration of 1m M and also agrees with the suggestion of (Wu et al., 2006) that conducive pH for Alum could be obtained by dosing within 1.6 mM Al.

4.6. Comparison with Pre-polymerized MFRs

A similar study was conducted by WESH group (at the Faculty of Science and Technology, NMBU) using polymerized reagents PAX-18 and PAX XL-61 and the graphical results were included here for relative comparison. The polymerized aluminum-based MFRs were applied into the BF-MBR mixed liquor at different working MLSS. First, the results are described shortly in similar graphical representation as earlier and discussed simultaneously. Summary of the comparison is then given at the end of the chapter.

4.6.1. PAX XL-61

The addition of PAX XL-61 to the BF-MBR mixed liquor influences the fouling factors in such a way that; the CST declines from 530 sec to 129 seconds, turbidity lowers by 12 times (from 35NTU to 2.7NTU) whereas Zeta potential improves from -12mV to -4 mV (figures 33 – 35). Initial points in the plots fall along zero dose implying points correspond to the raw sludge and the trend continues in response to the dosing. The optimal dosage was 0.4 mM-Me. g^{-1} SS and the filtration duration was enhanced by 10 min.



The pH declines from 5 to 4 pH units. A decrease in pH after dosing is familiar phenomenon due to addition of H^+ to the solution as the coagulant undergo hydrolysis reaction (eq. 2.5).

Figure 32. pH change before dosing and after dosing as a function of the dose at MLSS 5.87 mM-Me. g^{-1} SS

Figure 33 shows a correlation between the influence of the Zeta potential and filtration phase. This may indicate the improvement in the filtration duration was charge driven. Dosing the PAX XI-61 to the mixed liquor increased the ZP from -12mV to -4 mV and filtration phase by 10 times.

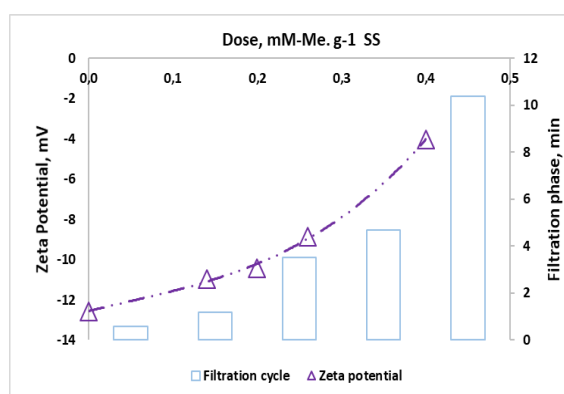
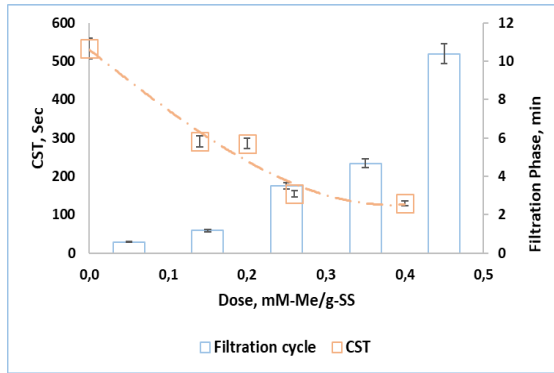


Figure 33. The variation of zeta potential and filtration phase as function of dosing at working MLSS 5.87 g. l^{-1}

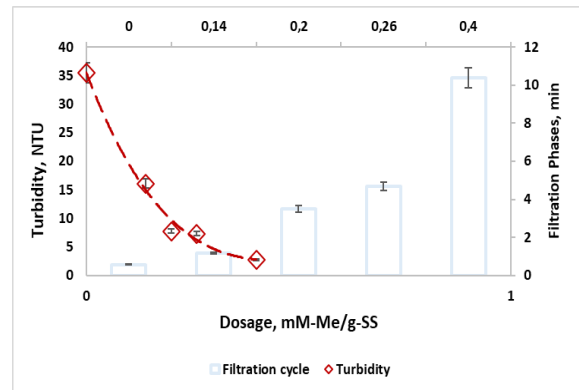


The CST declines from 530 sec to 129 seconds indicating the increase in dewaterability, indirect expression of the increase in hydrophobicity of the mixed liquor as a function of the dosing. It's in coherent with the increase of Zeta potential emphasizing both factors were influenced by the electro-neutralization, which similar effect on the filtration phase.

Figure 34. Graphical representation of the change in the CST in correlation with filtration phase as per dosing.

Following the dosing, the turbidity indices decline indicating removal of colloidal clouds through the process of flocculation. The turbidity initially at 35 NTU drops to 2.7NTU and hence the filtration increases.

Figure 35. The contrast between the filtration cycle and Turbidity as a function of dosage. The working MLSS was 5.87 g. l⁻¹.



4.6.2. PAX-18

This time the dosage was increased to evaluate the effect of the polymerized aluminum coagulant at different levels of concentration. The pH dropped from 6 to 4 pH units. The zeta potential increased from -12 mV to 3mV, which is a large change compared to both alum and PAX XL-61. However, the applied dose, in this case, was 10x higher than both MFRs. The capillary suction time initially at 150 Sec decreased to 35 Sec, implying an increase in hydrophobicity of the sludge. Though the filtration shows a significant increase until dosing point of 0.22 mM Al. g⁻¹ MLSS, it declines for the following dosing.

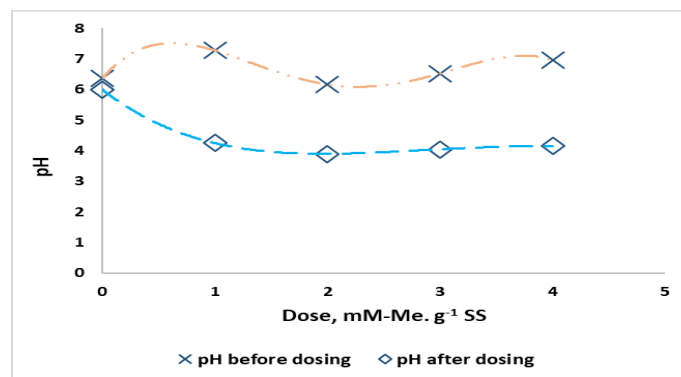
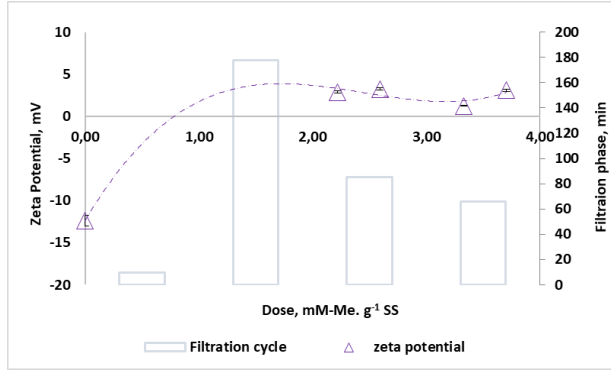


Figure 36. Change in pH before and after dosing as function of dosing at working MLSS concentration of 4.68 g. l⁻¹



At the optimum dose 1.5 mM-Me. g⁻¹ SS the zeta potential reached 3mV and the filtration phase increased to 150 minutes congruently. However, a slight decline in zeta potential reduced the filtration phase by half that provides a clear emphasis the impact of the charge on the filtration phase.

Figure 37. Evolution of surface net charge and its impact on filtration phase as function of dosing at MLSS 4.68 g. l⁻¹

The filtration phase and the CST look to have a contrasting relation where Filtration increase with decreasing CST as a function of dosing. Moreover, Figure 37 displays the change in capillary suction time is in agreement with the change in zeta potential. This signifies the effect of charge on the hydrophobicity properties of the particles and hence the influence on the filtration phase. It might explain that the re-stabilization of some colloids could partially regain their water liking property.

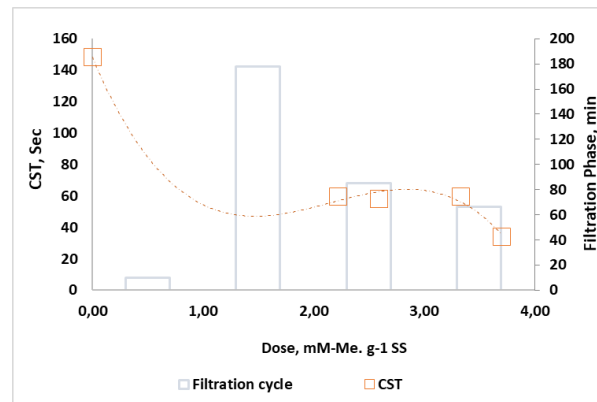
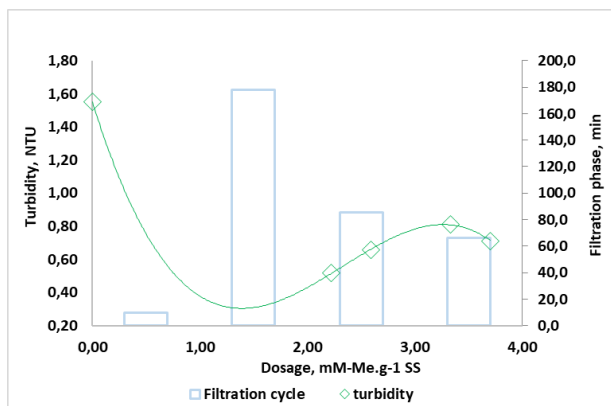


Figure 38. The contrast between the filtration cycle and zeta potential (a) and Filtration cycle versus CST (b) as a function of dosage at MLSS 4.68 g. l⁻¹.



A general decrease in Turbidity enhances the filtration phase. Dosing 2mM of PAX-18 large declined the turbidity before it tends to relatively increase again. The filtration was improved to the maximum at this low Turbidity indices. Filtration phase was enhanced 18 times where further dosing cause reduction in filtration phase by 2 fold for an equivalent increase in turbidity.

Figure 39. Turbidity indices in relation to the filtration phase as a function of dosing at working MLSS 4.68 g. l⁻¹.

Based on the observed results it could be summarized that;

- ✓ The Monomeric Alum and polymeric PAX XL-61 both have similarly influenced the increase the zeta potential, CST and hence the filtration phase which increased with doing.
- ✓ Dosing the PAX MFR However, increased the Zeta potential, CST and the filtration phase to great extent until a certain optimum dose where further adding causes a decline on the ZP, CST and consequently the filtration phase. This has happened for both BF-MBR and AS mixed liquors. This might be related to the relatively faster dissolvability and low basicity content nature of the PAX-18.
- ✓ Unlike to the study by (Wu et al., 2006) that observe the polymeric coagulants produce a better effect on the filterability enhancement, alum (monomeric) show better influence on the Mixed liquor properties (Table 5).

Table 6. Summary of the effect of the MFRs on the filtration Phase and ZP at Given MLSS, pH and optimal dose.

| FACTORS | REAGENT TYPES | | | |
|--|---------------|--------|--------|-----------------|
| | Pilot Plant | | | BEVAS |
| | PAX XL-61 | PAX-18 | ALS-LC | ASL-LC + PAX-18 |
| MLSS (g.l ⁻¹) | 5.87 | 4.68 | 4.55 | 6.06 |
| pH | 4.18 | 4.06 | 5.2 | 6.65 |
| Optimal dose (mM Al. g ⁻¹ SS) | 0.4 | 2 | 1.3 | 0.43 |
| Filtration Phase (min) | 10 | 18 | 75 | 23 |
| Zeta potential (mV) | -4 | 3 | -6 | -2 |

Based on the Summary in table 5, the coagulants could be ranked PAX-18, ALS-LC+ PAX-18, PAX XL-61, and ALS-LC in descending order of their effect on the net surface charge of the suspended solids. Yet, the filterability enhancement analysis showed ALS-LC had a better effect followed by ALS-CL+PAX-18, PAX-18, and PAX XL-61. However, this might be due to the low MLSS compared to PAX XL-61 and in addition different sludge characteristics for ALS-LC+PAX-18. The MLSS between PAX-18 and ALS-LC is nearly same (Table 6) and has same sludge source, yet the influence they had confirms the monomeric aluminum sulfate was efficient at a lower dose. pH was suggested as a possible affecting factor for the polymerized MFRs when its lower by (Wu et al., 2006) due to its influence on zeta potential however, the result show otherwise. Generally, the enhanced filtration duration suggests Alum has reduced the TMP increase rate significantly elucidating as the effective MFR for dosing below 1.6 mM-Me. g⁻¹ SS.

4. CONCLUSION

Given the results of the experiment, the monomeric and polymeric coagulants had a clear effect on the mixed liquor properties Zeta potential, Turbidity, Capillary suction time and Particles size. The addition of the coagulants has delivered positive charges to a different extent and electro-neutralized the net surface charges of the mixed liquor accordingly. Nevertheless, the influence on the electrical charge, clouds of colloids and dewaterability of the mixed liquor signifies the charge driven interaction triggered following the addition of the membrane fouling reducers indicating the experiment has met the purpose of the study. Furthermore, the extent of the influence on the fouling factors has signified the improvement on the mixed liquor filterability. Generally, the following conclusion can be drawn;

- The MFRs have influenced the filtration Phase positively.
- Variation between the influence of monomeric and polymeric coagulants in this study was that the selected range of the doses was low, which signify the monomeric was better in coagulation. Charge neutralization was the major mechanism fouling reduction. In contrary, it implicated the effect of the PAX XI-61 could be shown at higher doses instead and the influence might be collectively through sweep flocculation and bridging in addition to the charge neutralization. PAX-18 was dosed at higher range yet it has less effect than Alum.
- The change in pH explained the above inference. At pH 5 and given dose range, the effective interaction mechanism was charge driven interaction through the supplied positive charges. Furthermore, Ortho-phosphate had great adsorption at pH 5.
- The multi-MFR addition on the AS mixed liquor indicated excess reagent addition could cause destabilized flocs to re-stabilized. Besides, further dosing led to decrease in permeability, which happens in contrary to the effect on BF-MBR.
- At the given dose range it could be concluded that alum was better MFR followed by PAX-18 and PAX XL-61. The Optimum dose was 1.3 mM Al. g⁻¹ SS for Alum and 2 mM-Me. g⁻¹ SS for PAX-18.

5. REFERENCES

- AMTA, 2017, American Membrane Technology Association: Membrane Bioreactors for Wastewater Treatment, Volume 2017.
- Arabi, S., and Nakhla, G., 2008, Impact of calcium on the membrane fouling in membrane bioreactors: *Journal of Membrane Science*, v. 314, no. 1, p. 134-142.
- Bouhabila, E. H., Aïm, R. B., and Buisson, H., 2001, Fouling characterisation in membrane bioreactors: *Separation and Purification Technology*, v. 22, p. 123-132.
- Breite, D., Went, M., Prager, A., and Schulze, A., 2015, Tailoring membrane surface charges: A novel study on electrostatic interactions during membrane fouling: *Polymers*, v. 7, no. 10, p. 2017-2030.
- Buyukkamaci, N., 2004, Biological sludge conditioning by Fenton's reagent: *Process Biochemistry*, v. 39, no. 11, p. 1503-1506.
- Cembrane, 2015, Volume 2017.
- Chang, I.-S., and Lee, C.-H., 1998, Membrane filtration characteristics in membrane-coupled activated sludge system—the effect of physiological states of activated sludge on membrane fouling: *Desalination*, v. 120, no. 3, p. 221-233.
- Choo, K.-H., and Lee, C.-H., 1996, Membrane fouling mechanisms in the membrane-coupled anaerobic bioreactor: *Water Research*, v. 30, no. 8, p. 1771-1780.
- Chowdhury, Z. K., Amy, G. L., and Bales, R. C., 1991, Coagulation of submicron colloids in water treatment by incorporation into aluminum hydroxide floc: *Environmental science & technology*, v. 25, no. 10, p. 1766-1773.
- Cordell, D., Drangert, J.-O., and White, S., 2009, The story of phosphorus: global food security and food for thought: *Global environmental change*, v. 19, no. 2, p. 292-305.
- Diez, V., Ezquerro, D., Cabezas, J., García, A., and Ramos, C., 2014, A modified method for evaluation of critical flux, fouling rate and in situ determination of resistance and compressibility in MBR under different fouling conditions: *Journal of Membrane Science*, v. 453, p. 1-11.
- Duan, J., and Gregory, J., 2003, Coagulation by hydrolysing metal salts: *Advances in colloid and interface science*, v. 100, p. 475-502.
- EU-UWWTD, 1991, Volume 09.11.2017.
- Fang, H. H., Shi, X., and Zhang, T., 2006, Effect of activated carbon on fouling of activated sludge filtration: *Desalination*, v. 189, no. 1-3, p. 193-199.
- Fu, C., Yue, X., Shi, X., Ng, K. K., and Ng, H. Y., 2017, Membrane fouling between a membrane bioreactor and a moving bed membrane bioreactor: Effects of solids retention time: *Chemical Engineering Journal*, v. 309, p. 397-408.
- Geilvoet, S. P., 2010, The Delft Filtration Characterisation method: Assessing membrane bioreactor activated sludge filterability.
- Hofs, B., Ogier, J., Vries, D., Beerendonk, E. F., and Cornelissen, E. R., 2011, Comparison of ceramic and polymeric membrane permeability and fouling using surface water: *Separation and Purification Technology*, v. 79, no. 3, p. 365-374.
- Hong, H., Peng, W., Zhang, M., Chen, J., He, Y., Wang, F., Weng, X., Yu, H., and Lin, H., 2013, Thermodynamic analysis of membrane fouling in a submerged membrane bioreactor and its implications: *Bioresource Technology*, v. 146, no. Supplement C, p. 7-14.
- Houghton, J., Quarmby, J., and Stephenson, T., 2001, Municipal wastewater sludge dewaterability and the presence of microbial extracellular polymer: *Water Science and Technology*, v. 44, no. 2-3, p. 373-379.
- Hwang, B.-K., Lee, W.-N., Park, P.-K., Lee, C.-H., and Chang, I.-S., 2007, Effect of membrane fouling reducer on cake structure and membrane permeability in membrane bioreactor: *Journal of membrane science*, v. 288, no. 1, p. 149-156.
- Iorhemen, O. T., Hamza, R. A., and Tay, J. H., 2016, Membrane Bioreactor (MBR) technology for wastewater treatment and reclamation: membrane fouling: *Membranes*, v. 6, no. 2, p. 33.

- Jang, D., Hwang, Y., Shin, H., and Lee, W., 2013, Effects of salinity on the characteristics of biomass and membrane fouling in membrane bioreactors: *Bioresource Technology*, v. 141, no. Supplement C, p. 50-56.
- Khan, S. J., Visvanathan, C., and Jegatheesan, V., 2012, Effect of powdered activated carbon (PAC) and cationic polymer on biofouling mitigation in hybrid MBRs: *Bioresource technology*, v. 113, p. 165-168.
- Koros, W., Ma, Y., and Shimidzu, T., 1996, Terminology for membranes and membrane processes (IUPAC Recommendations 1996): *Pure and Applied Chemistry*, v. 68, no. 7, p. 1479-1489.
- Koseoglu, H., Yigit, N., Iversen, V., Drews, A., Kitis, M., Lesjean, B., and Kraume, M., 2008, Effects of several different flux enhancing chemicals on filterability and fouling reduction of membrane bioreactor (MBR) mixed liquors: *Journal of Membrane Science*, v. 320, no. 1, p. 57-64.
- Le-Clech, P., Chen, V., and Fane, T. A. G., 2006, Fouling in membrane bioreactors used in wastewater treatment: *Journal of Membrane Science*, v. 284, no. 1, p. 17-53.
- Lee, J., Ahn, W.-Y., and Lee, C.-H., 2001, Comparison of the filtration characteristics between attached and suspended growth microorganisms in submerged membrane bioreactor: *Water Research*, v. 35, no. 10, p. 2435-2445.
- Lee, W.-N., Chang, I.-S., Hwang, B.-K., Park, P.-K., Lee, C.-H., and Huang, X., 2007, Changes in biofilm architecture with addition of membrane fouling reducer in a membrane bioreactor: *Process Biochemistry*, v. 42, no. 4, p. 655-661.
- Lenntech, 2018, Volume 2018.
- Li, T., Zhu, Z., Wang, D., Yao, C., and Tang, H., 2006, Characterization of floc size, strength and structure under various coagulation mechanisms: *Powder technology*, v. 168, no. 2, p. 104-110.
- Liao, B., Allen, D., Droppo, I., Leppard, G., and Liss, S., 2001, Surface properties of sludge and their role in bioflocculation and settleability: *Water research*, v. 35, no. 2, p. 339-350.
- Lin, H., Gao, W., Leung, K., and Liao, B., 2011, Characteristics of different fractions of microbial flocs and their role in membrane fouling: *Water Science and Technology*, v. 63, no. 2, p. 262-269.
- Lin, H., Zhang, M., Wang, F., Meng, F., Liao, B.-Q., Hong, H., Chen, J., and Gao, W., 2014, A critical review of extracellular polymeric substances (EPSs) in membrane bioreactors: characteristics, roles in membrane fouling and control strategies: *Journal of Membrane science*, v. 460, p. 110-125.
- López-Maldonado, E. A., Oropeza-Guzman, M. T., Jurado-Baizaval, J. L., and Ochoa-Terán, A., 2014, Coagulation–flocculation mechanisms in wastewater treatment plants through zeta potential measurements: *Journal of Hazardous Materials*, v. 279, no. Supplement C, p. 1-10.
- Lyko, S., Al-Halbouni, D., Wintgens, T., Janot, A., Hollender, J., Dott, W., and Melin, T., 2007, Polymeric compounds in activated sludge supernatant — Characterisation and retention mechanisms at a full-scale municipal membrane bioreactor: *Water Research*, v. 41, no. 17, p. 3894-3902.
- Melin, T., Jefferson, B., Bixio, D., Thoeye, C., De Wilde, W., De Koning, J., van der Graaf, J., and Wintgens, T., 2006, Membrane bioreactor technology for wastewater treatment and reuse: *Desalination*, v. 187, no. 1, p. 271-282.
- Meng, F., Chae, S.-R., Drews, A., Kraume, M., Shin, H.-S., and Yang, F., 2009, Recent advances in membrane bioreactors (MBRs): membrane fouling and membrane material: *Water research*, v. 43, no. 6, p. 1489-1512.
- Meng, F., Zhang, H., Yang, F., Li, Y., Xiao, J., and Zhang, X., 2006, Effect of filamentous bacteria on membrane fouling in submerged membrane bioreactor: *Journal of Membrane Science*, v. 272, no. 1, p. 161-168.
- Meng, F., Zhang, H., Yang, F., and Liu, L., 2007, Characterization of cake layer in submerged membrane bioreactor: *Environmental science & technology*, v. 41, no. 11, p. 4065-4070.
- Mulder, J., 2012, Basic principles of membrane technology, Springer Science & Business Media.
- Nano, Z., 2017, Zeta Potential theory, Volume 2017: researchgate.net, Zetasizer Nano.

- Ng, H. Y., and Hermanowicz, S. W., 2005, Membrane bioreactor operation at short solids retention times: performance and biomass characteristics: *Water Research*, v. 39, no. 6, p. 981-992.
- Omoike, A., 1999, Removal of phosphorus and organic matter removal by alum during wastewater treatment: *Water Research*, v. 33, no. 17, p. 3617-3627.
- Ping Chu, H., and Li, X. y., 2005, Membrane fouling in a membrane bioreactor (MBR): sludge cake formation and fouling characteristics: *Biotechnology and bioengineering*, v. 90, no. 3, p. 323-331.
- Ratnaweera, H. C., 2017, *Renseteknologi for vann og avløp- internasjonalt: grunnkurs*, Universitetet for miljø- og biovitenskap.
- Rosenberger, S., Evenblij, H., Te Poele, S., Wintgens, T., and Laabs, C., 2005, The importance of liquid phase analyses to understand fouling in membrane assisted activated sludge processes—six case studies of different European research groups: *Journal of Membrane Science*, v. 263, no. 1, p. 113-126.
- Rusten, B., and Ødegaard, H., 2007, Design and operation of moving bed biofilm reactor plants for very low effluent nitrogen and phosphorus concentrations: *Water Practice*, v. 1, no. 5, p. 1-13.
- Shen, L.-g., Lei, Q., Chen, J.-R., Hong, H.-C., He, Y.-M., and Lin, H.-J., 2015, Membrane fouling in a submerged membrane bioreactor: impacts of floc size: *Chemical Engineering Journal*, v. 269, p. 328-334.
- Sheng, G.-P., Yu, H.-Q., and Li, X.-Y., 2010, Extracellular polymeric substances (EPS) of microbial aggregates in biological wastewater treatment systems: a review: *Biotechnology advances*, v. 28, no. 6, p. 882-894.
- Siembida, B., Cornel, P., Krause, S., and Zimmermann, B., 2010, Effect of mechanical cleaning with granular material on the permeability of submerged membranes in the MBR process: *Water research*, v. 44, no. 14, p. 4037-4046.
- Spettmann, D., Eppmann, S., Flemming, H.-C., and Wingender, J., 2007, Simultaneous visualisation of biofouling, organic and inorganic particle fouling on separation membranes: *Water science and technology*, v. 55, no. 8-9, p. 207-210.
- Tanada, S., Kabayama, M., Kawasaki, N., Sakiyama, T., Nakamura, T., Araki, M., and Tamura, T., 2003, Removal of phosphate by aluminum oxide hydroxide: *Journal of colloid and interface science*, v. 257, no. 1, p. 135-140.
- Tang, H., Xiao, F., and Wang, D., 2015, Speciation, stability, and coagulation mechanisms of hydroxyl aluminum clusters formed by PACl and alum: A critical review: *Advances in colloid and interface science*, v. 226, p. 78-85.
- van den Brink, P., Satpradit, O.-A., van Bentem, A., Zwijnenburg, A., Temmink, H., and van Loosdrecht, M., 2011, Effect of temperature shocks on membrane fouling in membrane bioreactors: *Water research*, v. 45, no. 15, p. 4491-4500.
- van der Marel, P., Zwijnenburg, A., Kemperman, A., Wessling, M., Temmink, H., and van der Meer, W., 2010, Influence of membrane properties on fouling in submerged membrane bioreactors: *Journal of membrane science*, v. 348, no. 1, p. 66-74.
- Vanysacker, L., Declerck, P., Bilad, M., and Vankelecom, I., 2014, Biofouling on microfiltration membranes in MBRs: Role of membrane type and microbial community: *Journal of Membrane Science*, v. 453, p. 394-401.
- Vinnerås, B., and Jönsson, H., 2002, The performance and potential of faecal separation and urine diversion to recycle plant nutrients in household wastewater: *Bioresource Technology*, v. 84, no. 3, p. 275-282.
- Wang, X.-m., Sun, F.-y., and Li, X.-y., 2011, Investigation of the role of biopolymer clusters in MBR membrane fouling using flash freezing and environmental scanning electron microscopy: *Chemosphere*, v. 85, no. 7, p. 1154-1159.
- Wong, L., Ng, C., Bashir, M., Koo, C., and Humaira, N., 2016, Enhancement of Membrane Fouling Control in Hybrid Aerobic Membrane Bioreactor System for Domestic Waste Water Application: Effect of Alum Concentration: *Procedia Engineering*, v. 148, p. 726-734.

- Wu, J. L., Chen, F. T., Huang, X., Geng, W. Y., and Wen, X. H., 2006, Using inorganic coagulants to control membrane fouling in a submerged membrane bioreactor: *Desalination*, v. 197, no. 1-3, p. 124-136.
- Yoon, S.-H., Collins, J. H., Musale, D., Sundararajan, S., Tsai, S.-P., Hallsby, G. A., Kong, J. F., Koppes, J., and Cachia, P., 2005, Effects of flux enhancing polymer on the characteristics of sludge in membrane bioreactor process: *Water Science and Technology*, v. 51, no. 6-7, p. 151-157.
- Ødegaard, H., Grutle, S., and Ratnaweera, H., 1992, An analysis of floc separation characteristics in chemical wastewater treatment, *Chemical Water and Wastewater Treatment II*, Springer, p. 97-114.

APPENDIX I: Processing of data from total recycle test

A. TMP Vs Time for MLSS 3.53 g.l⁻¹ from a BF-MBR plant

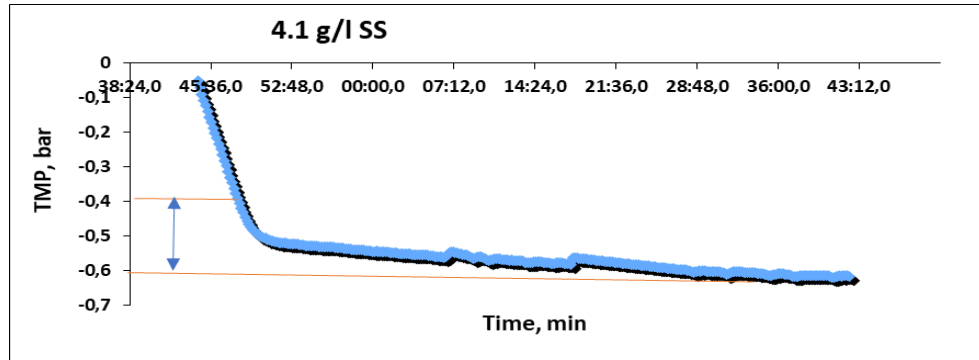


Figure 40. Change in TMP as function of time at 0.21 mM Al

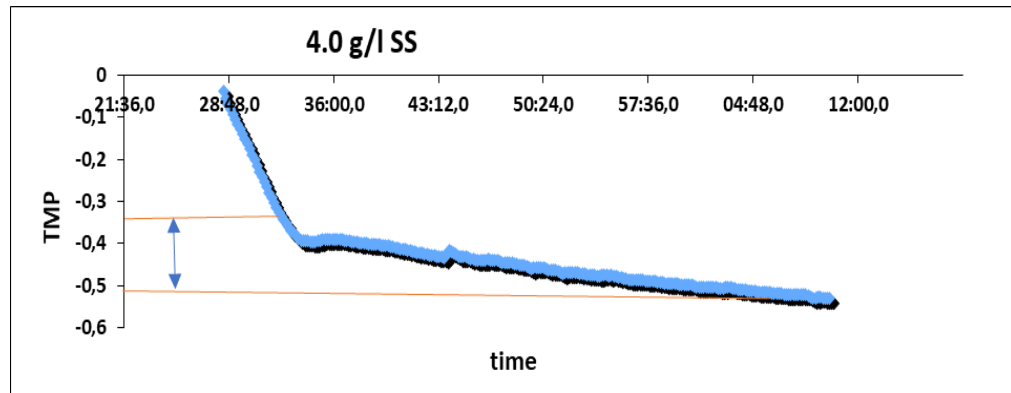


Figure 41. TMP as function of time at 0.43 mM Al

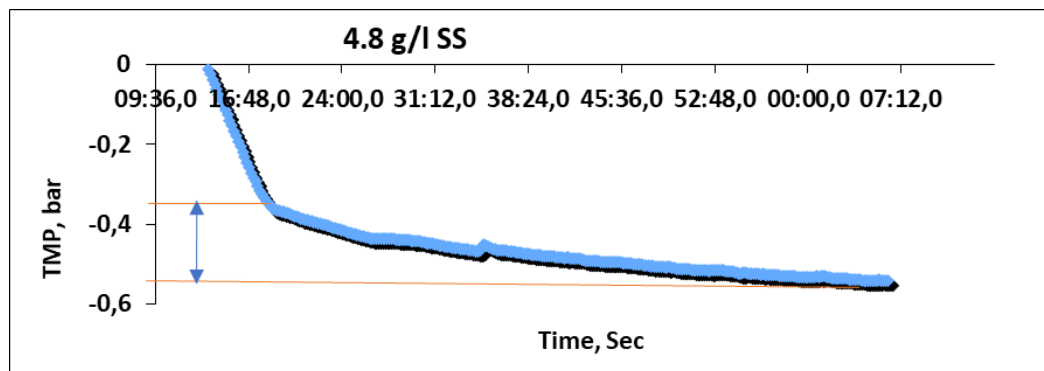


Figure 42. Change in TMP as function of time at 0.53 mM Al

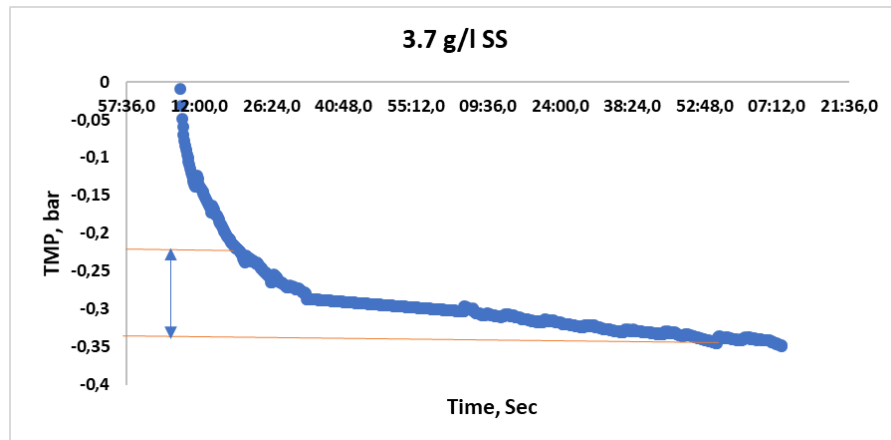


Figure 43. The Evolution of TMP as function of time at 0.64 mM Al

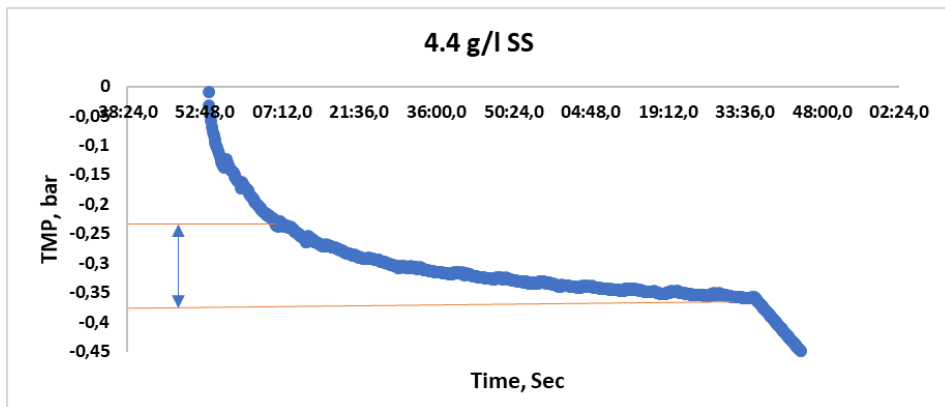


Figure 44. The three-stages of TMP as function of time at 0.74 mM Al

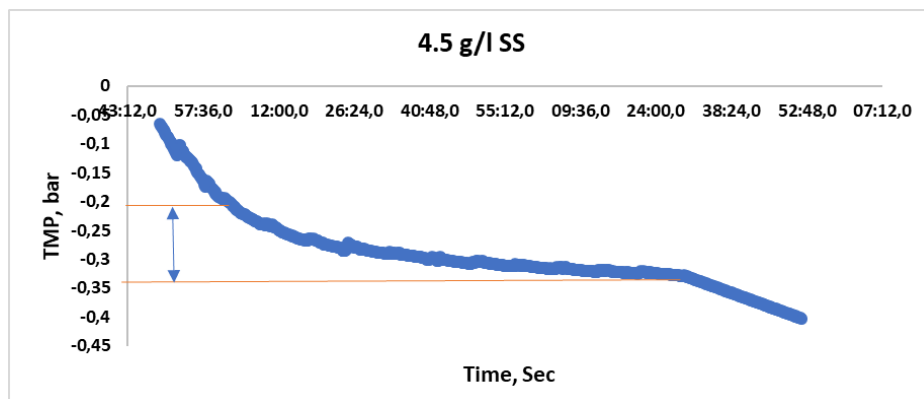


Figure 45. The variation of TMP as function of time at 0.85 mM Al

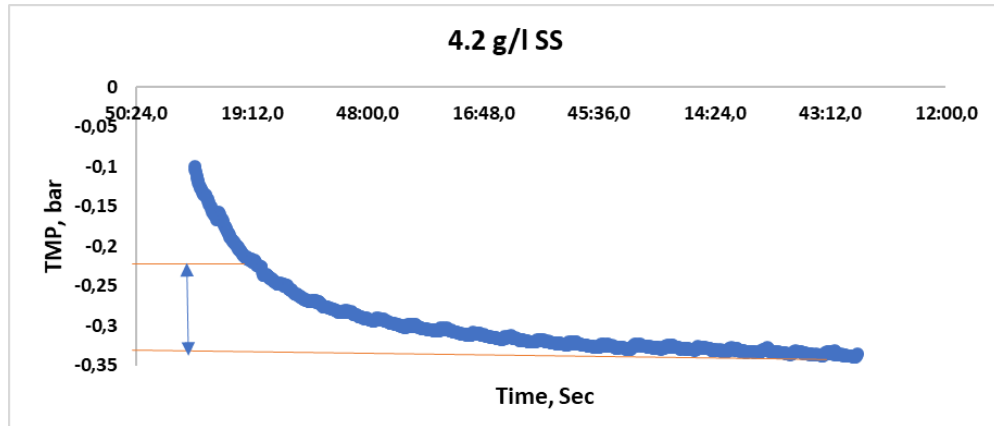


Figure 46. The Evolution of TMP as function of time at 0.96 mM Al

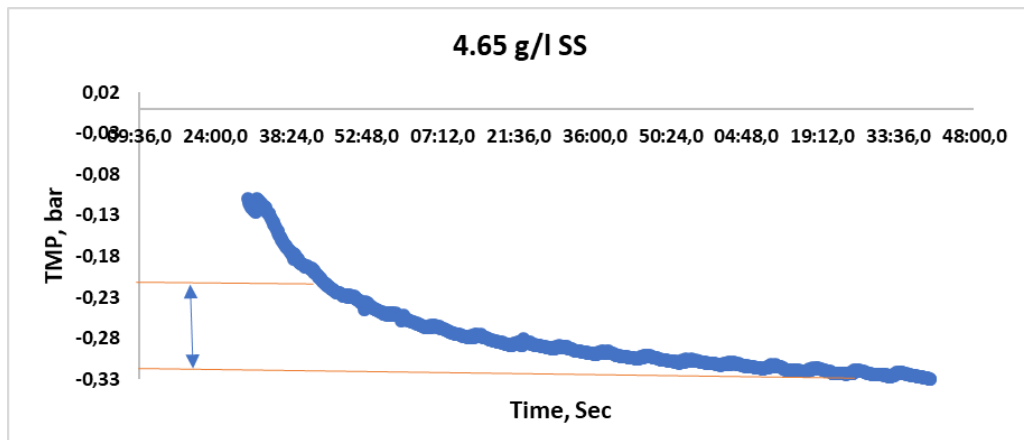


Figure 47. The change in TMP as function of time at 1.06 mM Al.

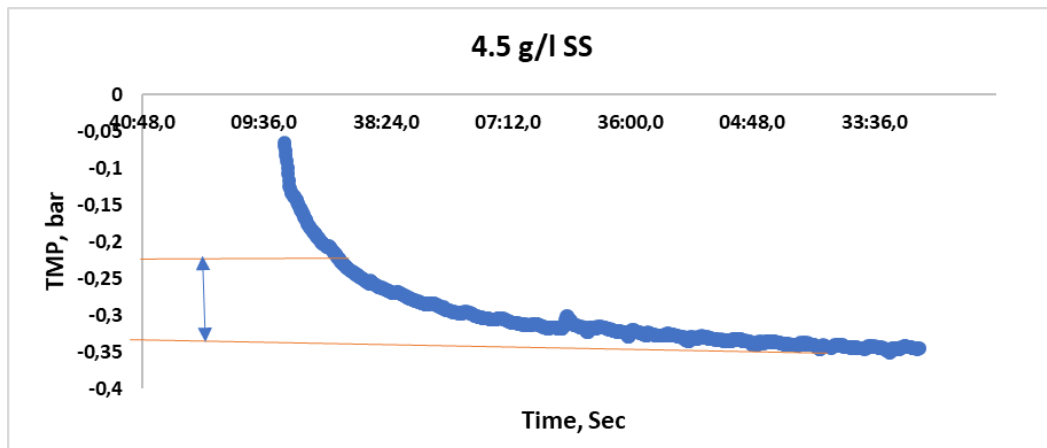


Figure 48. TMP increase as function of time at 1.3 mM Al

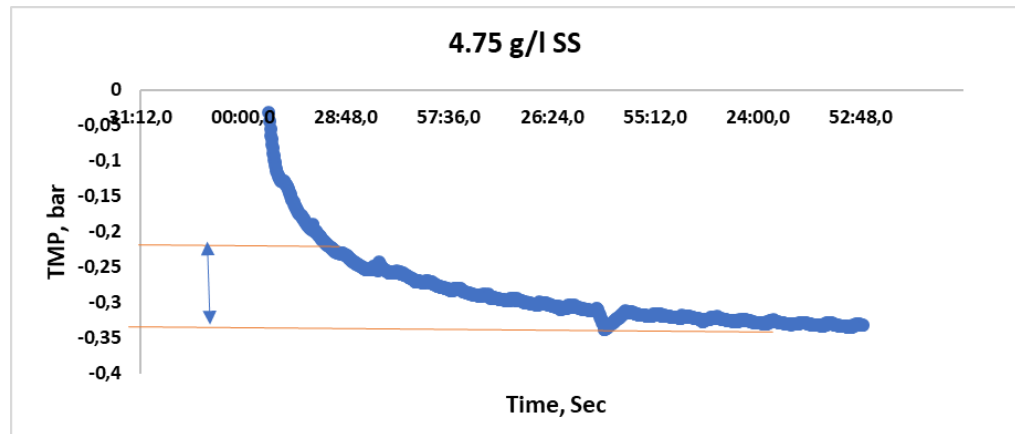


Figure 49. Evolution of TMP as function of time at 1.5 mM Al.

B. TMP Vs Time for MLSS 4.72 g.l⁻¹ from an AS

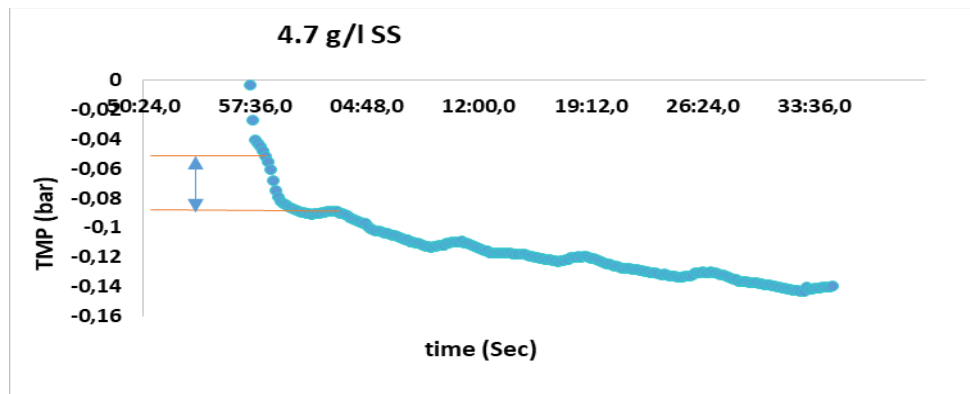


Figure 50. TMP increase as function of time at 0 mM Al

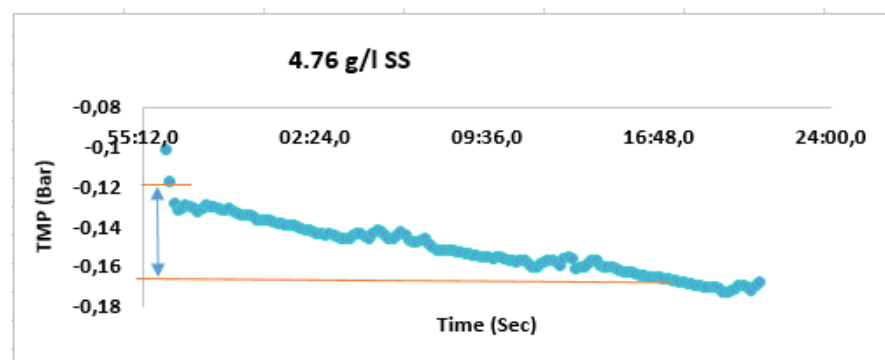


Figure 51. The change in TMP as function of time at 0.21 mM Al

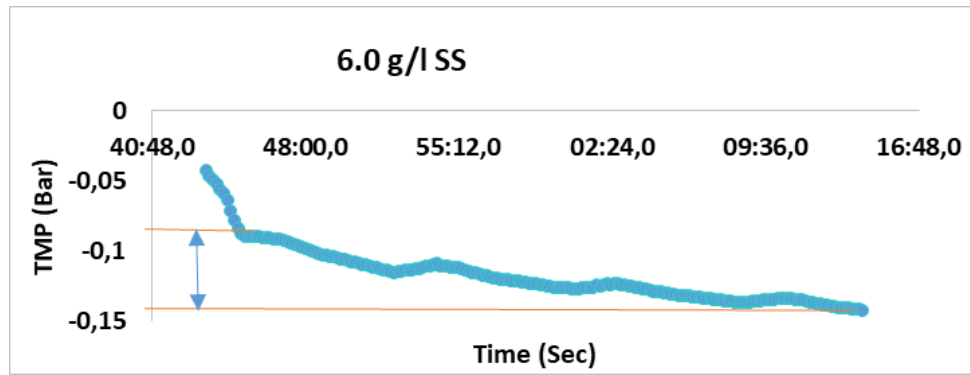


Figure 52. Evolution of TMP as function of time at 0.43 mM Al

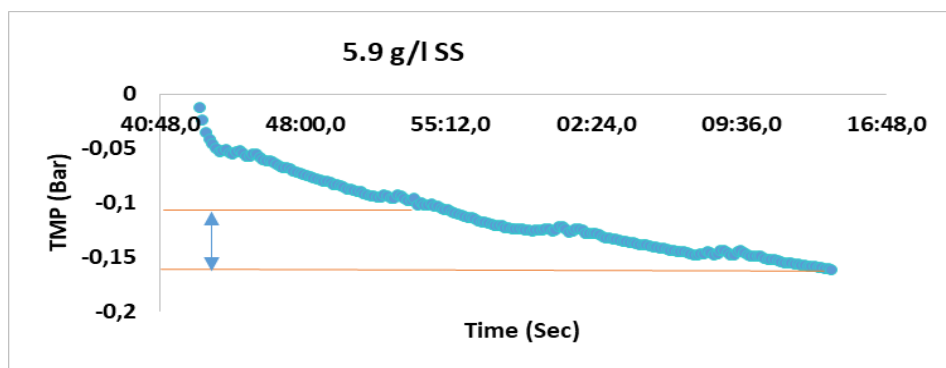


Figure 53. The variation of TMP as function of time at 0.53 mM Al

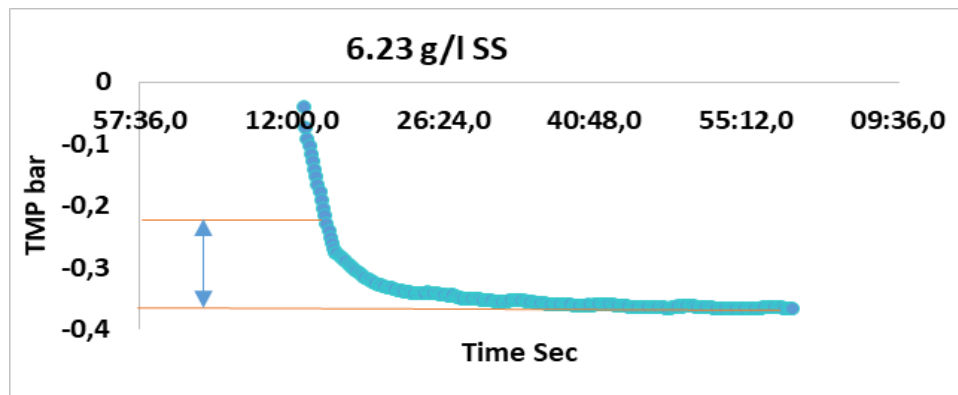


Figure 54. The change in TMP as function of time at 0.64 mM Al

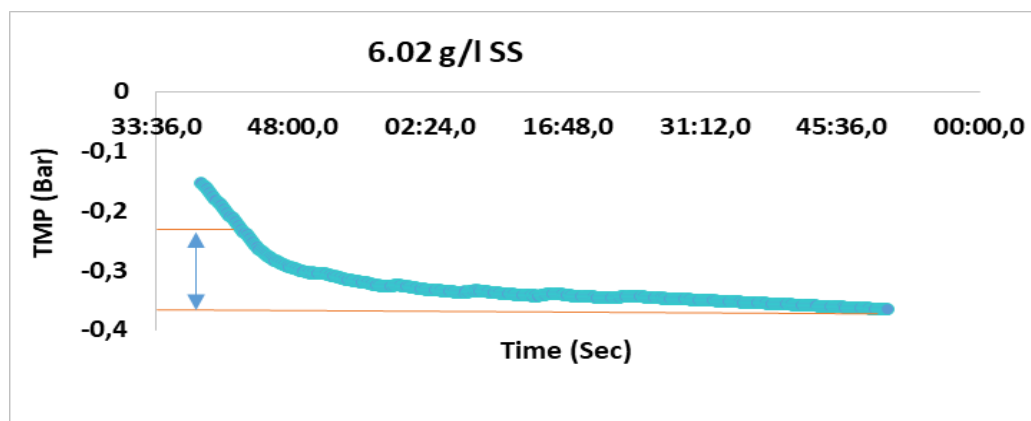


Figure 55 the evolution of TMP as function of time at 0.74 mM Al

Table 7, Filtration phase data source BF-MBR

| T in (Sec) | TMP in | Tfin | TMP fin | Filtration phase, min | Dose mM Al /g SS | MLSS g/l |
|------------|--------|--------|---------|-----------------------|------------------|----------|
| 139,0 | -0,3 | 249,0 | -0,4 | 1,8 | 0,0 | 3,5 |
| 249,0 | -0,4 | 2489,0 | -0,6 | 37,3 | 0,2 | 4,1 |
| 285,0 | -0,4 | 2535,0 | -0,5 | 37,5 | 0,4 | 4,0 |
| 341,0 | -0,4 | 3021,0 | -0,5 | 44,7 | 0,5 | 4,8 |
| 817,0 | -0,2 | 6037,0 | -0,3 | 87,0 | 0,6 | 4,2 |
| 929,0 | -0,2 | 7217,0 | -0,4 | 104,8 | 0,7 | 4,4 |
| 1823,0 | -0,3 | 8363,0 | -0,4 | 109,0 | 0,8 | 4,5 |
| 1115,0 | -0,2 | 9490,0 | -0,3 | 139,6 | 1,0 | 4,2 |
| 860,0 | -0,2 | 8860,0 | -0,3 | 133,3 | 1,1 | 4,6 |
| 850,0 | -0,2 | 9000,0 | -0,3 | 149,8 | 1,3 | 4,5 |
| 1030,0 | -0,2 | 9970,0 | -0,3 | 149,0 | 1,5 | 4,8 |

Table 8. Filtration phase data source AS

| Tin (Sec) | TMP in | T fin, Sec | TMP fin | Filtration, min | Dose, mM | MLSS (g/l) |
|-----------|--------|------------|---------|-----------------|----------|------------|
| 10 | -0,10 | 200,00 | -0,14 | 3,17 | 0,00 | 4,71 |
| 20 | -0,13 | 1510,00 | -0,17 | 24,83 | 0,21 | 4,76 |
| 272 | -0,11 | 1872,00 | -0,14 | 26,67 | 0,42 | 6,06 |
| 786 | -0,12 | 1926,00 | -0,16 | 19,00 | 0,53 | 6,33 |
| 157 | -0,28 | 2797,00 | -0,37 | 44,00 | 0,64 | 6,00 |
| 19 | -0,27 | 4049,00 | -0,35 | 67,17 | 0,74 | 6,15 |

APPENDIX II: Particle Size Growth and Distribution

A. Particle size change and distribution for BF-MBR at working MLSS 3.53 g.l⁻¹

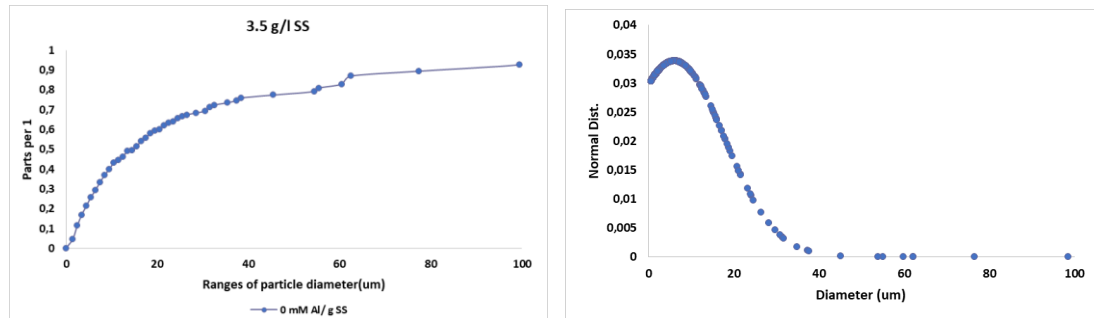


Figure 56. Illustrations of the particle size growth and distribution at dosing 0 mM Al

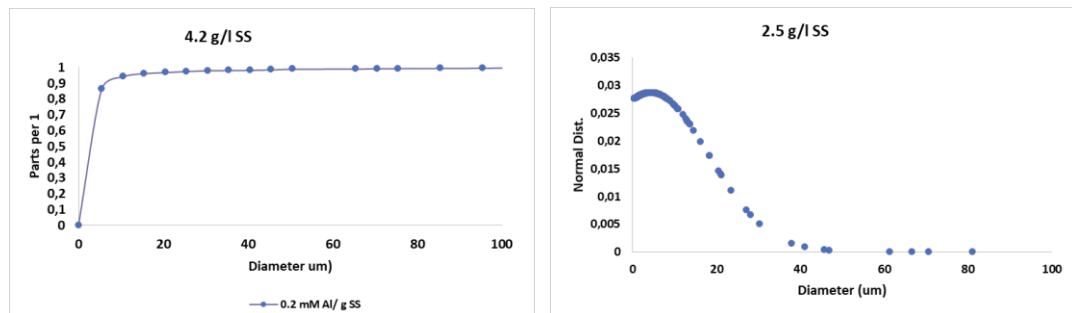


Figure 57. Graphical description of the particle size growth and distribution at dosing 0.21 mM Al

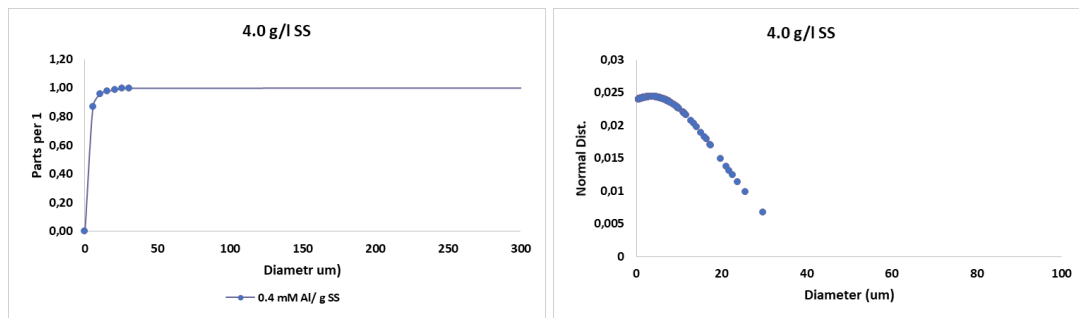


Figure 58. The particle size growth and distribution at dosing 0.42 mM Al

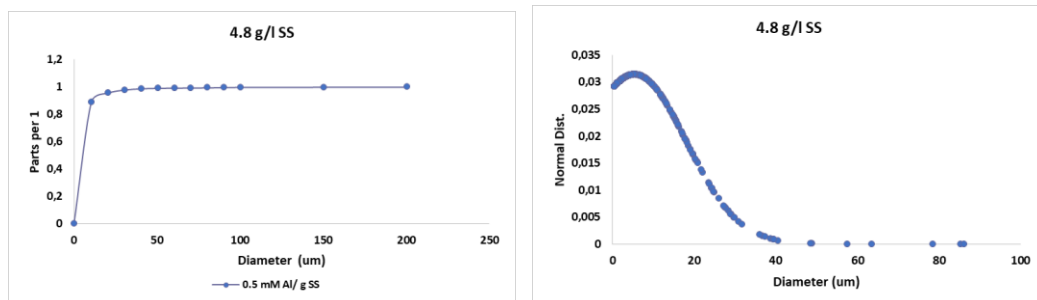


Figure 59. Graphical illustration of particle size growth and distribution at dosing 0.53 mM Al

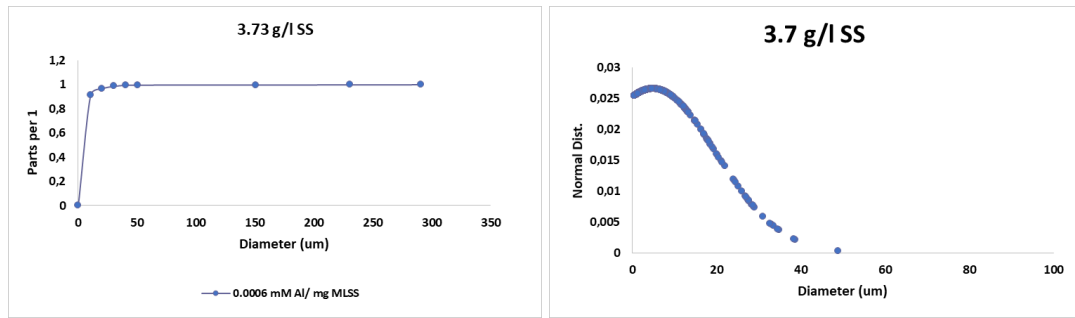


Figure 60. Shows the particle size growth and distribution at dosing 0.00064 mM Al

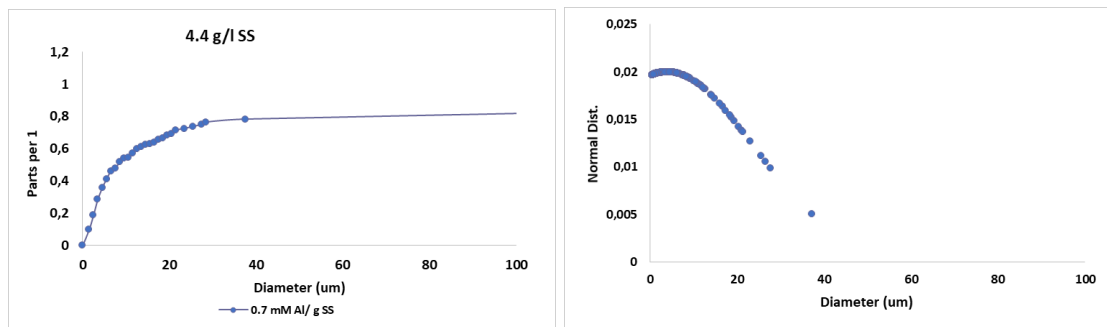


Figure 61. Graphical illustration of particle size growth and distribution at dosing 0.74 mM Al

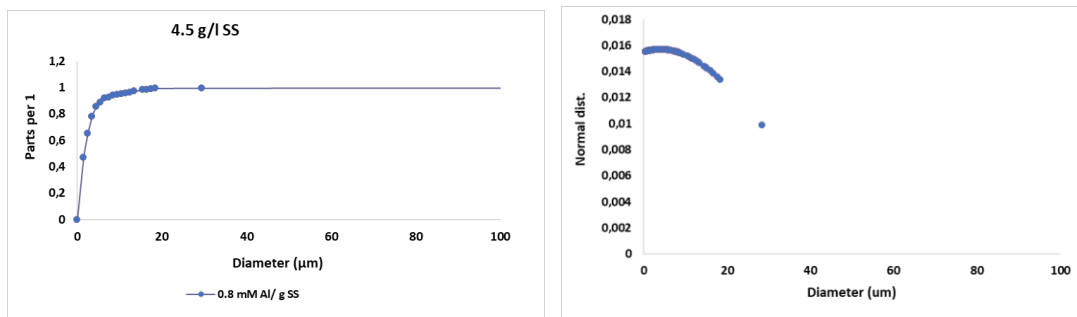


Figure 62. Graphic descriptions of the particle size growth and distribution at dosing 0.8 mM Al

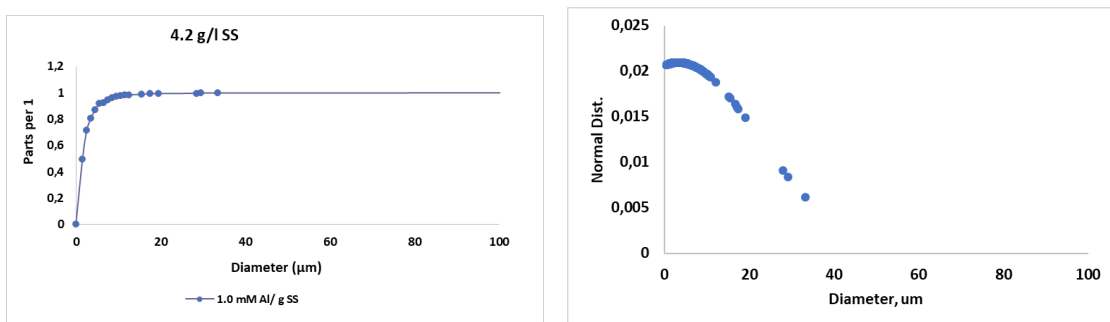


Figure 63. Illustrations of particle size growth and distribution 1.0 mM Al

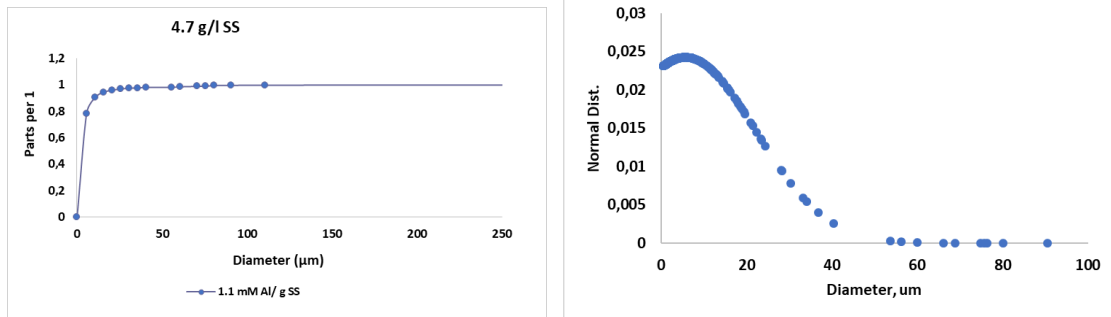


Figure 64. The change in particle size and distribution at dosing 1.1 mM Al

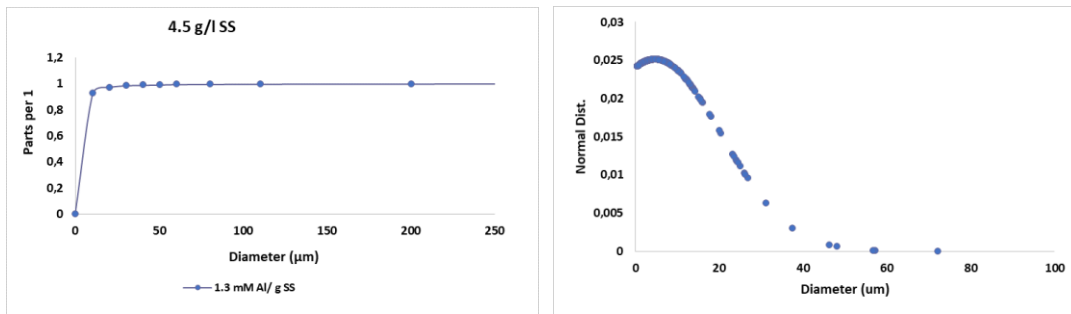


Figure 65. Shows the particle size growth and distribution at dosing 1.3 mM Al

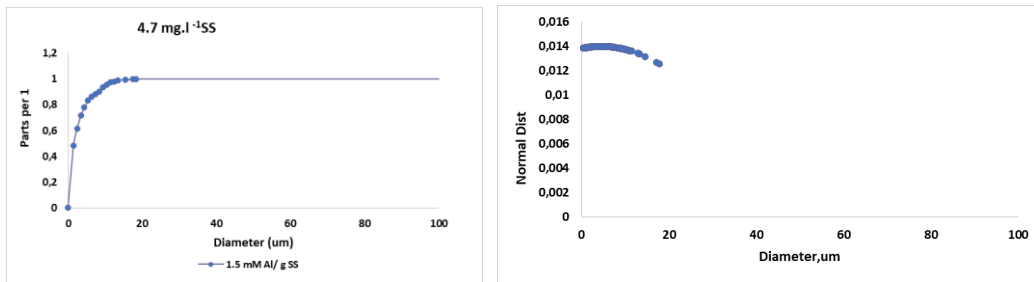


Figure 66. Display the particle size growth and distribution at dosing 1.5 mM Al

B. Particle size change and distribution for BEVAS MLSS

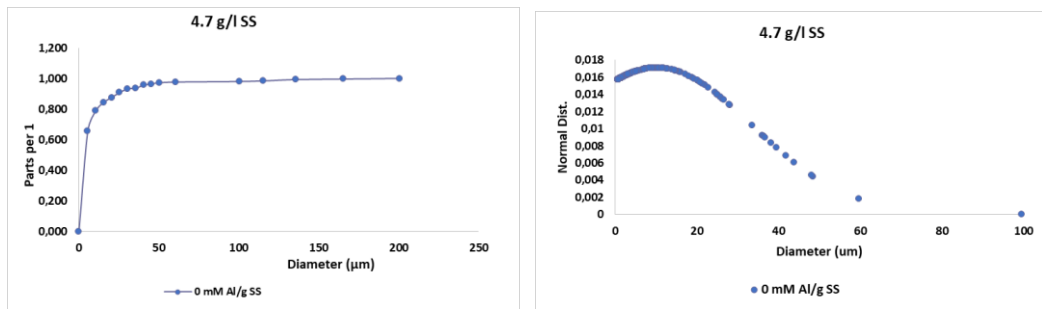


Figure 67. The particle size evolution and distribution at 0 mM Al

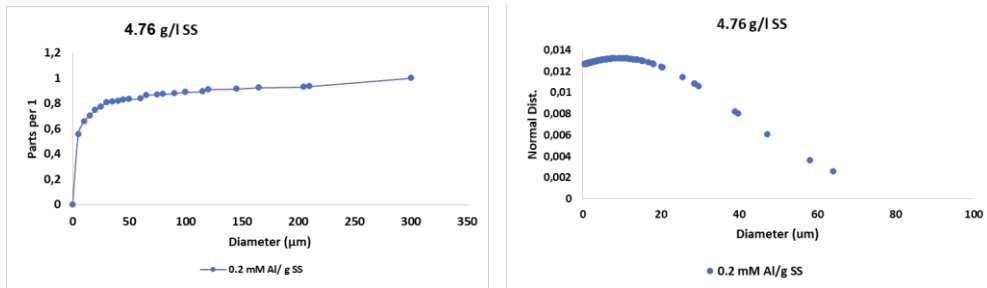


Figure 68. The improvement of the particle size and distribution at dosing 0.2 mM Al

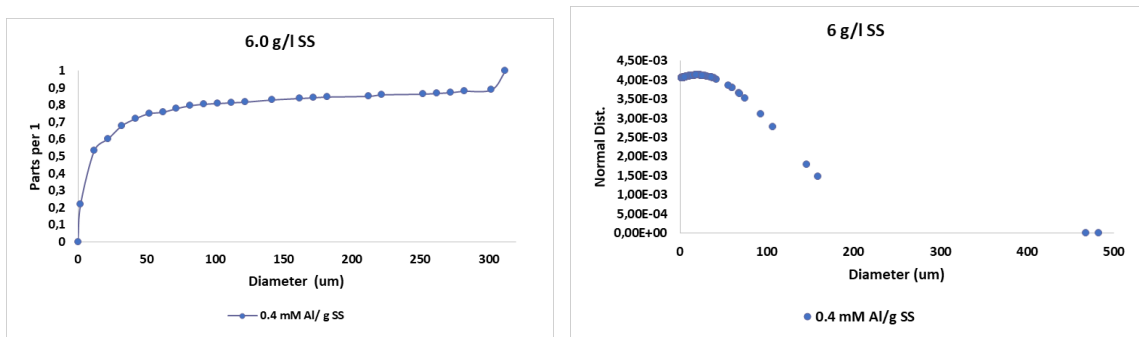


Figure 69. Graphical illustration of particle size growth and distribution at dosing 0.42 mM Al

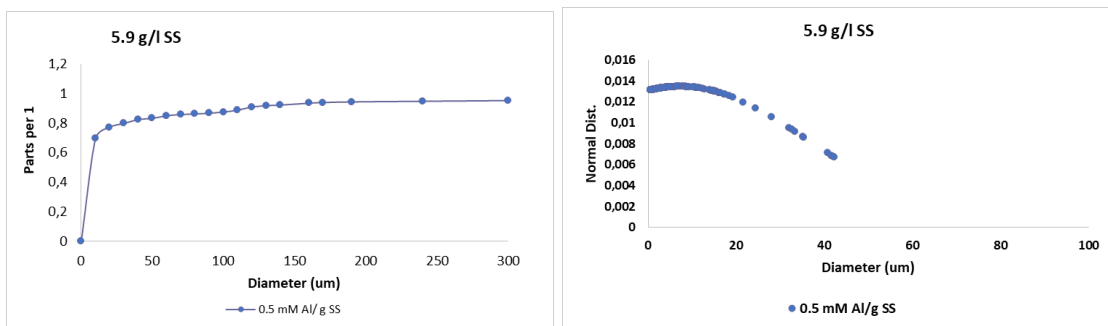


Figure 70. Illustrations of the growth in particle size and distribution at dosing 0.53 mM Al

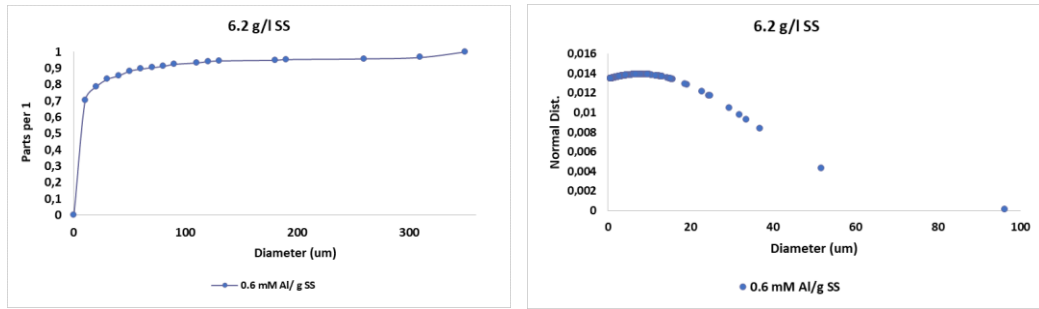


Figure 71. The influence on particle size and distribution at dosing 0.64 mM Al

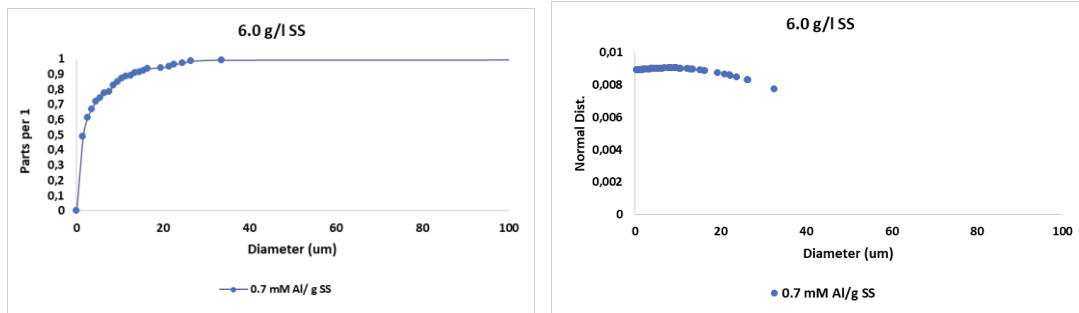


Figure 72. Graphical illustrations of particle size growth and distribution at dosing 0.74 mM Al



Norges miljø- og biovitenskapelige universitet
Noregs miljø- og biovitenskapelige universitet
Norwegian University of Life Sciences

Postboks 5003
NO-1432 Ås
Norway